Antitumor effects of novel targeted therapies (TAK-228 and TAK-117) with high selectivity against PI3K/AKT/mTOR pathway in bladder cancer. Defining molecular markers

Anna Hernández Prat

PhD THESIS UPF/2017

Thesis directors

Dr. Joaquim Bellmunt and Dra. Ana Rovira

Molecular Cancer Therapeutics Group

Cancer Research Program

Hospital del Mar Medical Research Institute (IMIM)

Als meus pares

What we know is a drop, what we don’t know is an ocean

Isaac Newton

This work was supported by the following institutions:

- ISCIII/FEDER (PI13/01893, RD12/0036/0051, CIBERONC CB16/12/00481).
- Generalitat de Catalunya (2014 SRG 740).
- We have established a Sponsored Research Agreement with industry (Millenium) for developing the targeted therapies TAK-228 and TAK-117 in the laboratory/translational setting.
- The IMIM (Institut Hospital del Mar d'Investigacions Mèdiques) provided funding for the publication of my PhD Thesis as hardcopies printed books.
- We thank Fundació Cellex (Barcelona) for a generous donation to the Hospital del Mar Medical Oncology Service.

ABSTRACT

Advanced bladder cancer is associated with a poor prognosis and with limited treatment options. Despite of the recent success with the use of immune check-point inhibitors, not all patients will respond to therapy and there is still need for alternative options. PI3K/AKT/mTOR pathway is frequently activated in this disease and can be a potential therapeutic target for treatment intervention. We studied the antitumor efficacy of two new targeted therapies, TAK-228 (an oral mTORC1/2 inhibitor) and TAK-117 (an oral PI3Kα inhibitor), and a classical mTOR inhibitor (Everolimus), in preclinical models of bladder cancer with signal transduction alterations in this pathway.

We demonstrated strong inhibition of cell proliferation *in vitro*, and reduction of the tumor growth *in vivo* with TAK-228. Potential biomarkers of response for TAK-228 were analysed. We also demonstrated that TAK-117 inhibits cell proliferation of cells with mutations in the PI3K gene and inhibits the tumor growth *in vivo*. We observed strong synergistic effects with the combination of TAK-228 and TAK-117. Furthermore, TAK-228 showed greater efficiency when combined with paclitaxel.

Our preclinical studies show that TAK-228 is a promising investigational agent that induces a strong effect on proliferation in bladder cancer models. Further studies with TAK-228 will be needed to see if this preclinical therapeutic efficacy is translated into clinical benefit for selected bladder cancer patients.

RESUM

El càncer de bufeta avançat està associat amb un mal pronòstic i les opcions terapèutiques són limitades. Tot i el recent èxit obtingut amb l'ús d'inhibidors de punts de control immunològics, no tots els pacients respondran a la teràpia i per tant encara hi ha la necessitat d'opcions alternatives. La via de PI3K/AKT/mTOR es troba activada freqüentment en aquesta patologia i pot ser una potencial diana terapèutica pel tractament. En aquest projecte hem estudiat l'eficàcia antitumoral de dues noves teràpies dirigides, el TAK-228 (inhibidor de mTORC1/2) i el TAK-117 (inhibidor de PI3Kα), i un inhibidor clàssic de mTOR, l'Everolimus, en models preclínics de càncer de bufeta amb alteracions de la senyalització d'aquesta via.

Vam demostrar una forta inhibició de la proliferació cel·lular *in vitro* en línies cel·lulars de càncer de bufeta i la reducció del creixement tumoral *in vivo* amb el TAK-228. Es van analitzar biomarcadors de resposta al TAK-228. També vam demostrar que el TAK-117 inhibeix la proliferació cel·lular de cèl·lules amb mutacions al gen de PI3K i la inhibició del creixement tumoral *in vivo*. Vam observar forts efectes sinèrgics amb la combinació de TAK-228 i TAK-117. A més, el TAK-228 va mostrar una major eficiència quan es combina amb el paclitaxel.

Els nostres estudis preclínics demostren que el TAK-228 és un fàrmac prometedor que indueix un fort efecte sobre la proliferació en els models de càncer de bufeta. Es necessitaran estudis addicionals amb el TAK-228 per veure si l'eficàcia terapèutica

observada a la preclínica es tradueix en un benefici clínic per a un subgrup de pacients amb càncer de bufeta.

PREFACE

The work presented in this PhD thesis has been conducted in the Molecular Cancer Therapeutics laboratory from the IMIM Cancer Research Program. The group is led by Dr. Joan Albanell, director of the Medical Oncology Service at the Hospital del Mar, and the preclinical laboratory is coordinated by Dr. Ana Rovira. The group is a multidisciplinary team composed by oncologists, pathologists, biologists and technicians with knowledge on different disciplines working together in traslational projects with clinicaly relevant interest.

Along the years as a predoctoral student in this group, since 2012, I have been working in a FIS project led by Dr. Joaquim Bellmunt and under the supervision of Dr. Ana Rovira for the experimental part. The results presented in this PhD thesis are derived from this project. The work was done in close collaboration with the Oncology and Pathology services of the Hospital del Mar and in collaboration with Dr. Federico Rojo from Fundación Jiménez Díaz, Madrid.

In this project we have studied the effects of new targeted-drugs for the treatment of bladder cancer. Two new drugs TAK-228 (mTORC1/2 inhibitor) and TAK-117 (PI3Kα inhibitor) were provided by Millennium Pharmaceuticals, Inc., through a MTA (material transfer agreement) in order to characterize their effects of them in our models of bladder cancer. Also, a Sponsored Research Agreement (SRA) between FIMIM and Millennium Pharmaceuticals, Inc was signed and the *in vivo* assays were conducted in accordance with the company.

In this study we have demonstrated the efficacy of these two new drugs as potential therapeutic strategies for the treatment of patients with advanced bladder cancer in the clinic.

We have also identified the ability of the drug TAK-228 to induce autophagy and the knowledge that I have acquired about this cellular process has allowed me to collaborate and to be the first co-author of a manuscript that we are preparing that summarize the main finding of another study of the group. It is focused on elucidating the involvement of the autophagia-lysosome system through modulation of the mTOR pathway in the efficacy of trastuzumab emtansine (T-DM1), a novel HER2-directed antibody-drug conjugate, in HER2 breast cancer.

During the last year, my research has been also focused on the relatively new field of immnunotherapy in bladder cancer. I have been involved as a research collaborator with a project since its start and we meet regularly with the research team (IP: Pilar Navarro) to provide input. The project: has been funded by the Spanish Association Against Cancer (AECC) to cancer research projects in Catalonia.

INDEX

INDEX

ABSTRACT ... XIII

RESUM ... XV

PREFACE ... XVII

INDEX ... XIX

ABBREVIATIONS ... XXVII

INTRODUCTION ... 1

- I.1. BLADDER CANCER OVERVIEW ... 3
  - I.1.1. Epidemiology of bladder cancer ... 3
  - I.1.2. Types and staging of bladder cancer ... 4
  - I.1.3. Management of localized and advanced bladder cancer 9
- I.2. MAJOR ALTERATIONS IN BLADDER CANCER AND THEIR CLINICAL SIGNIFICANCE ... 11
  - I.2.1. The Cancer Genome Atlas study and bladder cancer ... 11
  - I.2.2. PI3K/AKT/mTOR alterations in bladder cancer ... 13
  - I.2.3. Targeted therapy in bladder cancer ... 15
- I.3. PI3K/AKT/mTOR PATHWAY ... 18
  - I.3.1. Overview ... 18
  - I.3.2. Members of the PI3K/AKT/TOR pathway ... 20
    - I.3.2.1. Phosphatidylinositiol 3-kinase Lipids (PI3K) ... 20
    - I.3.2.2. AKT ... 25
    - I.3.2.3. Rheb protein and TSC1/TSC2 complex ... 26
    - I.3.2.4. mTORC1 and mTORC2 complex ... 28
    - I.3.2.5. mTORC1 Substrates: 4E-BP1 and S6K1 ... 32
      - I.3.2.5.1. 4E-BP1 ... 33
      - I.3.2.5.2. S6K1 and the ribosomal protein S6 ... 34

I.3.3. PI3K/AKT/mTOR signalling 36

I.3.3.1. AKT signalling 37

I.3.3.2. mTOR signalling 38

I.4. PHARMACOLOGICAL TARGETING OF THE PI3K/AKT/mTOR PATHWAY 41

I.4.1. Overview 41

I.4.1.1. mTORC1 inhibitors 45

I.4.1.2. mTORC1/2 inhibitors 48

I.4.1.2.1.TAK-228 50

I.4.1.3. PI3K inhibitors 51

I.4.1.3.1. TAK-117 53

1.4.2. Results of clinical targeting the PI3K/AKT/mTOR pathway in bladder cancer 54

1.4.3. Biomarkers in clinical samples that are potentially predictive of response to PI3K/AKT/mTOR inhibitors in bladder cancer 55

HYPOTHESIS 57

OBJECTIVES 61

RESULTS 65

R.1. CHARACTERIZATION OF HUMAN BLADDER CELL LINES 67

R.1.1. Cell morphology 67

R.1.2. Genetic background of the cell lines 68

R.1.3. Signaling molecule expression in human bladder cell lines 69

R.2. GENERATION OF BLADDER CANCER IN *IN VIVO* MODELS 71

R.3. CHARACTERIZATION OF THE EFFECTS OF DRUGS TARGETING THE PI3K/AKT/mTOR PATHWAY 75

R.3.1. Characterization of TAK-228 75

R.3.1.1. Effect of TAK-228 on BC cells 75

R.3.1.1.1. Effect of TAK-228 on cell viability 75

R.3.1.1.2. Effect of TAK-228 on cell cycle and apoptosis 76

R.3.1.1.3. Effect of TAK-228 on autophagy...................... 80

R.3.1.2. Molecular effects of TAK-228 on BC cells and tumor xenograft samples 83

R.3.1.2.1. Molecular effect of TAK-228 on BC cells......... 83

R.3.1.2.2. Molecular effects of TAK-228 on tumor xenograft samples 85

R.3.1.3. In vivo effects of TAK-228 on the RT4 xenograft model.. 87

R.3.1.3.1. Effect of TAK-228 on tumor growth................. 87

R.3.2. Characterization of everolimus 91

R.3.2.1. Cellular effects of everolimus on BC cells 91

R.3.2.1.1. Effect of everolimus on cell viability................. 91

R.3.2.2. Molecular effect of everolimus on BC cells 92

R.3.2.2.1. Molecular effect of everolimus on BC cells..... 92

R.3.3. Characterization of TAK-117.. 95

R.3.3.1. Cellular effect of TAK-117 on BC cell..................... 95

R.3.3.1.1. Effect of TAK-117 on cell viability 95

R.3.3.2. Molecular effect of TAK-117 on BC cells................ 97

R.3.3.3. In vivo effect of TAK-117 on the CAL-29 xenograft model.. 99

R.4. BIOMARKERS OF SENSITIVITY OR RESISTANCE TO TAK-228... 101

R.3.4.1. Basal expression and correlation.............................. 101

R.5. CHARACTERIZATION OF THE COMBINATION OF TAK-228 PLUS TAK-117.. 104

R.5.1. Cellular effects of TAK-228 plus TAK-117 on BC cells 104

R.5.1.1. Effects of TAK-228 plus TAK-117 on cell viability 104
R.5.1.2. Effect of TAK-228 plus TAK-117 on cell cycle 107
R.5.1.3. Effects of TAK-228 plus TAK-117 on autophagy. 109
R.5.2. Molecular effect of TAK-228 plus TAK-117 on BC cells 110
R.5.3. *In vivo* effects of TAK-228 plus TAK-117 on the RT4 xenograft model 113
R.5.3.1. Effects of TAK-228 plus TAK-117 on tumor growth 113
R.5.3.2. Effects of TAK-228 plus TAK-117 on tumor samples 114
R.6. CHARACTERIZATION OF THE COMBINATION OF TAK-228 PLUS PACLITAXEL 117
R.6.1. Cellular effects of TAK-228 plus paclitaxel on BC cells 117
R.6.1.1. Effects of TAK-228 plus paclitaxel on cell viability 117
R.6.1.2. Effects of TAK-228 plus Paclitaxel on cell cycle .. 120
R.6.1.3. Effects of TAK-228 plus Paclitaxel on autophagy 123
R.6.2. Molecular effects of TAK-228 plus Paclitaxel in BC cells 124
R.6.3. *In vivo* effects of TAK-228 plus Paclitaxel on the RT4 xenograft model 125
R.6.3.1. Establishing treatment conditions for in vivo experiments with paclitaxel 126
R.6.3.2. Effects of TAK-228 plus Paclitaxel on tumor growth 127
DISCUSSION 129
CONCLUSIONS 145
MATERIAL AND METHODS 149
M.1. CELL LINES AND CELL CULTURE 151

M.2. DRUGS 151

M.3. CELL PROLIFERATION AND CELL VIABILITY 152

M.3.1. MTS assay.. 152

M.3.1.1. Single agents assays... 153

M.3.1.2. Combinatorial assays 154

M.3.2. Automatic cell counting.. 154

M.3.3. Crystal violet assays 155

M.4. PROTEIN DETECTION 155

M.4.1. Total protein extraction 156

M.4.2. Protein quantification 156

M.4.3. Western blot analysis.. 157

M.4.4. Western blot quantification by QuantityOne............... 158

M.5. CELL CYCLE ANALYSIS.. 158

M.6. APOPTOSIS ANALYSIS 160

M.6.1. Apoptosis analysis by flow cytometry.......................... 160

M.6.2. Apoptosis analysis by western blot............................. 161

M.7. AUTOPHAGY ANALYSIS 161

M.7.1. Autophagic vesicles by microscopy............................. 162

M.7.2. Autophagy analysis by western blot 163

M.8. *IN VIVO* STUDIES.. 164

M.8.1. Animals 164

M.8.2. Set-up: Subcutaneous xenograft model in BALB/c nude mice 164

M.8.3. Survival studies.. 165

M.9. TUMOR SAMPLES ANALYSIS.. 165

M.9.1. Tumor samples analysis by immunohistochemistry... 166

M.9.1.1. IHC analysis of tumor samples treated ex vivo ... 166

M.9.1.2. IHC analysis of tumor samples from survival studies 167

M.9.2. Tumor samples analysis by western-blot 167

M.10. STATISTICAL ANALYSIS 168

M.10.1. Statistics for *in vitro* and *in vivo* assays 168

M.10.2. Statistics for biomarkers and drug response correlation 169

BIBLIOGRAPHY 171

ANNEX 185

ABBREVIATIONS

ABBREVIATIONS

ABD: Adaptor binding domain

ADP: Adenosine diphosphate

AGC: cAMP-dependent, cGMP-dependent and protein kinase C

AKT1-3/PKB: v-Akt murine thymoma viral oncogene homolog 1; protein kinase B

ATP: Adenosine triphosphate

BC: Bladder cancer

Bp: Base Pairs

C2: Protein kinase C homology 2

CD31: Platelet endothelial cell adhesion molecule1 (PECAM-1)

cDNA: complementay DNA

CI: Combinatorial index

CNA: Copy number alteration

CTLA4: Cytotoxic T-lymphocyte associated protein 4

DEPTOR: DEP domain-containing mTOR-interacting protein

4E BP1: Eukaryotic initiation factor 4E-binding protein 1

EGFR: ERBB1; Epidermal growth factor receptor

eIF4E: Eukaryotic translation initiation factor 4E

eIF4F: Eukaryotic initiation factor 4F

eIFs: Eukaryotic initiation factors

EMA: European medicines agency

ERK1/2: Extracellular regulated MAP kinase 1/2

FAT: FRAP-ATM-TRRAP

FATC: FRAP-ATM-TRRAP C terminal

FDA: Food and drug administration

FFPE: Formalin-fixed paraffin-embedded tumor tissue samples

FGFR3: Fibroblast growth factor receptor 3

FKBP12: FK506 binding protein 1A, 12kDa

FRAP1: FK506 binding protein 12-rapamycin associated protein 1

FRB: FKBP12-rapamycin binding

G0: growth phase 0; resting phase

G1: growth phase 1

G2: growth phase 2

GAP: GTPase-activating protein

GDP: guanosine diphosphate

GPCRs: G-protein coupled receptors

GSK3β: Glycogen synthase kinase 3 beta

GTP: guanosine triphosphate

H2AX: H2A histone family, member X

H3: histone H3

H&E: Hematoxylin & eosin

HEAT: Huntingtin, elongation factor3, alpha-regulatory subunit of protein phosphatase 2A and TOR 1

HER: Epidermal growth factor receptor family

HER2: ERBB2; Human epidermal growth factor receptor 2

HER3: Human epidermal growth factor receptor ¾

HRAS: v-Ha-ras Harvey rat sarcoma viral oncogene homolog

IC50: Half maximal inhibitory concentration

IHC: Immunohistochemistry

IRS-1: insulin receptor substrate 1

KDR: Vascular endothelial growth factor receptor 2; VEGFR-2

Ki-67: Antigen identified by monoclonal antibody Ki-67; MKI67

KRAS: v-Ki-ras2 Kirsten rat sarcoma viral oncogene homolog

LC3-I: Light chain 3 I

LC3-II: Light chain 3 II

M: mitosis phase

MAPK: mitogen activated protein kinase

MEK(1/2): MAPK/ERK kinase (1/2)

MIBCs: Muscle invasive bladder cancer

mLST8: Mammalian lethal with sec 13 protein 8

mRNA: messenger ribonucleic acid

mSIN1: MAPKAP1; mammalian stress-activated map kinase interacting protein 1

mTOR: mammalian target of rapamycin

mTORC1: mTOR complex 1

mTORC2: mTOR complex 2

NMIBCs: Non-muscle-invasive bladder cancer

p62/SQSTM1: Sequestosome 1

p70S6K: 70 kDa ribosomal protein S6 kinase 1

p90RSK: ribosomal protein S6 kinase, 90kDa

p110: Phosphatidylinositol-4,5-bisphosphate 3-kinase, catalytic subunit alpha protein

PARP: poly (ADP-ribose) polymerase

PBS: phosphate buffered saline

PD-1: Programmed cell death protein-1

PDK1: 3-Phosphoinositide dependent protein kinase 1

PD-L1: Programmed death ligand-1

PECAM-1: Platelet endothelial cell adhesion molecule1; CD31

PFS: progression free survival

PH: pleckstrin homology

PI3K: Phosphatidylinositol 3-kinase

PIK3CA: Phosphatidylinositol-4,5-bisphosphate 3-kinase, catalytic subunit alpha

PIKKs: Phosphatidylinositol 3-kinase-like kinases

PIP2: Phosphatidylinositol-4,5-biphosphate; PtdIns(4,5)P_2

PIP3: Phosphatidylinositol-3,4,5-triphosphate; PtdIns(3,4,5)P_3

PKB: Protein kinase B

PRAS40: 40kDa proline-rich AKT substrate

PROTOR: Protein observed with rictor-1

PTEN: Phosphatase and tensin homologue deleted on chromosome ten

RAPTOR: Regulatory-associated protein of mTOR

RBD: Ras binding domain

Rheb: Ras-homolog enriched in brain

RICTOR: Rapamycin-insensitive companion of mTOR

RNA: ribonucleic acid

rpS6: ribosomal protein S6

RTK: Receptor tyrosine kinases

S: DNA synthesis phase

S6K1: p70 S6 kinase 1

SD: Standard deviation

Ser: serine, amino acide

SH2: Src homology 2

TCC: Transitional cell carcinoma

TCGA: The cancer genome atlas

TGI: Tumor growth inhibition

Thr: Threonine, amino acide

TNM: Tumor node metastasis

TSC1: Tuberous sclerosis 1 (Hamartin)

TSC2: Tuberous sclerosis 2 (Tuberin)

UCC: Urothelial cell carcinoma

VEGF: Vascular endothelial growth factor

VEGF-A: Vascular endothelial growth factor A

VEGFR: Vascular endothelial growth factor receptor

INTRODUCTION

I.1. BLADDER CANCER OVERVIEW

Bladder is a balloon-shaped organ in pelvic area that stores urine. Bladder cancer (BC) includes neoplastic lesions arising from the tissues of the urinary bladder. Advanced BC is a heterogeneous and aggressive disease. Current treatment strategies have had limited success in the management of patients with advanced BC. The majority of these patients continue to have poor clinical outcomes.

I.1.1. Epidemiology of bladder cancer

BC is ninth most common cancer in the world and the second most common genitourinary malignancy in humans. The incidence is three times more frequent in men than in women and it occurs at a median age of 60 years [1]. The highest incidence rates are found in developed countries such as Europe and North America.

Various risks factors with different impacts on the incidence have been associated with bladder cancer. Smoking is the most important risk factor for bladder cancer in Western countries. The presence of arsenic in drinking water has been linked with a higher risk of bladder cancer in some parts of the world. Occupational exposure to carcinogens such as aromatic amines (benzidine and beta-naphthylamine), polycyclic and chlorinated hydrocarbons. Certain industrial chemicals are other associated risk factor. This exposure is likely to occur in industries that process dyes, rubber, textiles, metals, paints, leather and petroleum [2]. Parasitosis with *Schitosoma haematobium*, a parasite that infects the bladder to cause chronic cystitis, is the main risk in developing countries. Chronic inflammation of the bladder resulting from calculi, prolonged catheterization or chronic infections may also increase the risk of bladder cancer [3].

I.1.2. Types and staging of bladder cancer

The bladder is a hollow organ in the pelvis with flexible and muscular walls. Its main function is to store urine before it leaves the body. Urine is made by the kidneys and is then carried to the bladder through the ureters. The bladder's walls relax and expand to store urine, and contract and flatten to empty urine through the urethra.

The wall of the bladder has 4 main layers (**Figure I.1.**), which are made up of different types of cells:

- The innermost lining is called the *urothelium* or *transitional epithelium*.
- Beneath the urothelium is a thin layer of connective tissue, blood vessels, and nerves.
- Next is a thick layer of muscle.
- Outside of this muscle, a layer of fatty connective tissue separates the bladder from other nearby organs.

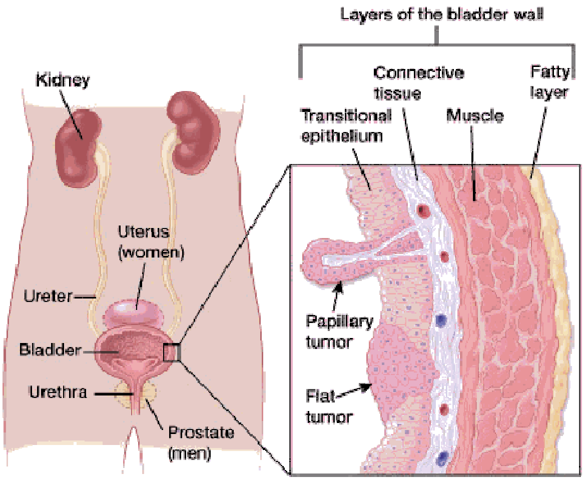
Layers of the bladder wall
Connective tissue
Fatty layer
Transitional epithelium
Muscle
Kidney
Uterus (women)
Ureter
Bladder
Urethra
Prostate (men)
Papillary tumor
Flat tumor

Figure I.1. Representative image of the wall of the bladder. Four layers form the wall of the bladder: transitional epithelium, connective tissue, muscle and fatty layer. Image obtained from the www.cancer.org

Nearly all bladder cancers start in the urothelium or transitional epithelium. As the cancer grows into or through the other layers in the bladder wall, it becomes more advanced and can be harder to treat. Over time, the cancer might grow outside the bladder and into nearby structures. It might spread to nearby lymph nodes, or to other parts of the body (it often goes first to distant lymph nodes, the bones, the lungs, or the liver.)

Several types of cancer can start in the bladder. Histologically, most cases of bladder cancer are Transitional cell carcinomas (TCC) (urothelilal carcinoma). This type accounts for about 90 % percent of bladder cancer. Bladder cancers are often described based on how far they have invaded into the wall of the bladder:

- **Non-invasive** cancers are still in the inner layer of cells (the transitional epithelium) but have not grown into the deeper layers.
- **Invasive** cancers have grown into deeper layers of the bladder wall. These cancers are more likely to spread and are harder to treat.

A bladder cancer can also be described as superficial or non-muscle invasive. These terms include both non-invasive tumors as well as any invasive tumors that have not grown into the main muscle layer of the bladder.

TCC are divided into two subtypes based on how they grow: a) Papillary carcinoma**:** This type of TCC grows out from the inner surface of the bladder toward the hollow center in fingerlike projections. Papillary tumors often grow toward the center of the bladder without growing into the deeper bladder layers often, these tumors are called “noninvasive papillary cancers,” meaning they don’t grow into the deeper layers of the bladder wall. When papillary TCC is very low grade, it may be called “papillary neoplasm of low-malignant potential” (PUNLMP), and typically has a very good outcome; b) Flat carcinomas: This type of TCC does not grow out of the urothelium toward the hollow part of the bladder. Rather, flat carcinomas remain on the surface of the bladder wall. If a flat carcinoma is confined to the urothelium, it is called “noninvasive flat carcinoma” or “flat carcinoma in situ (CIS).”

Several other types of cancer can start in the bladder, but these are all much less common than urothelial (transitional cell) cancer. Other histological cell types, in decreasing order of frequency are squamous cell carcinoma (3 - 5 %) (SCC; often associated with chronic inflammation); adenocarcinoma (0.5 to 2 %); small cell carcinoma (less than 0.5 %); and rare histological types such as sarcomatoid carcinoma, small-cell carcinoma, and lymphoepithelioma (less than 0.1 %) [4].

The stage of a bladder cancer describes how far it has spread. It's one of the most important factors in choosing treatment options and predicting a patient's prognosis.

BCs are staged according to TNM (Tumor-node-metastasis) system classification, which is based on 3 key pieces of information:

- **T** describes how far the main (primary) tumor has grown through the bladder wall and whether it has grown into nearby tissues.
- **N** indicates any cancer spread to lymph nodes near the bladder.
- **M** indicates whether or not the cancer has spread (metastasized) to distant sites, such as other organs or lymph nodes that are not near the bladder.

Numbers or letters appear after T, N, and M to provide more details about each of these factors. Higher numbers mean the cancer is more advanced.

The T category describes how far the main tumor has grown into the wall of the bladder (or beyond). Nearly all bladder cancers start in the urothelium. As the cancer grows into or through the other layers in the bladder, it becomes more advanced. According T category, BC is classified:

- NMIBCs (non-muscle-invasive BC):
    - Tis, non invasive, flat carcionoma in situ or cis
    - Ta, non invasive, papillary carcinoma
    - T1, the tumor has grown from the layer of cells lining the bladder into the connective tissue below. It has not grown into the muscle of the bladder

- MIBCs (muscle-invasive BC):
    - T2, the tumor has grown into the muscle layer
    - T3, The tumor has grown through the muscle layer of the bladder and into the fatty tissue layer that surronds it
    - T4, the tumor has spread beyond the fatty tissue and into nearby organs or structures. It may be growing into any of the following: the stroma (main tissue) of the prostate, the seminal vesicles, uterus, vagina, pelvic wall or abdominal wall

Bladder cancer can sometimes affect many areas of the bladder at the same time. If more than one tumor is found, the letter **m** is added to the appropriate T category.

Once the T, N, and M categories have been determined, this information is combined to find the overall cancer stage. Bladder cancer stages are defined using 0 and the Roman numerals I to IV

(1 to 4). Stage 0 is the earliest stage, while stage IV is the most advanced.

NMIBC frequently recur (50-70%) but infrequently progresses to invasion (10-15%), and five year survival is ~90%. MIBCs (stage T2 and above) have less favourable prognosis with five-year survival <50% and common progression to metastasis [5].

BCs are graded according to their cellular characteristics [5]. According to 2004 WHO/ ISUP (International Society of Urological Pathology) criteria, BCs are classified in three types:

- PUNLMP (papillary urothelial malignancy of low malignant potential) (Tis and Ta)
- Low-grade papillary urothelial carcinoma (T1 and T2)
- High-grade urothelial carcinoma (T2-T4)

I.1.3. Management of localized and advanced bladder cancer

Every bladder cancer patient is different and treatment for an individual patient with localized disease is designed based on tumor stage, size, and grade, as well as the overall health and preferences of the patient.

At the initial diagnosis of BC, 30% of cases present as MIBC, and approximately one-third of them might have distant metastases at presentation. 70% will be diagnosed with NMIBC and approximately 20% of this will progress to invasion of muscularis propia (MIBC).

The choice of treatment for NMIBC and for non-metastatic MIBCs is surgery, either transurethral resection or radical cystectomy of the bladder. Intravesical chemotherapy or BCG is given in patients with intermediate and high risk NMIBC. Neoadjuvant chemotherapy with platinum based agents is the standard of care for MIBC . Adjuvant chemotherapy can be considered in select patients after surgery.

BC is chemotherapy sensitive and the current standard of care for first-line systemic treatment of metastatic BC is combination chemotherapy with cisplatin and gemcitabine. Cisplatin o CDDP (cis-diaminocloroplatin (II)) is a platinum-based drug and gemcitabine is a drug that belongs to the nucleoside analog family. Both drugs, are chemotherapeutic agents, that work by inhibiting the DNA synthesis of proliferating cells.

There are limited options as second-line treatment for advanced BC. All the attempts to improve current chemotherapies such as dose intensification and combination doublets and triplet regimens have generally been unsuccessful. Only vinflunine is EMA-approved for second line treatment of metastatic disease. Vinflunine is a vinca alkaloid agent that works as an anti-mitotic and anti-microtubule agent by inhibiting the ability of cancer cells to divide [6].

Taxanes are commonly used as single agents in second line in USA. Taxanes have been tested in clinical trials as single agents or in combination with other therapies [7]. Taxanes such as paclitaxel, and docetaxel, are antineoplastic agents that inhibit the process of cell division by disruption of microtubules.

Despite the improvements seen during the last decade both in terms of surgical approach and systemic therapy, BC remains an aggressive disease with a poor prognosis, especially for patients with advanced disease who have a reduced overall survival of around 13-14 months with chemotherapy. New immunotherapeutic options with check-point inhibitors have opened great promises in the management of advanced BC patients.

I.2. MAJOR ALTERATIONS IN BLADDER CANCER AND THEIR CLINICAL SIGNIFICANCE

The first focused molecular analyses of patients with BC have revealed that urothelial carcinomas harbour frequent molecular dysregulations including recurrent mutations and frequent somatic copy number alterations (CNA), some of which could be potential therapeutic targets. Moreover, it has been shown that MIBC and non-MIBC are different specific entities with distinctive molecular characteristics. As of today, no molecularly targeted agents have so far been approved for the treatment of advanced BC.

I.2.1. The Cancer Genome Atlas study and bladder cancer

The Cancer Genome Atlas (TCGA) project is a collaboration, that begun in 2005, between the National Cancer Institute (NCI) and the National Human Genome Research Institute (NHGRI) with the purpose of cataloguing the genetic and epigenetic alterations responsible for cancer through the application of high-throughput genome analysis techniques, including large-scale genome sequencing and bioinformatics. The final goal of TCGA is to expand our understanding of the molecular basis of cancer in order to improve the ability to diagnose, treat and prevent this lethal disease.

The first TCGA analysis published integrate data from 131 with bladder cancer from patients who had not yet been treated. These analysis revealed three frequently mainly dysregulated pathways: p53/cell cycle (93%), PI3K signalling (72%) and chromatin remodelling pathways (76%) including alterations in the histone-modifying genes, and in the nucleosome remodelling complex [8].

PI3K signalling alterations included activating point mutations in *PI3KCA* and mutations or deletions of *TSC1* or *TSC2*. In addition, upstream activators of the PI3K pathway such as receptor tyrosine kinases (RTKs), EGFR, HER2, and HER3 were found to be overpressed or with mutations inducing PI3K activation and consequently activation of the pathway [5, 8].

A recent integrated analysis of mRNA, miRNA and protein data led to identification of 5 new distinct subsets of MIBC (luminal-papillary, luminal-infiltrated, luminal, basal-squamous, and neuronal subtypes) with specific molecular landscape. This classification should be used to validate and to assess therapeutic recommendations for each subtypes in the future.

I.2.2. PI3K/AKT/mTOR alterations in bladder cancer

The most important alterations correspond to mutations of several key genes regulating this pathway. This section is focused on the most relevant alterations.

Mutations in the regulatory subunit of PI3K (p85) and the catalytic subunit (p110α) have been identified in transformed cell lines and in human tumor samples [9]. *PIK3R1*, the gene that encodes the p85 subunit is mutated in a 5% of BC tumors. *PIK3CA*, the gene that encodes the p110α subunit is frequently mutated in human cancer and induces a constitutive activation of the pathway. Approximately 80% of *PI3KCA* mutations occur within three hotspot sites. Mutations occur more commonly in the helical domain (E545K and E542K) than in the kinase domain (H1047R), and are found in ~25% of NMIBCs and less frequently in MIBCs [5, 10, 11] (**Figure I.2.**). The two classes of *PI3KCA* mutations promote constitutive PI3K signaling through distinct mechanisms [12]. Tumors harboring these mutations potentially benefit from PI3K inhibitors.

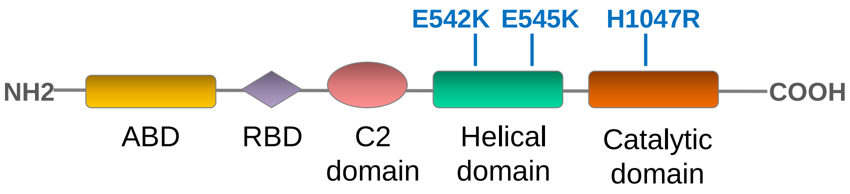

Figure I.2. Mutations in the *PI3KCA* gene relative to the functional domains of the encoded protein. Schematic representation of the protein showing functional domains and the position of the most relevant mutations (E542K, E545K and H1047R) of the *PI3KCA* gene in BC.

Mutations in the *TSC1* and *TSC2* genes causes the hamartomatous syndrome tuberous sclerosis complex (TSC) that is characterized by benign, noninvasive, tumor-like lesions in multiple organ systems. The TCGA identified mutations in the *TSC1* and *TSC2* genes in several tumor types including bladder cancer. Inactivating mutations of *TSC1* (9q34) are found in 11-16% of bladder tumors (in both MIBC and NMIBC) and inactivating mutations of *TSC2* (16p13) in a 2% of bladder tumors [5, 8]. Tumors harboring these mutations potentially benefit from mTOR inhibitors.

PTEN gene is mutated in a frequency of 25-58% in MIBC and it commonly shows LOH. Downregulated expression of PTEN is associated with poor outcome.

Activating mutations in *AKT1* are a rare event occurring in 2-3% [13, 14]. Moreover, hyper activation of the PI3K signaling pathway can also result from molecular alterations in upstream components including RTKs such as the ERRB family of proteins (found in 2% to 11%) and FGFR3 (found in 3% to 11%), as well through the activation of RAS (found in 1% to 5%). Integrated analysis of genetic alterations in the RTK/RAS/PI3K/AKT/mTOR pathway reveals that this signaling network is altered in 72% of BC [8]. This high frequency of alterations and the development of several small molecule inhibitors make the PI3K signaling pathway a strong contender for target therapy in BC.

I.2.3. Targeted therapy in bladder cancer

The genomic alterations found in BC have potential therapeutic implications and could be treated by drugs that are already available in other diseases or in a clinical trial setting. The main agents are inhibitors of EGFR, HER2 and FGFR families, antiangiogenic agents and inhibitors of the PI3K/AKT/mTOR pathway [15] (**Figure I.3.**).

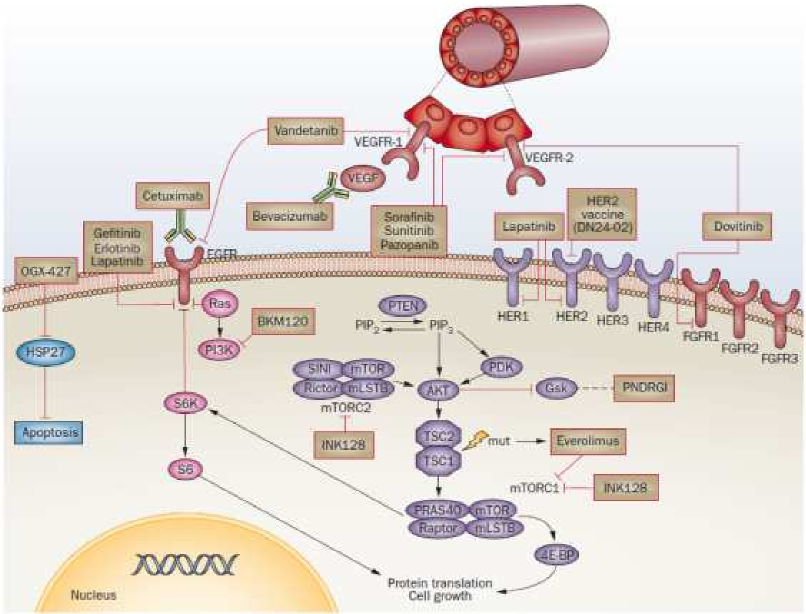
Vandetanib
VEGFR-1
VEGFR-2
VEGF
Cetuximab
Bevacizumab
Sorafinib
Sunitinib
Pazopanib
Lapatinib
HER2
vaccine
(DN24-02)
Dovitinib
Gefitinib
Erlotinib
Lapatinib
EGFR
OGX-427
Ras
BKM120
PI3K
PTEN
PIP_2
PIP_3
HER1
HER2
HER3
HER4
FGFR1
FGFR2
FGFR3
HSP27
Apoptosis
SINI
mTOR
Rictor
mLSTB
mTORC2
PDK
AKT
Gsk
PNDRGI
S6K
INK128
TSC2
TSC1
mut
Everolimus
mTORC1
INK128
S6
PRAS40
mTOR
Raptor
mLSTB
4E-BP
Nucleus
Protein translation
Cell growth

Figure I.3. Therapeutic targets in urothelial tumors. The inhibitors acting on single or multiple signalling proteins which are involved in cellular processes such us cell growth, apoptosis and angiogenesis are shown [15].

The epidermal growth factor receptor (EGFR) is a transmembrane glycoprotein that constitutes one of the members of the erbB family of tyrosine kinase receptors. Other members are the human epidermal growth factor receptors: HER2 (ErbB2), HER3 (ErbB3) and HER4 (ErbB2). EGFR immunohistochemical overexpression has been described in patients with BC [8, 16]. Therefore EGFR pathway represents a potential therapeutic target in BC. Results for drugs targeting the EGFR family showed promising antitumor activity in certain preclinical models. Nevertheless, small-molecule and antibody-based inhibitors of EGFR such as lapatinib (EGFR and HER2 inhibitor) [17], erlotinib (EGFR inhibitor) [18] and cetuximab (EGFR inhibitor) [19], have demonstrated disappointing activity in the clinic for urothelial carcinoma. Attempts to combine anti-EGFR agents with chemotherapy have been unsuccessful.

Mutations of the *FGFR3* gene are prevalent in both NMIBC and MIBC. Fibroblast growth factor receptor (FGFR3) is a transmembrane RTK that transduces cellular growth signals in response to external stimuli, and is considered an oncogene in bladder cancer. Dovitinib (TK1258), a small-molecule multikinase inhibitor that targets FGFR3 kinase, was evaluated in patients with metastatic urothelial carcinoma with FGFR3 genomic alterations. In this study, treatment with dovitinib resulted in an overall response rate of 3% in patients with wild-type *FGFR3* and no response in patients with *FGFR3* mutations [20]. Potential explanations for these disappointing results are the limited efficacy of dovitinib or the inadequacy of the genomic testing used.

The availability of antiangiogenic agents and the central role that angiogenesis has in urothelial carcinoma has prompted their testing in the metastatic setting. The Vascular endothelial growth factors (*VEGF)* family of ligands that stimulate the growth of new blood vessels is important in the pathophysiology of urothelial cancer. It is often overexpressed in bladder cancer. A high level of VEGF in both serum and urine is correlated with tumor progression, a higher recurrence rate and poor survival [21]. The VEGF family binds with high affinity to three tyrosine kinase receptors (VEGFR-1, VEGFR-2, and VEGFR-3), mostly through interaction with VEGFR-2. VEGFR-2 is expressed in 50% of urothelial carcinomas, and expression is significantly higher in MIBC than in non-MIBC [22]. Various VEGF-targeting agents have been tested as monotherapy or in combination with other therapies including small-molecule inhibitors of multiple tyrosine kinase receptors, including VEGFR (sorafenib, sunitinib, pazopanib) [23, 24] and anti-VEGF monoclonal antibodies (bevacizumab) [25]. Although targeting angiogenesis is a promising strategy for BC, the results with these agents have not been encouraging. The results of the CALGB trial testing bevacizumab added to chemotherapy in first line are awaited. Ramucirumab (IMC-1121B, LY3009806), a fully humanized monoclonal antibody that blocks the binding of VEGF to VEGFR-2, has recently shown to provide limited progression free survival (PFS) benefit in second line [26].

Recently, immunotherapy has demonstrated significant antitumor effect, with superior survival benefit seen in second line when compared to chemotherapy. Immunotherapy has focused on inhibitors of immune checkpoint proteins which are molecules that impede immune function, thereby allowing tumor cells to grow and proliferate unregulated. Several checkpoint targets PD-L1 (programmed death ligand-1), PD-1 (programmed cell death protien-1), and CTLA4 (cytotoxic T-lymphocyte associated protein 4) have received the most attention in the treatment of bladder cancer as is in other tumor types. Atezolizumab and other PD-L1 inhibitors (durvalumab and avelumab) and PD-1 inhibitors (nivolumab and pembrolizumab) have positive results for BC and and have been FDA approved [27]. Nivolumab has received recent EMA approval with positive opinion received for atezolizumab and pembrolizumab.

There is a significant unmet clinical need for an effective treatment of bladder cancer. Several drugs targeting PI3K/AKT/mTOR pathway are being evaluated in preclinical studies and clinical trials. The next sections describe the key members of the pathway and specific inhibitors.

I.3. PI3K/AKT/mTOR PATHWAY

Since this pathway is frequently mutated in bladder cancer we focused our work in the study of this oncogenic pathway. The role of this pathway and the functions of the most important members are discussed in this section.

I.3.1. Overview

The PI3K/AKT/mTOR signaling pathway is one of the main pro-growth signaling pathways. When stimulated, it generally promotes cell growth, differentiation and cell division [28]. The 3 major players in the pathway are: Phosphatidylinositol 3-kinase (PI3K), AKT (a serine/threonine kinase also known as PKB), and mammalian target of rapamycin (mTOR) that exists in two functionally distinct complexes: mTORC1 and mTORC2. A detailed explanation of these proteins is included below.

As a brief summary of the mechanism of the pathway, phosphoinos itide 3kinase (PI3K is initially stimulated by the binding of ligands to receptor tyrosine kinases receptor (RTKs) or G protein- coupled receptors (GPCRs). PI3K then phosphorylates phosphatidylinositol 4,5-bisphosphate ($PtdIns(4,5)P_2$ or PIP2) to create phosphatidylinositol (3,4,5)-trisphosphate ($PtdIns(3,4,5)P_3$ or PIP3). The reverse reaction is catalized by PTEN. PIP3 generation stimulates the activation of AKT by PDK1 and mTORC2. AKT then goes on to phosphorylate certain mTOR complex 1 inhibitors, resulting in the activation of mTORC1. Specifically, AKT relieves the inhibitory effect of PRAS40 on mTORC1. AKT also phosphorylates TSC2 to inhibit the TSC1/2 complex function leading to increased association of the small G-protein Rheb with GTP. GTP-Rheb stimulates mTORC1. An activated mTORC1 can then phosphorylate downstream effectors like p70 S6 kinase (S6K) and eukaryotic initiation factor 4E-binding protein-1 (4E-BP1), ultimately causing increases in protein translation and the promotion of cell division.

A more detailed overview of the pathway is shown in **Figure I.4.**

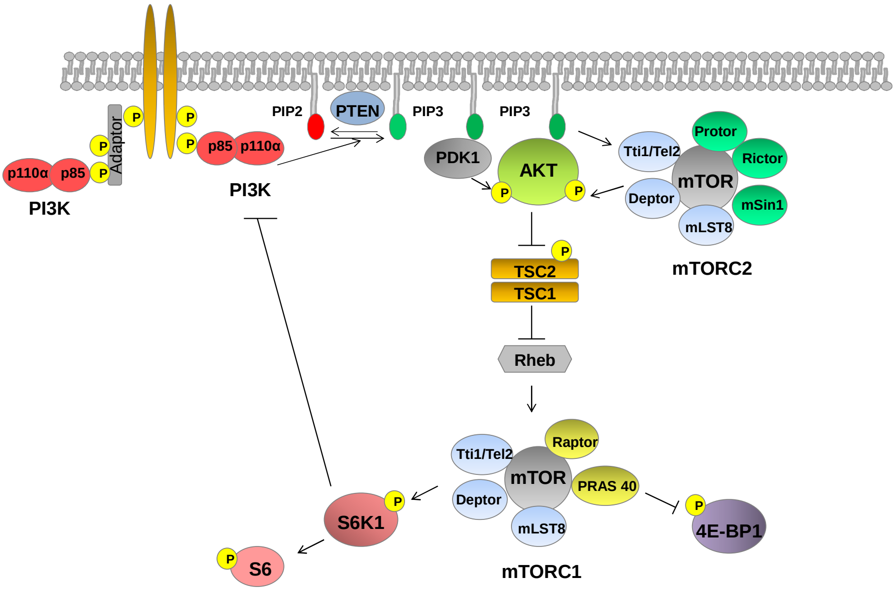
PIP2
PTEN
PIP3
PIP3
p110α
p85
P
P
Adaptor
P
P
P
p85
p110α
PI3K
PI3K
PDK1
AKT
P
P
Tti1/Tel2
Protor
Rictor
mTOR
Deptor
mSin1
mLST8
mTORC2
P
TSC2
TSC1
Rheb
Raptor
Tti1/Tel2
mTOR
PRAS 40
Deptor
mLST8
mTORC1
P
S6K1
P
S6
P
4E-BP1

Figure I.4. Overview of the PI3K/AKT/mTOR signaling pathway. PI3K activates AKT/mTOR pathway resulting in different cellular outcomes. Adapted from [29, 30].

I.3.2. Members of the PI3K/AKT/TOR pathway

The most important members of the pathway are described in detail in below.

I.3.2.1. Phosphatidylinositiol 3-kinase Lipids (PI3K)

PI3Ks (phosphatidylinositol 3-kinases) proteins are just downstream of the growth factor receptors in this signaling cascade. PI3Ks are lipid kinases that generate second messengers that govern cellular activities and properties [9].

PIK3Ks form a family that is divided into three classes (I, II and III) that differ in structure, substrate preference, tissue distribution, mechanism of activation and, ultimately, in function [9]. Only Class I PI3Ks are involved in cancer; there are no data linking Class II PI3Ks or Class III PI3K (Vsp34p) to oncogenesis.

There are two subgroups within the class I PI3Ks: class IA and class IB. Both classes are heterodimeric enzymes consisting of a catalytic and a regulatory subunit, and their major function is to convert phosphatidylinositol-4-5-biphosphate (PIP2) into PIP3 by phosphorylating PIP2 [31].

Class IA PI3K is composed of a heterodimer between a p110 catalytic subunit and a p85 regulatory subunit. The members of this class contain one of three possible variants of the p110 catalytic subunit (designated p110α, p110β, p110δ subunit) and one of five variants of the p85 regulatory subunit (designated p85α, p55α, p50α, p85β and p55γ). The catalytic subunits are encoded by the separate genes: *PI3KCA*, *PIK3CB* and *PIK3CD* for p110α, p110β and p110δ, respectively. The first p110α and p110β isoforms are expressed in all cells, but p110δ is expressed primarily in leukocytes. On the other hand, the p85α, p55α, p50α regulatory subunits are all splice variants of the same gene PIK3R1, the other two being expressed by other genes (*PIK3R2* and *PIK3R3*, p85β, and p55γ, respectively).

In contrast, the class IB PI3Ks are much simpler; there is only on catalytic subunit, p110γ (encoded by PIK3CG and only expressed i n a limited subset of tissues) and two possible regulatory subunits, p101 and p84 (encoded by PIK3R5and PIK3R6 respectively) [31, 32]. The classification of PI3K is shown in the **Figure I.5.**

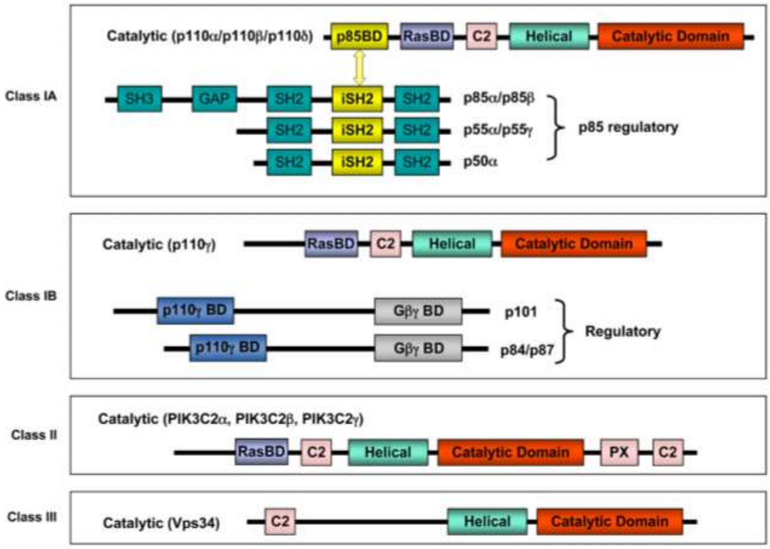
Class IA
Catalytic (p110α/p110β/p110δ)
p85BD
RasBD
C2
Helical
Catalytic Domain
SH3
GAP
SH2
iSH2
SH2
p85α/p85β
p55α/p55γ
p50α
p85 regulatory
Class IB
Catalytic (p110γ)
p110γ BD
Gβγ BD
p101
p84/p87
Regulatory
Class II
Catalytic (PIK3C2α, PIK3C2β, PIK3C2γ)
PX
Class III
Catalytic (Vps34)

Figure I.5. The members of the PI3K family. PI3K have been divided into three classes according their structural characteristics and substrate specificity [32].

The catalytic subunits of Class I PI3K share a common structure composed of an N-terminal adaptor binding domain (ABD), a Ras binding domain (RBD), a C2 (protein kinase C homology 2) domain, a helical domain, and a C-terminal lipid kinase domain [9]. The full length of p85 regulatory subunits contain a SH3 domain, a BH domain sandwiched between two proline-rich regions, two SH2 domains, nSH2 and cSH2 separated by an intervening coiled-coiled domain (iSH2) [9].

Each of these PI3K classes is associated with a particular class of receptors; class IA PI3Ks are associated with RTKs, and class IB PI3Ks are associated with GPRCRs [31-33]. GPCRs can activate PI3K/AKT/mTOR signalling directly, through Gβγ subunits, or indirectly by transactivating RTKs [34].

One of the class I PI3Ks (PI3Kα, PI3Kβ, PI3Kδ and PI3Kγ), PI3Kα, is frequently mutated in diverse tumor types.

The most important PI3K proteins implicated in tumorigenesis and proliferation are the PI3Kα proteins (with the catalytic subunit p110α and the regulatory subunit p85) [9, 10, 35].

The PI3Kα proteins are regulated by RTK (receptor tyrosine kinases) and RAS. In the first case, RTKs are transmembrane proteins that, upon ligand binding, phosphorylate tyrosine residues located either on the protein itself or on an adapter protein. When those specific tyrosines are phosphorylated, they are then able to recruit SH2 domain containing molecules [31]. Such molecules include the regulatory domains of class IA PI3Ks. This recruitment of PI3Ks to the membrane by RTKs initiates PI3K/AKT/mTOR signaling.

PI3K is recruited to the membrane via interaction of its p85 subunit to tyrosine phosphate motifs on activated receptors directly (e.g. PDGFR) or to adaptor proteins associated with the receptors (e.g. insulin receptor substrate 1, IRS-1). The binding of p85 to receptor tyrosine kinases or their adaptor proteins activates p110α. The high-affinity substrate of p110α is PIP2 (phosphatidylinositol 4,5-bisphosphate). This is phosphorylated by the PI3K to become PIP3 (Phosphatidylinositol (3,4,5)-trisphosphate (PtdIns(3,4,5)P_3), abbreviated PIP3). The activated p110 catalytic subunit generates phosphatidylinositol-3,4,5-trisphosphate, PI(3,4,5)P_3, which in turn activates multiple downstream signaling pathways which activates multiple downstream signaling proteins, among them PDK1 and AKT [9].The phospholipid PI(3,4,5)P_3 generated by activated class I PI3Ks is the key second messenger that drives multiple downstream signaling cascades regulating cellular processes. PIP3 acts recruiting a number of proteins that contain PIP3 binding domains to the membrane. These proteins are recruited via the pleckstrin homology (PH) domain, a structurally conserved area of around 100 amino acids which bind inositol lipids with high affinity.

Another method by which RTKs might activate PI3K involves the protein RAS. GTP bound RAS is produced as a result of the activation of several different RTKs, and it appears to be able to bind and possibly activate the p110 catalytic subunit of class IA PI3Ks. In addition, PI3K can be activated by the interaction between p110α and the RAS protein [9].

PTEN

The cellular level of the key second messenger PI(3,4,5)P_3 is tightly regulated by the opposing activity of PTEN (Tensin homologue deleted on chromosome ten). PTEN, an important tumor suppressor, functionally antagonizes PI3K activity via its intrinsic lipid phosphatase activity that reduces the cellular pool of PIP_3 by converting PI(3,4,5)P_3 back to PI(4,5)P_2. By doing so, PTEN reduces the activation of AKT and prevents all of the downstream signaling events that are controlled by AKT. Loss of PTEN will result in unrestrained signaling by the PI3K pathway leading to cancer.

PDK1 (3-phosphoinositide dependent kinase 1) and AKT belong to the AGC family and have a PH domain with affinity for the PIP3. Binding of both proteins to PIP3 has the dual function to promote the physical contact between the two kinases and facilitate the phosphorylation of AKT on Thr308 by PDK1 [36].

I.3.2.2. AKT

The serine/threonine kinase AKT, also known as protein kinase B (PKB), exists as three isoforms in mammalian cells AKT1 (PKBα), AKT2 (PKBβ) and AKT3 (PKBγ) encoded by three separate genes. AKT1 is the most commonly expressed isoform in normal cells. AKT resides in the cytosol in an inactive conformation, until the cell is stimulated and it translocates to the plasma membrane. The three AKT isoforms are well characterized as downstream effectors of PI3K signalling and they all contain an N-terminal PIP3-binding PH (pleckstrin-homology) domain. PIP3 generated by PI3K as a lipid second messenger and recruit AKT and phosphatidylinositide-dependent protein kinase 1 (PDK1) to the plasma membrane, through their PH domains.

Through its PIP3 binding PH domains AKT, binds the PIP3 generated by an activated PI3K. The generation of PIP3 colocalises PDK1 and AKT kinases at the plasma membrane AKT is then phosphorylated and activated at Thr308 in the activation loop by PDK1 and at Ser473 in the carboxy-terminus by mTORC2. Ser473 phosphorylation is required for maximum activation of protein and stabilizes Thr308 phosphorylation despite not to be essential for the activation of AKT. Then, AKT moves from the cell membrane to the cytoplasm and the nucleus, and phosphorylates (on serine and threonine residues) a number of downstream targets.

More than 100 proteins were reported in the literature as direct targets of AKT and consequently AKT has been implicated in a number of cellular processes. The best characterized substrates of

AKT are summarized in **Figure I.6.**, including protein and lipid kinases, transcription factors, regulators of small G proteins and vesicle trafficking, metabolic enzymes, E3 ubiquitin ligases, cell cycle regulators, and many others) [37, 38]. Among them TSC2 is important in the regulation of mTORC1 (as discussed below).

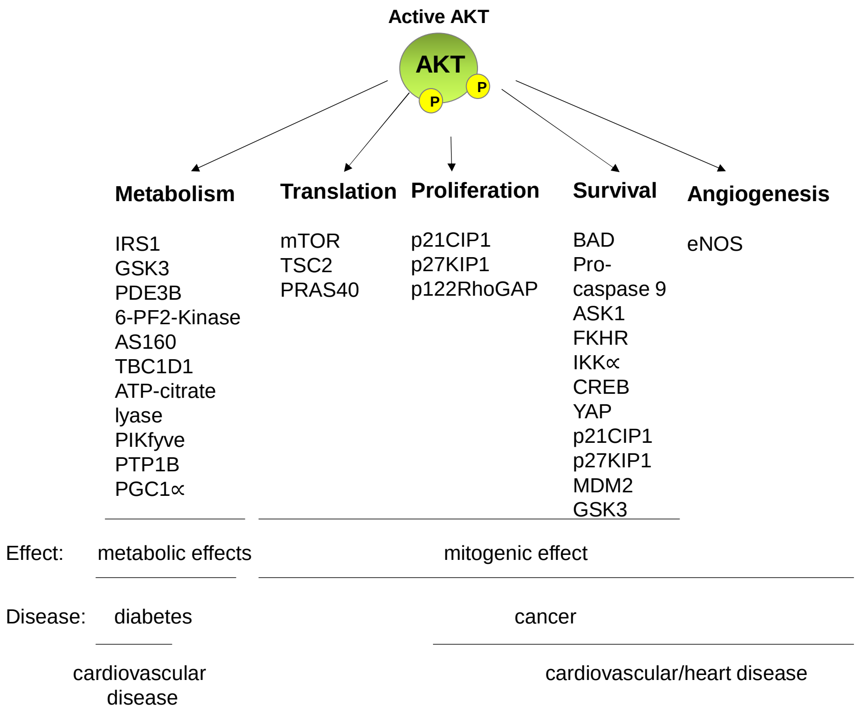
Active AKT
AKT
P
P
Metabolism
IRS1
GSK3
PDE3B
6-PF2-Kinase
AS160
TBC1D1
ATP-citrate lyase
PIKfyve
PTP1B
PGC1∝
Translation
mTOR
TSC2
PRAS40
Proliferation
p21CIP1
p27KIP1
p122RhoGAP
Survival
BAD
Pro-caspase 9
ASK1
FKHR
IKK∝
CREB
YAP
p21CIP1
p27KIP1
MDM2
GSK3
Angiogenesis
eNOS
Effect:
metabolic effects
mitogenic effect
Disease:
diabetes
cancer
cardiovascular disease
cardiovascular/heart disease

Figure I.6. Best characterized AKT substrates. Only the most extensively characterized cancer relevant substrates are presented here [39].

I.3.2.3. Rheb protein and TSC1/TSC2 complex

There are two links between AKT and mTORC1: Rheb (Ras-homolog enriched in brain), and its negative regulator, the tuberous sclerosis complex (TSC) complex composed of the TSC tumor suppressors, TSC1 and TSC2. Regulation of a switch involving AKT, the TSC complex, and Rheb, is the primary mechanism through which PI3K signaling activates mTORC1.

Rheb activates mTORC1 kinase activity. Rheb is a ~21 kDa small GTPase and a member of the Ras superfamily. The activity of Rheb is regulated by a GTP-GDP cycle. Rheb is active when GTP is bound, and this induces a conformational change that permits interaction with downstream effectors. But Rheb becomes inactive following hydrolysis of the bound GTP to GDP. GTPase-activating protein (GAP) accelerates the rate of GTP hydrolysis of GTPase (**Figure I.7.**).

The tuberous sclerosis (TSC1/TSC2) complex, formed by the tuberous sclerosis complex 1 and 2 (TSC1/2) proteins is an inhibitor of mTORC1 signaling through its GAP activity towards Rheb (Rheb-GAP activity).

TSC1/TSC2 complex

TSC1/TSC2 complex is an heterodimer consisting of two proteins, tuberous sclerosis 1, TSC1 (also known as hamartin) and tuberous sclerosis 2, TSC2 (also known as tuberin) which are encoded by the tumor suppressor genes *tsc1* and *tsc2* respectively [28, 40].

TSC1/TSC2 heterodimer represses mTOR activity. This complex functions as a GAP for the Rheb protein which activates the kinase activity of mTORC1. TSC2 contains the GAP domain that stimulates stimulates Rheb GTP hydrolytic activity and hence the conversion of Rheb-GTP into Rheb-GDP (**Figure I.7.**). TSC1 is required to stabilize TSC2 and protect of its ubiquitin-mediated degradation. TSC2 is inactivated by AKT-dependent phosphorylation in multiple residues which destabilizes the complex and inhibits the function of this complex [41, 42].

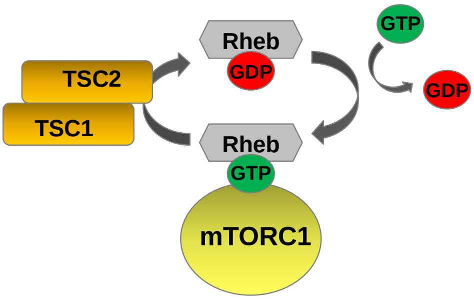

Figure I.7. Regulation of mTORC1 by TSC1-TSC2 and Rheb. When TSC1-TSC2 complex is activated functions as a GAP domain which stimulates the hydrolysis of Rheb-GTP to Rheb-GDP inhibiting the activity of Rheb. However, when AKT phosphorylates TSC2 inhibits the TSC complex and mTORC1 is activated through Rheb-GTP.

I.3.2.4. mTORC1 and mTORC2 complex

Mammalian target of rapamaycin (mTOR) is a serine-threonine kinase that belongs to the PIKKs (phosphatidylionsitol 3-kinase-like kinases). mTOR is an ubiquitous protein that is mainly localized into cytoplasm and controls cellular growth in a nutrient and amino acid sensitive manner.

mTOR interacts with several proteins to form two distinct complexes, mTOR complex 1 (mTORC1) and mTOR complex 2 (mTORC2) that have shared and unique components (**Figure I.8.**). . Both complex have distinct functions and are activated in response to different stimuli. In addition they have different sensitivities to rapamycin [28].

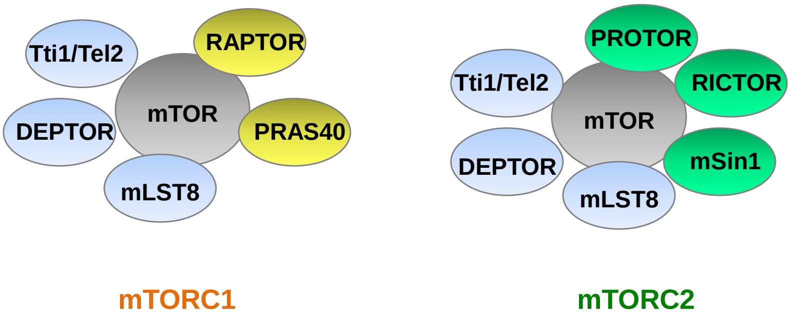

mTORC1

mTORC2

Figure I.8. Structure of the mTORC1 and mTORC2 complexes. Both complexes have shared (mTOR, mLST8, Deptor, and Ttil/Tel2) and unique domains (mTORC1 is composed of RAPTOR and PRAS40 and mTORC2 is composed of RICTOR, PROTOR and mSin1).

The mTORC1 and mTORC2 complexes both contain mTOR, mammalian lethal with Sec13 protein 8 (mLST8 also known as GβL) and DEP domain-containing mTOR-interacting protein (DEPTOR) and the Tti1/Tel2 complex. mTORC1 is composed also of the following members: Regulatory-associated protein of mTOR (RAPTOR) and 40 kDa Proline-rich AKT substrate (PRAS40). On the other hand, Rapamycin-insensitive companion of mTOR (RICTOR), mammalian stress-activated map kinase interacting protein 1 (mSIN1; also known as MAPKAP1) are specific to mTORC2.

mTOR

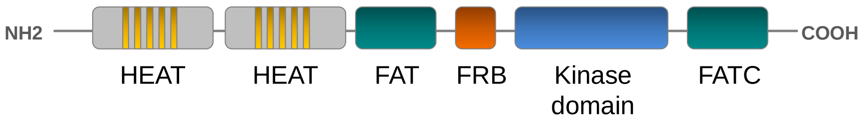

Figure I.9. Structural domains of the mTOR protein. Schematic representation of the protein showing functional domains. Adapted from [43].

mTOR contains multiple domains, which are required for a large functional complex formation (**Figure I.9.**). The N-terminal portion contains up to 20 tandemly repeated HEAT motifs (Huntingtin, Elongation Factor 3, Alpha-regulatory subunit of protein phosphatase 2A and TOR1) that serve to mediate protein-protein interactions: Raptor (in mTORC1) and Rictor (in mTORC2) binds to these HEAT repeats within mTOR to form the complex. These HEAT repeats are followed by a FAT (FRAP-ATM-TRRAP) domain that is made up of around 500 residues with unclear function. Adjacent to the FAT domain lies an area known as the FKBP12–rapamycin binding (FRB) domain. Rapamycin binds with the FKBP12 (FK509-binding protein) and this complex interacts with the FRB domain. Other members including Rheb and one of the mTORC1 components, raptor, also interact with FRB. The C-terminal portion of mTOR contains the Ser/Thr kinase catalytic domain (KIN). Within the KIN domain is a region, NRD, which contains serine and threonine residues that are phosphorylated (Thr2246, Ser2448 and Thr2246) and involved in the regulation of mTOR activity [44]. The C-terminus also contains a FATC (FRAP-ATM-TRRAP C-terminal) domain that is paired with the upstream

FAT domain to modulate mTOR kinase activity in an unknown manner.

mTORC1 and mTORC2 complexes

Regarding the other common members of both mTOR complexes, mLST8 is highly conserved; its seven WD40 domains form a b-propeller that mediates protein-protein interactions. The function of mLST8 is unknown and not affect mTORC1 activity, however is essential for mTORC2 activity. DEPTOR consists of tandem DEP domains (Dishevelled, EGL-10 and pleckstrin domains) that are followed by a single PDZ domain (postsynaptic density of 95 kDa, Discs large and zonula occludens 1 domain). DEPTOR acts as mTOR inhibitor.Tti1/Tel2 complex are scaffold proteins regulating the assembly and the stability of mTORC1 and mTORC2 [28].

Regarding the specific proteins for mTORC1, RAPTOR has a scaffolding function reflected by its composition of protein-binding domains; it consist of several HEAT repeats, followed by seven WD40 domains, which are probably arranged in a □-propeller. RAPTOR present substrates to mTORC1. Raptor binds to the TOS (TOR signaling) motifs present in mTOR downstream proteins (such as the S6Ks, 4EBPs, and STAT3) [45] and carries them to the mTOR catalytic domain. In addition, Raptor competes with rapamycin for the binding to the FRB domain [28, 44]. PRAS40 as well as DEPTOR are inhibitors of mTORC1. PRAS40 regulates the interaction between mTOR and Raptor, and negatively regulates mTOR signalling by blocking mTORC1 access to its substrates. When mTORC1 is activated, it is able to directly phosphorylate and reduce PRAS40 and DEPTOR function. PRAS40 has a conserved

Leu charged domain (LCD), at which phosphorylation by AKT occurs.

Regarding the specific proteins of mTORC2: mSin1 contains a Ras binding domain (RBD), an a pleckstrin homology (PH) domain that is likely to interact with phospholipids. mSin1 is a scaffold protein that controls the assembly of the complex and the interaction of an mTOR downstream protein, SGK1.

PROTOR 1/2 increases mTORC2 mediated-activation of SGK1 [28]. RICTOR is a scaffold protein that regulates the assembly, localization and substrate binding of mTORC2. PROTOR and RICTOR have no clearly identificable domains or motifs.

mTORC1 is involved in the control of different cellular processes (lipid synthesis, lysosome biogenesis, energy metabolism and autophagy), the best-characterized process is the regulation of protein synthesis through 4E-BP1 and S6K1.

Compared to mTORC1, much less is known about the mTORC2 pathway. mTORC2 signaling is sensitive to growth factors and controls metabolism, cell survival and cytoskeletal organization [28].

I.3.2.5. mTORC1 Substrates: 4E-BP1 and S6K1

Eukaryotic initiation factor 4E-binding protein 1 (4E BP1) and the the p70 S6 kinase 1 (S6K1) are the best-characterized substrates of mTORC1 kinase activity that mediate the role of mTORC1 in many of its cell biological functions including cap dependent translation, cell growth, and cell cycle progression. Thus, this section will focus on mTORC1 substrates, S6K1 and 4E-BP1. Other mTORC1 substrates are ULK1/2, Atg13, and HIF1α and will be discussed under “I.3.3.2. mTOR signaling” section.

I.3.2.5.1. 4E-BP1

4E-BP1 belongs to a family of eIF4E-binding proteins divided into three members (4E-BP1, 4E-BP2 and 4E-BP3) encoded by three different genes.

The active form of the protein is the hypophosphorylated and acts as a translation repressor protein inhibiting the cap-dependent translation by binding eIF4E (eukaryotic translation initiation factor 4E).

4E-BP1 is phosphorylated at multiple sites (Thr37, Thr46, Ser65, Thr70, Ser83, Ser101 and Ser 112). The first four sites are linked to mTORC1 kinase activity. Phosphorylation of Thr37 and Thr46 are thought to be the priming event for subsequent phosphorylation of the Thr70 and Ser65 sites [46]. Phosphorylation of 4E-BP1 causes it to dissociate from eukaryotic initiation factors 4E (eIF4E). Without phosphorylation 4E-BP1 is bound to eIF4E, inhibiting the translational initiation activity eIF4E. eIF4E binds and recognises the cap, which contains a 7-methyl guanosine moiety, at the 5’ end of mRNA and mediates transcription of the mRNA. (one member of the eIFs family involved in the control of mRNA translation).

eIF4E is a member of the eIF4F complex (eukaryotic initiation factor 4F) which recruits ribosomes to the mRNA. eIF4F is composed of two more initiation factors (eIF4A and eIF4G). The association of the eIF4F complex on the mRNA 5’ cap structure (m7GTP) is required for the binding of the 40S small ribosomal subunit to the mRNA. Other initiation factors, also participate in this process.

The hyperphosphorylated 4E-BP1 dissociates from eIF4E, allowing the factor to bind to eIF4F complex, as a consequence the overall protein synthesis is increased [47, 48] (**Figure I.10.**).

I.3.2.5.2. S6K1 and the ribosomal protein S6

S6 kinases (S6Ks) are serine/threonine protein kinases of the AGC kinases super-family There are two members with similar functions, S6K1 and S6K2, being the S6K1 the most well characterized [49, 50]. S6K1 has cytosolic and nuclear isoforms (p70-S6K1 and p85-S6K1, respectively) [51].

Activation of S6K1 is controlled by multiple phosphorylation, at least eight threonine and serine sites have been reported. mTORC1 phosphorylates the Thr389 residue, followed by phosphorylation of the Thr229 residue by PDK1 [49, 50].

S6K is implicated in the control of cell growth via increasing mRNA translation. S6K promotes the translation of 5’TOP mRNAs, which contain a short polypyrimidine tract immediately adjacent to the 5’ cap. These mRNAs encode for components of the translation machinery. The effects of S6K on mRNA translation are indirect via its downstream effectors. S6Ks have several substrates being the ribosomal protein S6 the main target. Other targets of S6K1, such as eIF4B, have effects on translation and cell growth [52]. (**Figure I.10.**)

Ribosomal protein S6 (rpS6) is a component of the 40S ribosomal subunit and therefore is involved in protein translation. Also regulates cell size, cell-cycle and glucose homeostasis.

S6 has five sites of phosphorylation located within a small, c-terminal region of the protein. rpS6 is phosphorylated in sequential order beginning with the Ser236 and followed by Ser235, Ser240, Ser244 and Ser247. S6 phosphorylation is a good marker of the S6K activity [51, 52].

Phosphorylation of rpS6 increases the affinity of ribosomes for TOP mRNAs and thus facilitates the translation initiation of this class of mRNAs [51].

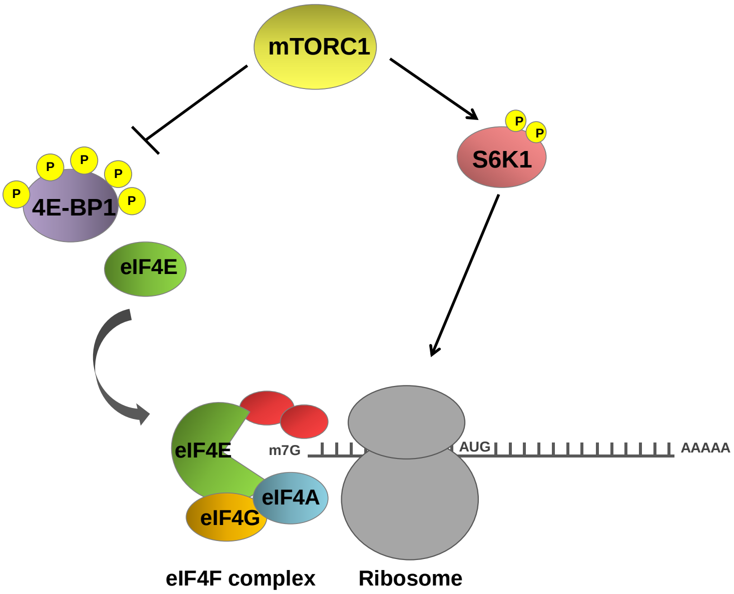
mTORC1
P
P
S6K1
P
P
P
P
P
4E-BP1
eIF4E
eIF4E
m7G
AUG
AAAAA
eIF4A
eIF4G
eIF4F complex
Ribosome

Figure I.10. Cap dependent translation by 4E-BP1 and S6. Activation of mTORC1 induces the dissociation of 4E-BP1 from eIF4E and the binding of the factor to the eIF4F complex and the following binding to the mRNA. Also mTORC1 activates S6K1 which promotes protein translation via its substrates.

I.3.3. PI3K/AKT/mTOR signalling

PI3K/AKT/mTOR pathway is involved in the control of many major cellular functions such as metabolism, cell growth, proliferation, migration, angiogenesis, survival, autophagy and lysosome biogenesis. Given its central role, it is not surprising that it is one of the most frequently deregulated pathways in cancer. PI3K and their downstream mediators AKT and mTOR constitute the key components of the pathway.

Several growth factors and nutrients can initiate the process activating PI3K. These molecules activate RTK leading to autophosphorilation and binding to PI3K in this site. However, in some cases, RTK mediates the recruitment of an adaptor protein necessary to bind RTK to PI3K. Then, PI3K mediates the transmission of the extracellular signal to the interior of the cell. The RTK can also activate PI3K through the engagement of Ras to RBD of the PI3K [53].

I.3.3.1. AKT signalling

AKT is the main effector of PI3K. Multiple substrates of AKT have been identified involved in the regulation of survival, cell cycle and cell growth [54, 55] (**Figure I.11.**).

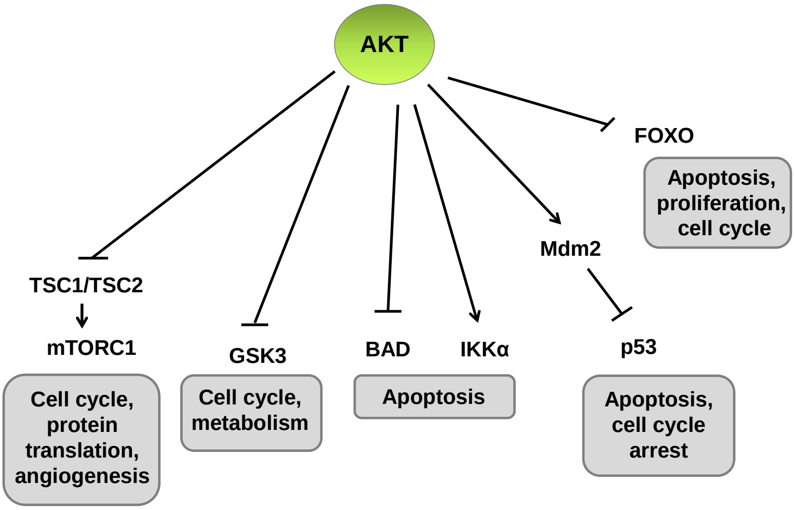
AKT
FOXO
Apoptosis, proliferation, cell cycle
Mdm2
TSC1/TSC2
mTORC1
GSK3
BAD
IKKα
p53
Cell cycle, protein translation, angiogenesis
Cell cycle, metabolism
Apoptosis
Apoptosis, cell cycle arrest

Figure I.11. AKT signaling. The main substrates of AKT involved in the regulation of cell cycle progression, protein translation, angiogenesis, metabolism, apoptosis and survival are shown. Adapted from [54-56].

AKT is implicated in cell survival since regulate apoptosis, the process of programmed cell death controlled by multiple factors. AKT phosphorylates and inactivates the pro-apoptotic factor BAD and the FOXO transcription factors, which are involved in the expression of pro-apoptotic genes and gens that regulate cell cycle [57]. Also is thought that AKT phosphorylates and regulates MDM2 (Mouse double minute 2 homolog) function in response to survival signals. MDM2 is an E3 ubiquitin ligase which mediates ubiquitination and proteasome-dependent degradation of the p53 tumor suppressor protein [58]. The role of AKT in cell cycle progression is in part by phosphorylating and inhibiting the GSK3β protein, which mediates cyclin D1 protein degradation. In addition, AKT can phosphorylate the cell cycle inhibitors $p21^{WAF1}$ and $p27^{Kip1}$ and impeding the function in the nucleous [38, 59]. AKT regulates cell growth activating mTORC1 mainly through TSC2 and PRAS40.

I.3.3.2. mTOR signalling

The mTORC1 pathway integrates inputs from at least five major intracellular and extracellular cues (growth factors, stress, energy status, oxygen, and amino acids). Activated mTORC1 promotes macromolecule biosynthesis, cell cycle progression and cell growth whereas inhibits autophagy and lysosome biogenesis. mTORC2 regulates cell survival, cytoskeletal organization and metabolism [28] (**Figure I.12.**).

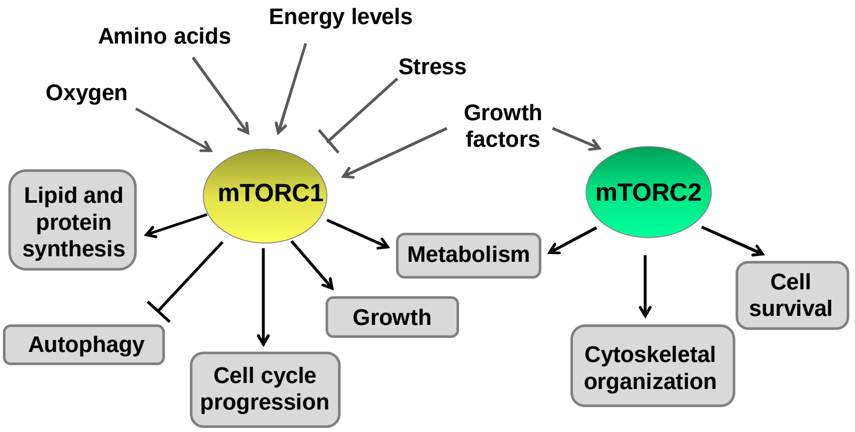
Energy levels
Amino acids
Stress
Oxygen
Growth factors
mTORC1
mTORC2
Lipid and protein synthesis
Metabolism
Cell survival
Growth
Autophagy
Cell cycle progression
Cytoskeletal organization

Figure I.12. mTOR signaling. mTORC1 responds to amino acids, stress, oxygen, energy and growth factors. It promotes cell growth and cell cycle progression and also affects autophagy, metabolism and lipid and protein synthesis. mTORC2 responds to growth factors and regulates cell survival, metabolism and cytoskeletal organization. Adapted from [28].

Protein synthesis is the best-characterized process controlled by mTORC1. Direct downstream effectors of mTORC1 are 4E-BP1 and S6K1 which promote protein synthesis and regulate cell growth and cell cycle progression. It is speculated that 4E-BP1 regulate cell cycle progression while S6Ks play a crucial role in cell growth [48]. mTORC1/4E-BP1 axis may contribute to cancer by promoting the translation of mRNAs coding for proteins regulating cell cycle progression (cyclin D1, cyclin dependent kinases (CDK1 and CDK2)), cell survival (Bcl-2, survivin), energy metabolism and angiogenesis (VEGF) [28].

mTORC1 is emerging as a key regulator of genic transcription. It regulates several transcription factors such as SREBPs (Sterol-Regulatory-Element-Binding), HIFα (Hypoxia Inducible Factor 1) and TFEB (Transcription Factor EB) which are mainly implicated in metabolic pathways. mTORC1 controls the synthesis of lipids, required for the generation of the membranes of the proliferating cells, by controlling SREBP. Under hypoxic conditions, mTORC1 induces the expression of HIFα, a transcription factor which regulates glycolytic genes and also promotes VEGF expression which promotes angiogenesis. mTORC1 negatively regulates the biogenesis of lysosomes through TFEB, a transcription factor involved in the expression of many lysosomal genes [28, 60].

Active mTORC1 inhibits autophagy, the process of degradation of cellular organelles and proteins, that is critical for maintain the cellular homeostasis. Autophagy is initiated with the formation of double-membrane vesicles, known as autophagosomes that internalize cytoplasmic components. Then, the autophagosomes fuse with the lysosomes leading to the degradation of the sequestered contents and the recycling of cellular components. mTORC1 phosphorylates Atg13 and inhibits the formation of the ULK complex (ULK1/2–Atg13–FIP200) that is responsible of initiate autophagy [61]. Constitutive activation of PI3K-mTORC1 signaling strongly inhibits autophagy [28].

Compared to mTORC1, much less is known about the mTORC2 pathway. mTORC2 signaling is sensitive to growth factors and controls metabolism, cell survival and cytoskeletal organization. There are three main substrates of mTORC2: AKT, SGK1 (serum- and glucocorticoid-induced protein kinase 1) and PKC-α (protein kinase C- α). Like AKT, SGK1 contributes to the phosphorylation and inactivation of the FOXO transcription factors. The mTORC2 complex in turn constitutes an important regulator of the cytoskeleton through the activation of PKC-α and other proteins (RhoA, Rac1 and Paxilin).

I.4. PHARMACOLOGICAL TARGETING OF THE PI3K/AKT/mTOR PATHWAY

I.4.1. Overview

PI3K/AKT/mTOR pathway represents an attractive target for cancer therapeutics since it is frequently activated and deregulated in cancer. A large number of therapeutic agents targeting members of the PI3K-AKT-mTOR axis have been developed and evaluated in preclinical studies as well as in clinical trials.

These drugs are small molecule inhibitors targeting key nodes in the pathway including: dual PI3K/mTOR inhibitors, Pan-PI3K inhibitors, isoform-specific PI3K inhibitors, AKT inhibitors, and mTOR inhibitors (mTORC1 inhibitors and mTORC1/2 inhibitors) [29, 62]. Yet currently, the only FDA-approved PI3K pathway inhibitors target a single node of this pathway, the mammalian target of rapamycin (mTOR).

The First-Generation PI3K Pathway- Targeting Agents were a naturally occurring PI3K inhibitor, wortmannin, and a morpholine derivative of quercetin, LY294002. These compounds were instrumental in defining the biological role of PI3K, but they demonstrated poor pharmacokinetics and thus had limited therapeutic potential.

The first inhibitors of the pathway to enter the clinic were those targeting the downstream effector mTOR. Rapamycin (sirolimus) is a naturally occurring compound isolated from the soil bacterium *Streptomyces hydroscopius*, a potent inhibitor of mTORC1. Limitations in the solubility and pharmacokinetic properties of rapamycin led to development of rapamycin analogues with improved characteristics, including temsirolimus and everolimus.

Randomized phase III trials confirmed efficacy of these agents and led to their FDA approval for a range of oncology indications. Currently, only the rapalog inhibitors of the PI3K-AKT-mTOR pathway have entered the clinic for the treatment of renal cell, neuroendocrine, and breast cancers.. Clinical benefit has been observed with rapalogues but they showed activity only in limited number of solid tumor types. They have certain limitations that make them less effective than expected. Limited activity of the rapalogues is suggested to result from various regulatory feedback loops which activate PI3K-AKT signalling upon mTOR inhibition [63]. This can seriously undermine the efficacy of mTOR inhibitors, and nearly all patients treated with these agents eventually relapse.

This factled to development upstream inhibitors, which could overcome hyperactivation and potentially have more clinical activity. Therefore, other drugs have been developed with the aim to improve rapalogues.Multiple clinical trials are underway to test efficiency of dual PI3K/mTOR, PI3K, mTORC1/2 inhibitors, and AKT inhibitors in various solid malignancies.

Due to the multitude of drugs targeting the pathway, drug investigation is full of challenges. Some of them are to select the optimal drug in each context, to establish possible synergies between drugs, to establish the doses that can be tolerated, to define biomarkers of resistance or sensitivity to the drugs, and to overcome drug resistance.

Bladder cancer is a disease for which PI3K/mTOR targeted therapy is still in early stages. Clinical trials of mTORC1 inhibitors in patients with bladder cancer have been initiated in recent years.This PHD work has been performed with a mTORC1/2 inhibitor and few experiments with a specific PI3K inhibitor and mTORC1 inhibitor. The work focuses on the characterization of their mechanism of action and predictive biomarkers for efficacy.

Because of the grata number of such drugs in development the introduction sections has been mainly dedicated to the description of such kind of drugs.

On the basis of these considerations, we will only briefly describe the other kind of inhibitors that are not the focus of this PHD Thesis

Dual PI3K-mTOR inhibitors

To target the PI3K/AKT/mTOR pathway both up- and down-stream, small molecules able to concomitantly inhibit not only all class I PI3K isoforms but also mTORC1 and mTORC2 were synthesized. These drugs have dual activity against PI3K and mTOR, which is due to the fact that their catalytic domains are structurally similar thus having a strongest effectiveness in switching off the PI3K signaling pathway [30]. Dual PI3K-mTOR inhibitors disable both inputs to AKT: PI3KPDK1 and mTORC2, and may bypass feedback loops.

An example of dual PI3K-mTOR inhibitors is NVP-BEZ235. The pan-PI3K/mTOR inhibitor, NVP-BEZ235 (hereafter BEZ235) NVP-BEZ235 has been shown to reversibly block the p110α catalytic subunit of PI3K and mTOR [64]. Treatment with NVP-BEZ125 has resulted in a significant decrease in phosphorylation levels of mTORC1 and mTORC2 substrates (S6K1, 4E-BP1, and AKT), and higher antiproliferative effect than everolimus in BT474 breast cancer cells and in xenografts derived from them [65]. However, this broad inhibition can also be toxic to normal cells [66].

AKT kinase inhibitors

Inhibitors of AKT, are beginning to progress through clinical development. There are three isoforms of AKT (AKT1, 2, and 3) and thus far only pan-AKT inhibitors have been developed. Due to the structural similarities between the three isoforms, producing isoform-specific inhibitors has proved challenging. Several sites on the AKT protein provide important regions that are suitable for binding small molecule inhibitors. Thus ATP inhibitors are either ATP competitive inhibitors, allosteric inhibitors, inhibitors of PIP_3 and substrate-competitive inhibitors [39, 55]. The most promising inhibitors are the allosteric and the ATP competitive inhibitors. The allosteric inhibitor MK-2206 and the ATP-competitive inhibitors AZD5363, GSK2110183 and GSK21411795 have shown preliminary activity in phase I clinical trials, and are being tested in a range of solid tumors. However, as AKT regulates several important cellular processes potential toxicities should be monitored during clinical trials [67].

I.4.1.1. mTORC1 inhibitors

The first generation of mTOR inhibitors are derivatives of rapamycin – “rapalogues” that specifically inhibit the mTORC1 complex, examples include RAD001 (everolimus), CCI- 779 (temsirolimus) and ridaforolimus [68].

Rapamycin (also known as sirolimus) is a macrolide antibiotic produced by the bacteria *Streptomyces hygroscopicus*. Rapamycin was discovered during the 1970’s in a soil sample from Easter Island and it was originally developed by as an anti-fungal. Later it was discovered its potential immunosuppressive activity leading to the approval of rapamycin in 1997 as an anti-rejection agent. Rapamycin is approved as an immunosuppressant drug following transplantation. Moreover studies at the NCI also observed rapamycin anti-tumor activity within both in vivo and in vitro studies.

Rapamycin was the first identified mTOR inhibitor. Precisely, rapamycin is a highly selective allosteric inhibitor of mTORC1. The mechanism of action of rapamycin involves its interaction with an intracellular receptor protein, the immunophilin FK506-binding protein (FKBP12). The resulting rapamycin/FKBP12 complex then targets mTOR via the FKBP12 rapamycin binding (FRB) domain adjacent to the catalytic site of the mTORC protein and inhibiting its activity [69]. The mechanism by which rapamycin inhibits mTORC1 catalytic activity is unclear, the rapamycin-FKBP12 complex has been proposed to act as a physical obstruction between the mTOR catalytic domain and its substrates. The formation of this complex also appears to destabilise the interaction between mTOR and raptor, despite raptor binding further than 1000 residues away from the FRB domain (**Figure I.13.**). The resulting loss of the mTOR raptor complex may contribute to the loss of mTOR catalytic activity as the mTOR/RAPTOR complex is required for catalytic activity.

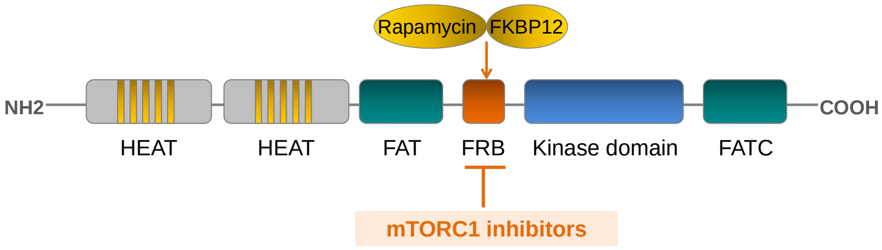

Figure I.13. mTORC1 inhibitors interaction with the FRB domain of the mTOR protein. Rapamycin/FKBP12 complex binds to FRB domain adjacent to the catalytic site of the mTOR protein and inhibits its activity.

Rapamycin is a highly selective molecule, inhibiting only one of the two mTOR complexes, mTORC1. A number of studies have shown that mTORC2 is rapamycin insensitive. However, it has also been shown that long-term exposure to rapamycin can also inhibit mTORC2 and that it is tissue specific [29]

Rapamycin is given via oral administration; it has rapid absorption with peak concentration reached at 2h. However, bioavailability of rapamycin is low (only around 15 %) and can vary greatly between patients. Intestinal CYP450 3A enzymes and P-glycoproteins can influence absorption of rapamycin [70].

A series of semisynthetic derivatives of rapamycin, known as rapalogues have been developed to improve the pharmacokinetics and pharmacodynamics properties of rapamycin. All rapalogues are very structurally similar to rapamycin and act via the same mode of action as rapamycin. Four ‘rapalogues’ have so far been developed: Everolimus (RAD001 from Novartis), Temsirolimus (or CCI-779 from Wyeth), Deforolimus (or Ridaforolimus) (AP23573 from Ariad) and Zotarolimus (ABT-578 from Abbott).

At a cellular level, rapalogues have many effects useful for the treatment of cancer. Inhibition of mTORC1 leads to the decrease of protein translation, cellular growth and cell cycle arrest, usually in G1 phase. Rapalogues also induce autophagy in some cancer cells. Despite not to be the main mechanism of action, rapalogues can also cause increase in apoptosis in certain cells. In addition, rapalogues inhibit the growth of tumor xenografts.

I.4.1.1.1. Everolimus

Everolimus (also known as RAD001 or Afinitor) is an oral rapamycin analog which shares the mechanism of action with rapamycin.

It has been reported that Everolimus has effects in various tumor cells and *in vivo* models including BC models [71-73].

Everolimus has been FDA approved for the treatment of various malignancies including advanced renal cell carcinoma and ER+ breast cancer. Everolimus is being tested in clinical trials for the treatment of different tumor types as monotherapy or in combination with other therapies. Clinical trials with rapalogues combined with classical chemotherapies or other antineoplastic drugs have provided better and promising clinical results than monotherapy.

Despite the efficiency demonstrated as an antineoplasic agent, the effects obtained in clinic were disappointing and did not achieve the expected results. Several hypotheses may explain the limited success of rapalogues. First, the mechanism of action of rapalogues is mainly cytostatic with poor proapoptotic effects. Second, the poor ability of rapalogues to dephosphorylate 4E-BP1 in the Thr37/46 sites which are good substrates of mTORC1. Finally, S6K1-dependent feed-back loops that lead to reactivation of PI3K/AKT and Ras/Raf/MEK/ERK pathways [29, 74].

Few predictive biomarkers of response have been identified. Results provided from the genome analysis of tumors from patients treated with Everolimus suggested that mTORC1 inhibitors may be highly effective in patients whose tumors harbor TSC1, NF2, or MTOR mutations [75, 76].

I.4.1.2. mTORC1/2 inhibitors

The second generation of mTOR inhibitors targeting the ATP site of the kinase domain of mTOR, are able to block both mTORC1 and mTORC2 complexes [77].

mTORC1/2 inhibitors are the new generation of mTOR inhibitors that are ATP-competitive inhibitors. These molecules suppress the kinase activity of mTOR by competing with ATP for the binding to the catalytic domain of mTOR. ATP is the substrate that donates the phosphate group by which mTOR phosphorylates its target proteins (**Figure I.14.**). These drugs potently inhibit both mTORC1 and mTORC2 complexes [43].

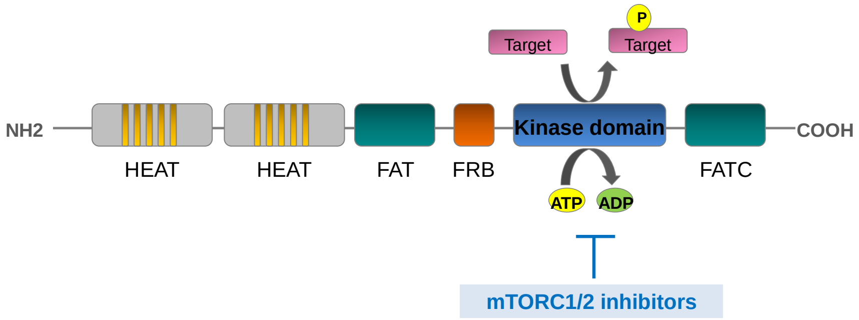

Figure I.14. mTORC1/2 inhibitors interaction with the kinase domain of the mTOR protein. mTORC1/2 inhibitors inhibits the kinase activity of mTOR by competing with ATP for the binding to the catalytic site.

mTORC1/2 inhibitors have been developed with the aim to improve the efficacy of rapalogues and to reduce the toxicity of the dual PI3K/mTOR inhibitors. It should be considered that the inhibition of all the functions of mTOR could generate toxicity. However, some studies suggest that blocking mTORC2 could be tolerated *in vivo* [74].

In preclinical studies, mTORC1/2 inhibitors have shown stronger antiproliferative and propapoptotic effects as well as better mTORC1 inhibition compared with rapalogues. mTORC1/2 inhibitors improve rapalogues since they eliminate activation of AKT by mTORC2 and induce a more profound inhibition of 4E-BP1 [29, 62].

The first reported molecule for this class of inhibitors was PP242 [78]. Several drugs are being studied such as Torin1 [79], PP30 [78], OSI-027 [80] and Ku-0063794 [81].

Preclinical data demonstrated that treatment with these drugs reduce cell proliferation in different cancer cell types, and in rapamycin-sensitive and rapamycin-insensitive cell lines. Also, they have shown robust antitumor activity in several human xenografts models. These drugs decrease the overall rates of protein synthesis in cell lines [79]. Also, anti-angiogenic effects have been shown with the treatment with catalytic mTOR inhibitors [82]. OSI-027 in combination with Lapatinib has shown antitumor synergistic effects in bladder cancer cells [83].

mTORC1/2 inhibitors are in phase I/II clinical trials. Results of the first clinical trials with these drugs have identified single-agent activity apparently higher than that seen previously with rapalogues. AZD-2014, OSI-027, AZD-8055 and TAK-228 have been tested in clinical trials and have shown signs of clinical activity in patients with advanced solid tumors and hematologic malignancies [67, 84].

I.4.1.2.1.TAK-228

TAK-228 (formerly known as INK128 and MLN0128) is a novel dual mTORC1/2 inhibitor, an orally bioavailable, potent and highly selective, catalytic inhibitor of mTOR.

TAK-228 showed anti-proliferative effects in human cell lines of various tumor types and genetic backgrounds. TAK-228 has been effective in *in vitro* and *in vivo* models of solid tumors as breast cancer, NSCLC, prostate cancer and colorectal cancer [85-89] and haematological malignancies [66, 90]. Cellular assays have confirmed that TAK-228 inhibits mTORC1/2 signaling and prevents cellular proliferation in cancer cells. In addition, TAK-228 induces cell cycle arrest at G0/G1 phase and activates apoptosis in some types of tumor cell lines. TAK-228 has demonstrated effects on cell migration and invasion. In addition, preclinical studies of mTORC1/2 inhibitors in combination with chemotherapy or targeted-therapies have shown greater effects than in the monotherapy.

TAK-228 has been or is being tested, in more than 30 clinical trials according to ClinicalTrials.gov, for advanced solid tumors and hematologic malignances as single-agent and in combination with other therapies such as paclitaxel.

I.4.1.3. PI3K inhibitors

PI3K inhibitors are basically divided into two subgroups: pan-class IA and isoform-specific inhibitors.

Pan-class IA inhibitors are inhibitors able to bind the four isoforms of class I PI3K (α, β, δ and γ). Wortmannin and LY294002, the first two prototype PI3K inhibitors, represented for a long time a useful tool in the study of PI3K function in cellular processes, given their effectiveness at low concentration (nM). Nevertheless, given their poor pharmacokinetic properties and lack of selectivity, these compounds have limited their therapeutic potential. Therefore, several novel compounds have been further developed.Currently, there are several pan-class IA PI3K inhibitors being tested in low-phase clinical trials. These drugs are e.g. BKM120, CH5132799 and XL-147, which might be efficacious in trastuzumab resistant cells [91-93].

A second group of PI3K inhibitors has been developed to overcome the toxicity displayed by the treatment with pan-PI3K inhibitors. They are characterized by greater selective activity (isoform-specific). Isoform-specific inhibitors selectively inhibit p110 α, β, δ or γ catalytic subunits. Several molecules are currently under evaluation in preclinical and clinical studies. These include GSK2636771 which is a selective inhibitor of p110β and CAL-101 is a selective inhibitor of p110δ. BYL719, GDC-0032 and INK-1117 are specific inhibitors of p110α. We have been working with the latest.

PI3Kα inhibitors selectively suppress the activity of the class I PI3K catalytic subunit p110α. The high specificity of these drugs suggests that they may have therapeutic utility in tumors with specific alterations of the PI3K pathway. An advantage of the isoform-specific inhibitors is that may present fewer side effects than pan-PI3K inhibitors [62].

Preclinical studies have shown sensitivity of different tumor cell types to isoform-specific inhibitors. Cellular assays have reported that PI3K inhibitors reduce the PI3K signalling, and induce cytostatic and cytotoxic effects in *in vitro* models. It has been demonstrated that GDC-0941 (a potent inhibitor of PI3Kα/δ) has efficacy as an anti-tumoral drug in urothelial cell [94]. Also, synergistic antitumor activity has been reported with PI3K inhibitors in combination with other treatments such as in breast cancer [95, 96].

Several new isoform-specific inhibitors of PI3K are currently evaluated in clinical trials.

I.4.1.3.1. TAK-117

TAK-117 (formerly known as INK1117 and TAK-117) is a potent and highly selective small molecule, ATP-competitive inhibitor of the class I PI3K catalytic subunit p110α. TAK-117 is more than 100-fold less potent on the other catalytic subunits (β, δ or γ) and does not inhibit class II and III PI3K family members [67, 97].

There are few studies of TAK-117 effects in preclinical models and in the clinic. TAK-117 has demonstrated efficiency as anti-tumor drug in cell lines and xenograft models of tumors bearing *PIK3CA* mutations. TAK-117 inhibits cell proliferation and reduces phosphorylation and activity of AKT [98]. Results of a phase I clinical trial suggests that TAK-117 has an acceptable safety profile. Antitumor activity was observed with TAK-117, but its single-agent efficacy was limited, further evaluation in combination approaches is warranted [97].

TAK-117 has been or is being tested, in 9 clinical trials according to ClinicalTrials.gov, for advanced solid tumors as single-agent and in combination with other therapies.

1.4.2. Results of clinical targeting the PI3K/AKT/mTOR pathway in bladder cancer

Only rapalogues that selectively target mTORC1 have been tested so far in clinical trials for bladder cancer. Preclinical studies showed the efficacy of mTOR inhibitors rapamycin and everolimus, in inhibiting the growth of bladder cancer cells in vitro [99, 100].

Although these data represent a strong biological rationale to use mTOR inhibitors in bladder cancers, results from early-phase studies were globally disappointing despite some long-term responses from several patients [76, 84, 101].

There are reports of four different clinical trials that used rapalogues as a second line treatment in patients with metastatic bladder cancer, after the failure of platinum based chemotherapy [76, 101-103]. The overall results from all the trials were disappointing and expected efficacy of rapalogues was not observed. However, some of the trials had a small fraction of patients that responded to rapalogues and a retrospective molecular analysis has been performed from these responders. From these studies some candidates as biomarker of resistance have been proposed and are described in detail in the next section.

1.4.3. Biomarkers in clinical samples that are potentially predictive of response to PI3K/AKT/mTOR inhibitors in bladder cancer

Results from early-phase studies with mTOR inhibitors have been globally disappointing despite some long-term responses from several patients. Focused molecular analyses in patients with objective response included in these trials of revealed some biomarker of sensitivity candidates.

In one study, loss of PTEN expression correlated with resistance to rapalogues, while a complete responder in another study had an inactivating mutation in *TSC1* [75, 101].

These findings suggest that TSC1 might mediate everolimus sensitivity and raise the possibility that mTOR inhibition could be an effective therapeutic strategy for patients with metastatic urothelial carcinoma whose tumors harbor TSC1 mutations [15].

In a clinical trial of different solid tumors treated with a combination of a rapalog and pazopanib, a multi-TKI, an exceptional responder with bladder cancer had mutations in mTOR [104].

While these associations offer interesting insights into the molecular determinants of sensitivity to rapalogues, it should be remembered that they are case reports of single patients in a small cohort. The association between alterations in PTEN and *TSC1* and sensitivity to rapalogues could not be confirmed mechanistically using cell line models [101, 105].

These findings need to be studied further to enable the development of a robust clinical biomarker and the molecular determinants of sensitivity to rapalogues currently remain unclear. However, these data support the hypothesis that response to inhibitors targeting the PI3K network might be dependent on specific molecular alterations that activate signaling within this pathway.

We have addressed this issue in this PhD thesis.

HYPOTHESIS

HYPOTHESIS

- Due to genetic alterations seen in the PI3K/AKT/mTOR pathway in bladder cancers (BC) we hypothesize that mTOR and PI3K inhibitors could be active in this kind of tumors

- Not all treatments must be equally effective in all BC. There must be differences depending on the targeted protein, drug mechanism of action, and genetic and molecular characteristics of the tumor

OBJECTIVES

OBJECTIVES

1. To characterize the effects of two new drugs targeting the PI3K/AKT/mTOR pathway (TAK-228 and TAK-117) on bladder cancer cell lines and xenografts models. To determine the outcome while analyzing the mechanism of action.

2. To describe the key molecular and genetic alterations present in these cells that could predict sensitivity to these drugs.

3. To define *in vitro* and *in vivo* the antitumor effects of TAK-228 in combination with other therapies.

RESULTS

RESULTS

R.1. CHARACTERIZATION OF HUMAN BLADDER CELL LINES

R.1.1. Cell morphology

For our preclinical work we selected six BC cell lines (RT4, T24, CAL-29, TCCSUP, HT-1197, and UM-UC-3) classified as transition cell carcinoma, the most frequent type of urothelial carcinoma. Almost all these cells are adherent epithelial cells that grow as a layer a single cell thick (monolayer), attached to plastic tissue culture dishes. In contrast, RT4 cells grow as small islands, not in a single cell layer (**Figure R.1.**). In all the experiments, every two to three days the cells were supplied with fresh culture medium. In order to keep the cultures healthy and actively growing we subcultured them at regular intervals, checking the general cell morphology and growth patterns using an inverted microscope, and carefully looking for any microscopic evidence of microbial contamination. In addition to these daily examinations, the cultured cells were periodically tested for mycoplasm contamination at the IMIM Tissue Culture Core Facility.

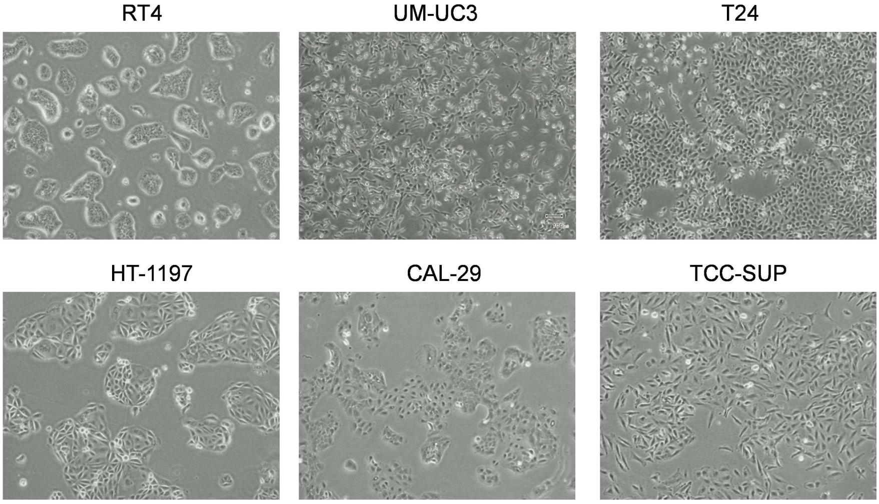

Figure R.1. Cell morphology of BC cell lines. Light microscopy images showing the growth patterns of BC cell lines.

R.1.2. Genetic background of the cell lines

We selected these six BC cell lines as they harbor some of the most frequent alterations in members of the PI3K/AKT/mTOR pathway described in bladder cancer patients. The genetic background data for the cell lines was taken from the open data found in the Cosmic Catalog of Somatic Mutations in Cancer and the Broad-Novartis Cancer Cell Line Encyclopedia [106] (**Table R.1.**).

Gene	RT4	T24	CAL29	TCCSUP	HT-1197	UM-UC-3
PIK3CA			p.H1047R	p.E545K	p.E545K	
TSC1	▨					
TSC2						▨
PTEN		▨				▨
RAS		HRAS			NRAS	KRAS
AKT						
mTOR						
EIF4EBP1		▨				▨

Table R.1. Mutation status of cell lines. Grey represents presence of known alterations in these genes. Known mutations in the PI3KCA gene are indicated.

We confirmed the presence of some of these mutations in our cells through Sanger sequencing. We found the *PIK3CA* gene mutations in TCC-SUP, CAL-29, and HT-1197 cells, and the *TSC1* gene alterations in RT4 cells.

R.1.3. Signaling molecule expression in human bladder cell lines

Next, we wanted to analyze the expression of different members of the PI3K/AKT/mTOR pathway under basal, non-stimulated culture conditions. To do this, we evaluated the phosphorylated and total levels of the main pathway targets: AKT, S6, and 4E-BP1. We checked the phosphorylation of AKT at the Ser473 site, S6 at the Ser235/236 sites, and 4E-BP1 at the Thr34/46 sites (**Figure R.2.**)

Similar levels of phosphorylated AKT were observed in the BC cell lines studied in basal conditions, with the exception of RT4 cells, which did not express phosphorylated AKT.

We also detected similar levels of phosphorylated S6 in the 6 BC cell lines. UM-UC-3 expressed low levels compared with the others.

There were important differences in the expression of total and phosphorylated 4E-BP1 between the cell lines. Three cell lines, T24, UM-UC-3, and TCC-SUP expressed higher levels of total and phosphorylated protein than the others. Regarding the phospho-4E-BP1 Thr37/46 results, when using this antibody 3 to 4 four bands between 20 and 12 kDa are expected, representing the different 4E-BP1 isoforms when phosphorylated at multiple sites. Of note, the upper and lower bands represent the more phosphorylated and unphosphorylated 4E-BP1 isoforms, respectively.

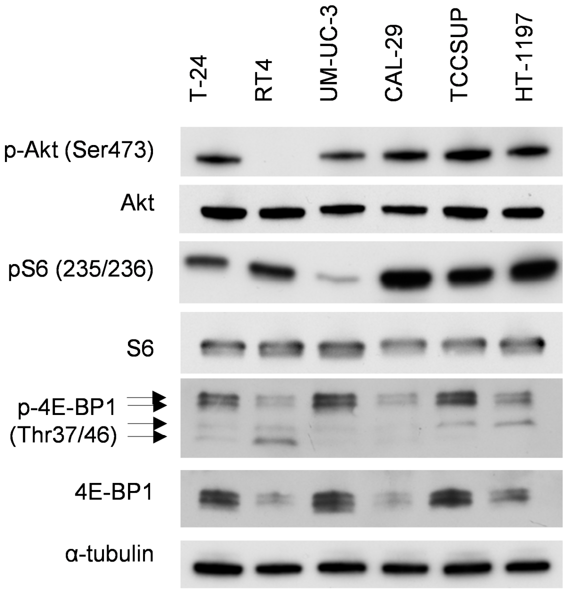
T-24
RT4
UM-UC-3
CAL-29
TCCSUP
HT-1197
p-Akt (Ser473)
Akt
pS6 (235/236)
S6
p-4E-BP1
(Thr37/46)
4E-BP1
α-tubulin

Figure R.2. Expression of PI3K/AKT/mTOR pathway molecule levels in BC cell lines. The cells were cultured for 48 hours, then whole-cell lysates were analyzed by western blot with the indicated antibodies. The images are representative of three sets of biological replicates.

R.2. GENERATION OF BLADDER CANCER IN *IN VIVO* MODELS

We established *in vivo* models of human urothelial cancer. Four of the six BC cell lines (TCCSUP, CAL-29, T24, and RT4) were tested *in vivo*. A total of $20x10^6$ cells were injected into the right flanks of mice and the animals were examined twice a week for signs of tumor growth.

After 5 months of follow-up, there were no signs of tumor growth in any of the mice injected with TCCSUP cells. In contrast, we found that three of the cell lines, RT4, T24, and CAL-29 were tumorigenic in mice. However, each tumor model displayed different growth rates.

With the RT4 cells, 5 out of 5 mice developed a tumor. The injected cells formed tumors that grew rapidly (approximately 6-7 days after cell implantation), and we decided to inoculate fewer tumor cells in subsequent experiments. After trials, we established $5x10^6$ cells/mice as the optimal quantity for injection. Under these conditions, RT4 vehicle-treated tumors reached approximately $700mm^3$ in 5-6 weeks, and the entire set of treatment experiments lasted approximately 7-8 weeks. (**Figure R.3.**).

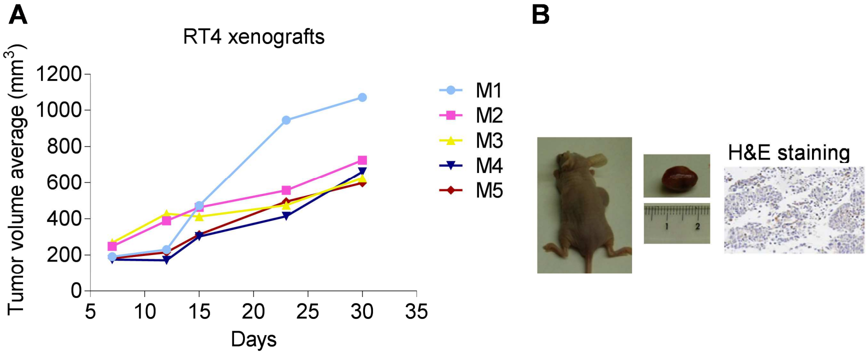

Figure R.3. Tumor growth of subcutaneous RT4 xenografts. A. Tumor growth over 35 days. The mice are indicated as M1-M5. **B.** Representative photographs of tumor-bearing mice*,* the excised tumors, and H&E staining of RT4 tumor sections.

With the CAL-29 cells, once again 5 out of 5 mice developed tumors. Although as many as $20x10^6$ cells were injected, the CAL-29-derived tumors grew extremely slowly, as previously reported [107]. It was necessary to wait at least one month post-injection for the tumors to reach the optimal size for treatment to begin. Because of this slow growth, we decided to use this cell line as the source of material for starting xenografts only in selected confirmatory experiments (**Figure R.4.**).

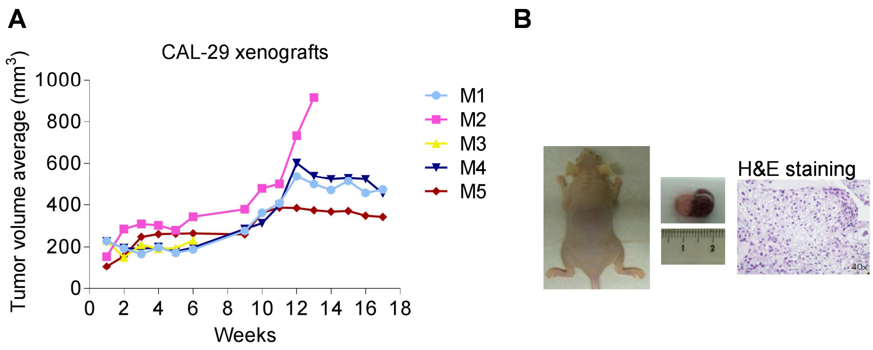

Figure R.4. Tumor growth of subcutaneous CAL-29 xenografts. A. Tumor growth over 18 weeks. The mice are indicated as M1-M5. **B.** Representative photographs of tumor-bearing mice, the excised tumors, and H&E staining of CAL-29 tumor sections.

With the T24 cells, only 3 out of 5 mice developed tumors after being injected with 20x106 cells. These were also very slow-growing tumors. T24 cells did not induce tumors in 2 out 5 mice (no tumor was detected six months after injection). In order to improve this model, we decide to inoculate the T24 parental cells in a mouse to form a “donor” tumor mass. The tumor was then excised and a tumor fragment was surgically implanted subcutaneously into each new mouse (one implant/mouse) with further using passage of the tumors in mice. Generally, when undertaking this procedure the implanted tumor tissue should be no smaller than 0.25 cm. After each passage surgery, we saved a tumor fragment from the donor tumor for histology. This model achieved a 3/3 level of effectiveness (**Figure R.5.**).

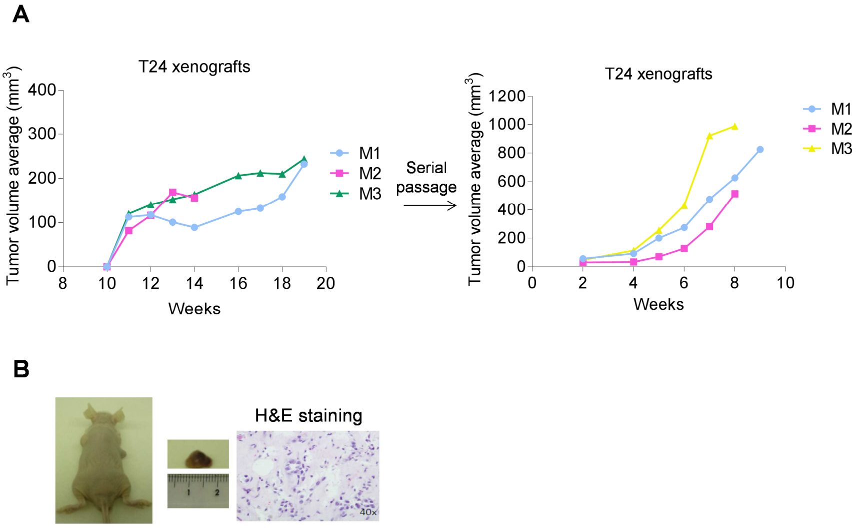

Figure R.5. Tumor growth of subcutaneous T24 xenografts. A Tumor growth over 20 weeks. Serial passage of tumor fragments implanted in mice. The mice are indicated as M1-M5. **B.** Representative photographs of tumor-bearing mice, the excised tumors, and H&E staining of T24 tumor sections.

Based on the characteristics of these three models, we decided to perform all *in vivo* analyses of the targeted drugs both individually and in the combinations using the RT4 model.

R.3. CHARACTERIZATION OF THE EFFECTS OF DRUGS TARGETING THE PI3K/AKT/mTOR PATHWAY

In order to study the effects of different PI3K/AKT/mTOR pathway inhibitors, we use three targeted therapies: TAK-228 (mTORC1/2 inhibitor), everolimus (mTORC1 inhibitor), and TAK-117 (PI3Kα inhibitor). We focused on characterizing the new inhibitor TAK-228 and then we compared the effects of TAK-228 on the BC models with the effects of the two other drugs.

R.3.1. Characterization of TAK-228

We first examined the effects of TAK-228 on the BC cell lines *in vitro,* and we then confirmed the results in the RT4 xenograft model *in vivo*.

R.3.1.1. Effect of TAK-228 on BC cells

We analyzed the effects of TAK-228 on cell proliferation in the six BC cell lines. Then, in order to elucidate the mechanism of action of the drug we evaluated the effect of TAK-228 on cell-cycle regulation, apoptosis and autophagy in two of the six cell lines: RT4 and CAL29 cells.

R.3.1.1.1. Effect of TAK-228 on cell viability

Cells were treated with different concentrations of TAK-228 and cell viability was determined. TAK-228 reduced proliferation of all bladder cancer cell lines in a concentration-dependent manner (**Figure R.6A**) with IC50 values ranging from 24 to 41.6nM (**Figure R.6B**). RT4 cells with inactivating TSC1 mutation were significantly more sensitive than the rest of the cell panel ($p<0.001$).

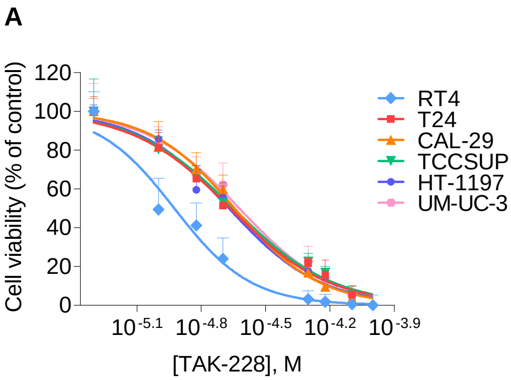

B

Cell line	IC50 TAK-228 [nM]
RT4	24.3 ± 7.2
T24	41.6 ± 2.7
CAL-29	30.1 ± 5.7
TCCSUP	36.1 ± 10.6
HT-1197	30.0 ± 3.5
UM-UC-3	38.4 ± 7.9

Figure R.6. Sensitivity of BC cell lines to TAK-228. **A.** Sensitivity of BC to TAK-228 at 72 hours assessed using MTS assay. Values shown are the mean percentage +/- SD of cell viability relative to controls and plotted as dose-response curves using GraphPad Prism. **B.** IC50 values of TAK-228 for the six cell lines. Incorporates data from three replicate experiments.

R.3.1.1.2. Effect of TAK-228 on cell cycle and apoptosis

We treated RT4 and CAL-29 cells with TAK-228 and the cell cycle distribution was analyzed through flow cytometry. In RT4 cells, TAK-228 significantly increased the number of cells in the G0/G1 phase and reduced the cells in the S phase ($p<0.05$). Also, the quantity of cells in the G2/M phase decreased. The same trend was observed in CAL-29 cells, despite the differences not being significant (**Figure R.7A**). The percentage of cells in each of the cell cycle phases is shown in **Table R.2.**

To better understand the effects of TAK-228 on the cell cycle, we used western blot to evaluate cyclin D1 levels after treatment with the drug. We observed inhibition of cyclin D1 in RT4 cells after 48 hours of treatment with the drug, indicating that TAK-228 decreases cyclin D1 levels. This suggests that TAK-228 may induce cell cycle arrest at the G0/G1 phase by inducing cyclin D1 degradation. Nevertheless, this result was not observed in CAL-29 cells, indicating that cyclin D1 may not be essential for cell cycle arrest in this cell line (**Figure R.7B**).

RT4			
Phase	**Control**	**TAK-228 [30nM]**	**TAK-228 [50nM]**
G0/G1	66.8 ± 7.6	86.4 ± 0.4	88.7 ± 2.5
S	14.0 ± 0.3	6.4 ± 2.5	4.8 ± 1.4
G2/M	18.6 ± 7.3	6.9 ± 2.5	6.1 ± 3.8
Sub G0/G1	8.2 ± 0.4	6.7 ± 2.2	5.6 ± 1.6

CAL-29			
Phase	**Control**	**TAK-228 [30nM]**	**TAK-228 [50nM]**
G0/G1	46.1 ± 1.9	58.7 ± 9.6	67.1 ± 1.2
S	20.5 ± 0.7	14.1 ± 4.1	11.2 ± 2.1
G2/M	26.5 ± 2.8	20.5 ± 1.1	17.8 ± 2.9
Sub G0/G1	5.7 ± 4.5	6.0 ± 6.2	3.3 ± 1.8

Table R.2. Percentage of cells in each of the cell cycle phases after treatment with TAK-228. Each value represents the mean ± standard error of the mean.

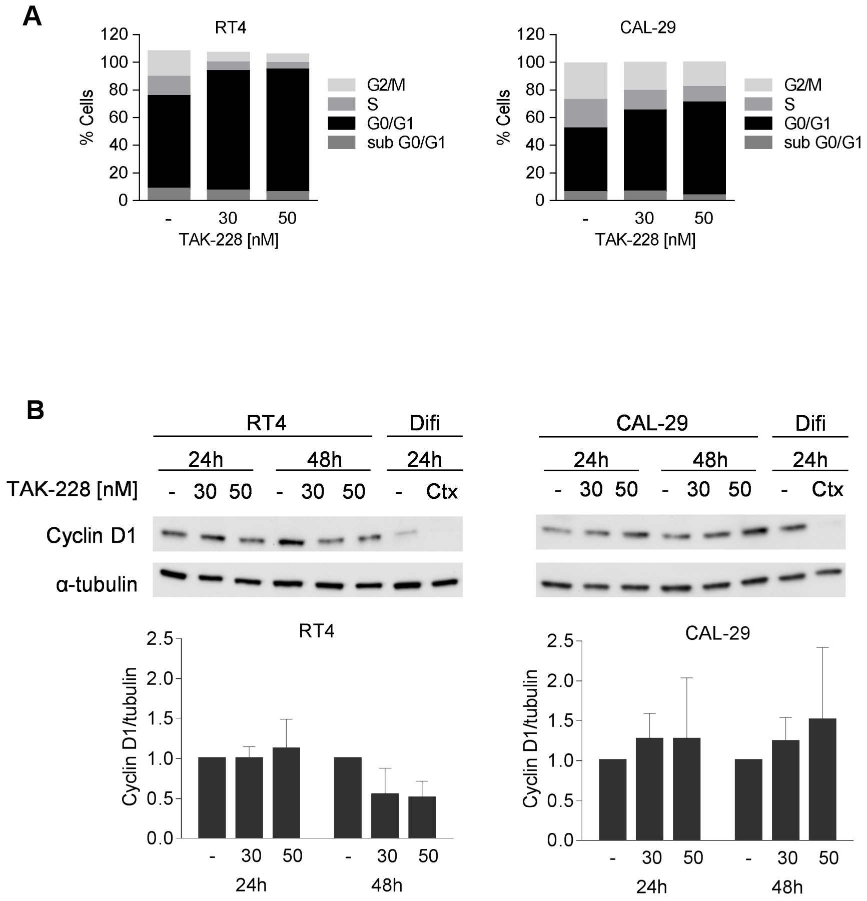

Figure R.7. The action of TAK-228 on cell cycle in RT4 and CAL-29 cells. A. Cell cycle distribution after 24 hours of treatment with TAK-228 [30nM and 50nM]. Fixed and propidium iodide stained cells were analyzed through flow cytometry. The bar chart shows the percentage of cells at different cell stages. **B.** Whole-cell lysates were analyzed using western blot with cyclin D1 after 24 and 48 hours of treatment with TAK-228 [30nM and 50nM]. The graphs show the cyclin D1 levels in each condition expressed as fold induction versus control arbitrarily set at 1.

It has been described that TAK-228 induces apoptosis in cancer cells in vitro [85, 108, 109]. We wondered if TAK-228 was able to induce apoptosis in bladder cancer cells. We treated the RT4 and CAL-29 cells with TAK-228 and we checked the effects of the drug through western blot (cleaved-PARP) and Muse Cell Analyzer using the Muse® Annexin V & dead cell kit. As a positive control for apoptosis we used Difi cells treated with Cetuximab [110]. We detected neither apoptotic cells nor cleaved-PARP (**Figure R.8.**). These results therefore suggested that apoptosis is not activated by the drug under these conditions.

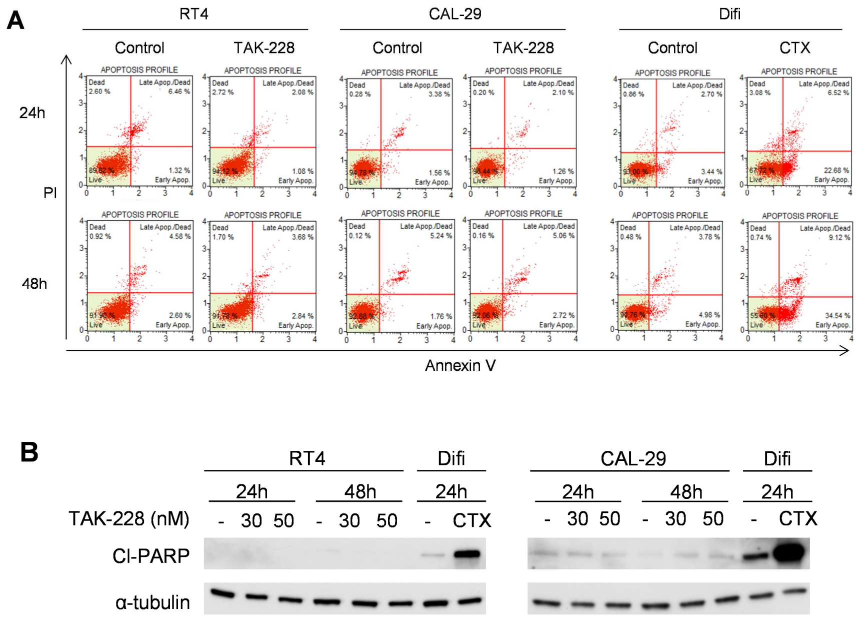

Figure R.8. Action of TAK-228 on apoptosis in RT4 and CAL-29 cells. A. Representative flow cytometry dot plots of two independent experiments are shown after treatment with [30nM and 50nM] over 24 and 48 hours. As a positive control for apoptosis we used Difi cells treated with Cetuximab [10µg/ml] (CTX). **B.** Whole-cell lysates were analyzed using western blot with cleaved-PARP after treatment with TAK-228 [30nM and 50nM] over 24 and 48 hours.

		RT4		CAL-29		Difi	
Time	**% of cells**	**Control**	**TAK-228 [50nM]**	**Control**	**TAK-228 [50nM]**	**Control**	**CTX [10µg/ml]**
24h	**Live**	87.1 ± 3.6	92.0 ± 3.0	93.0 ± 2.5	94.0 ± 3.3	93.0	67.7
	Total apoptotic	10.3 ± 3.6	5.6 ± 3.4	6.7 ± 2.6	5.7 ± 3.2	6.14	29,2
48h	**Live**	91.1 ± 1.1	88.4 ± 4.8	91.0 ± 2.7	93.4 ± 1.8	90.7	55.6
	Total apoptotic	7.4 ± 0.3	10.2 ± 5.2	8.3 ± 1,8	6.3 ± 2.1	8.8	43.7

Table R.3. Percentage of live and apoptotic cells after the treatment with TAK-228 in RT4 and CAL-29 cells. As a positive control for apoptosis we used Difi cells treated with Cetuximab [10µg/ml]. Each value represents the mean ± standard error of the mean.

R.3.1.1.3. Effect of TAK-228 on autophagy

It has been reported that the classical inhibitors of mTOR (e.g. everolimus or rapamycin) and the dual mTORC1/2 inhibitors induce autophagy [61]. In order to analyze the effects of TAK-228 in this process we checked the levels of two proteins involved in autophagy: LC3-II and p62/SQSTM1.

Cells were treated with TAK-228 [50nM] in the presence or absence of the autophagy inhibitor chloroquine [5 µM, CLQ] for 24 hours. Everolimus-treated cells [100nM] were used as a positive control of autophagy induction.

We demonstrated that TAK-228 decreases the levels of p62/SQSMT1 in both cell lines. Higher levels of LC3-II compared to the control demonstrate that TAK-228 increases the conversion of LC3-I to LC3-II. This effect was better shown in the presence of chloroquine which blocks the degradation of the autophagic vesicles (**Figure R.9.**).

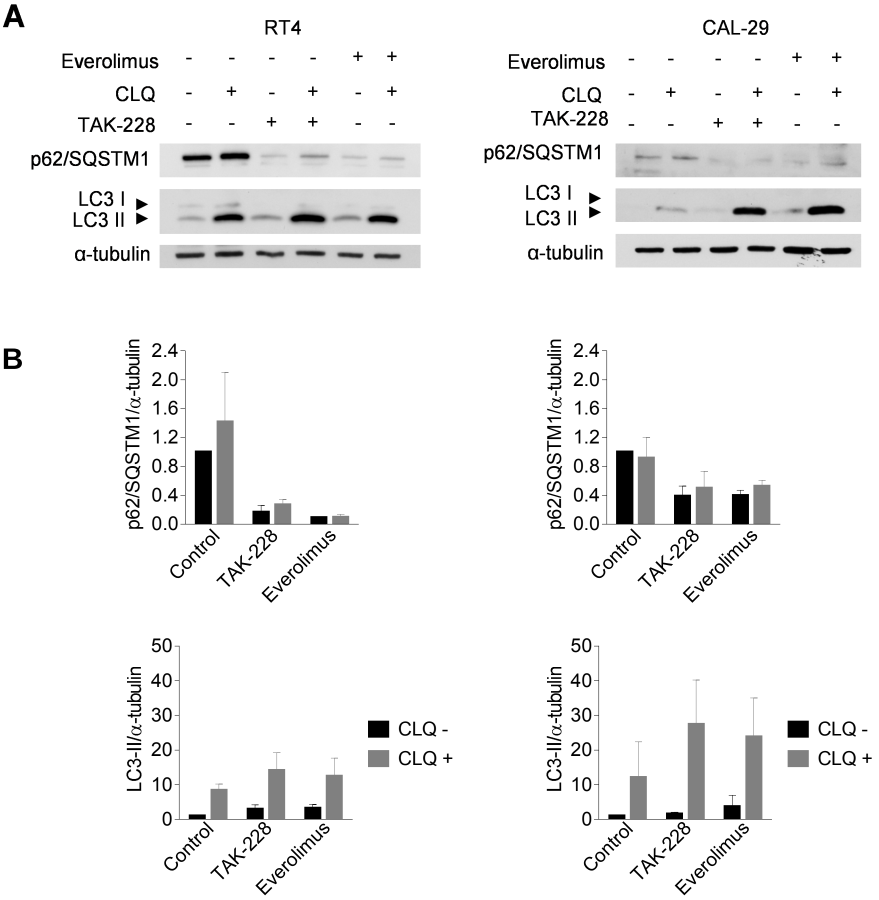

Figure R.9. The action of TAK-228 on autophagy in RT4 and CAL-29 cells. **A.** Lysates of cells treated with TAK-228 [50nM] or everolimus [100nM], in the presence or absence of chloroquine (CLQ) [5µM], for 24 hours, were analyzed by western blot for p62/SQSMT1 and LC3-II. Representative images of three separate experiments are shown. **B.** The graphs show the levels of p62/SQSMT1 and LC3-II under each condition expressed as fold induction versus control arbitrarily set at 1.

To better analyze the effects of the drug on the autophagy process, we used the Cyto-ID® kit which specifically stains autophagic vesicles. A high accumulation of vesicles in RT4 cells was detected with fluorescence microscopy after treatment with TAK-228 or everolimus (**Figure R.10.**).

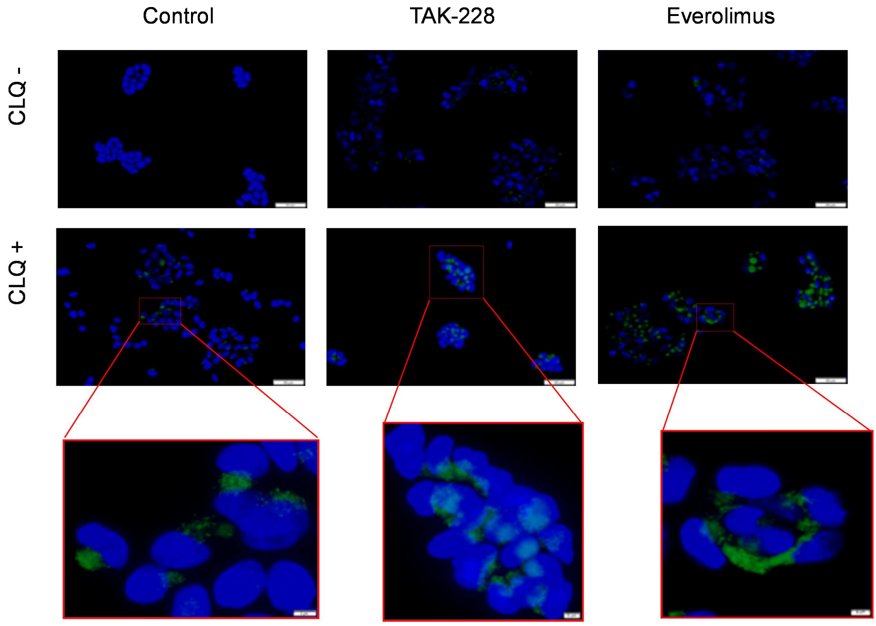

Figure R.10. Detection of autophagic vesicles using fluorescence microscopy. A high-intensity fluorescent punctate pattern corresponds to the production of autophagic vesicles. Representative microscopy pictures of three independent experiments are shown.

Similar results were obtained for TAK-228 as for the everolimus-treated cells used as a positive control. Based on these results we can conclude that autophagy was activated by TAK-228 in RT4 and CAL-29 cells.

R.3.1.2. Molecular effects of TAK-228 on BC cells and tumor xenograft samples

We evaluated the inhibitory effects of TAK-228 on the PI3K/AKT/mTOR pathway using western blot in three cell lines (CAL-29, T24 and RT4) and by immunohistochemistry in samples from tumor xenogratfs of CAL-29, T24 and RT4.

R.3.1.2.1. Molecular effect of TAK-228 on BC cells

To assess the effects of TAK-228 on mTORC2 we analyzed AKT activation through phosphorylation at the Ser473 site. TAK-228 inhibited the phosphorylation of AKT at Ser473 in CAL29 and T24 cells at 2 hours and 24 hours. AKT phosphorylation at S473 was almost recovered at 24 hours in T24 cells but not in CAL29 cells. AKT phosphorylation at T308 was inhibited at 2 hours but had recovered at 24 hours in T24 and CAL29 cells. Phosphorylation of AKT was not observed in basal conditions in RT4 cells. Total AKT levels were unchanged after treatment in the three cell lines tested.

Phosphorylation of S6, a direct downstream target of mTORC1, was found to be completely eliminated by TAK-228 2 hours after treatment and this effect was sustained for 24 hours in the three cell lines tested. We observed that total S6 levels decreased slightly when the cells were treated with the drug. In addition, TAK-228 significantly reduced the phosphorylation of 4E-BP1 Thr37/46, another downstream event in mTORC1, in RT4 cells, and we observed that this inhibition was dose-dependent (**Figure R.11C**).

There was a slight decrease of 4E-BP1 phosphorylation in CAL29 and T24.

These data confirm that TAK-228 inhibits both mTORC1 and mTORC2 in bladder cancer cell lines with mutations in the PI3K/AKT/mTOR pathway (**Figure R.11.**)

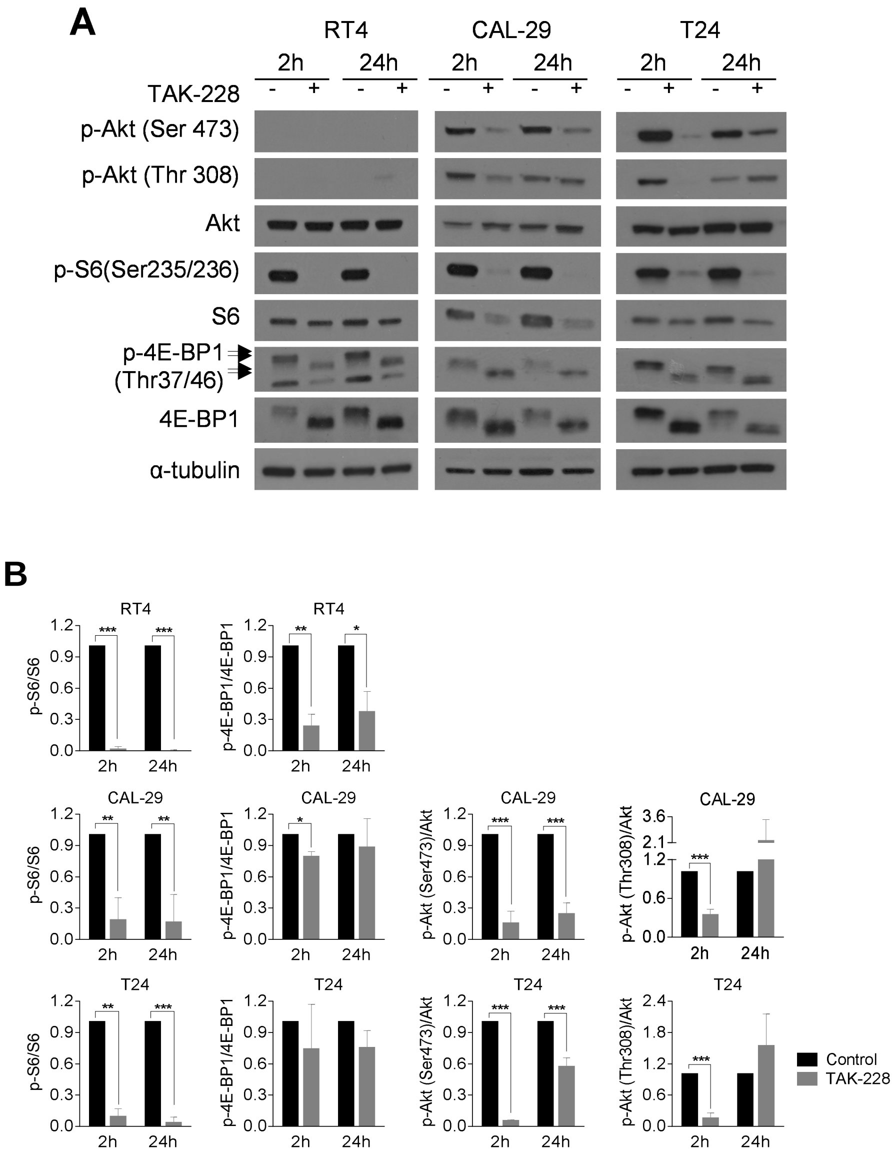

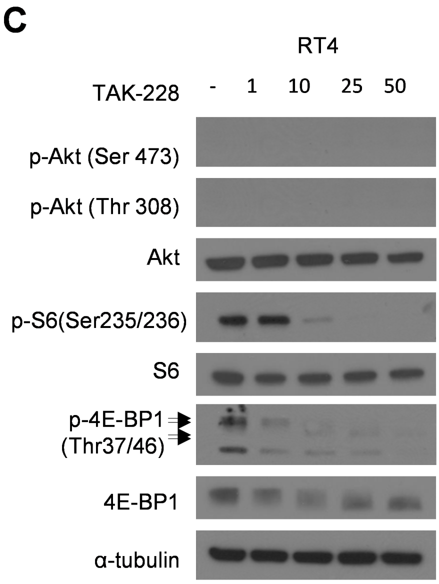
C
RT4
TAK-228
-
1
10
25
50
p-Akt (Ser 473)
p-Akt (Thr 308)
Akt
p-S6(Ser235/236)
S6
p-4E-BP1
(Thr37/46)
4E-BP1
α-tubulin

Figure R.11. Molecular effects of TAK-228 on the PI3K/mTOR signaling pathway. A. RT4, CAL-29, and T24 cells were treated with 50nM of TAK-228 for 2 and 24 hours. Whole-cell lysates were subjected to immunoblot analysis with the indicated antibodies. **B.** The graphs show the ratio of phosphorylated to total protein in each condition expressed as fold induction versus control arbitrarily set at 1. ular effects of TAK-228 on the PI3K/mTOR signaling pathway. **C.** RT4 cells were treated with the indicated doses of TAK-228 for 24 hours. Whole-cell lysates were subjected to immunoblot analysis with the indicated antibodies.

R.3.1.2.2. Molecular effects of TAK-228 on tumor xenograft samples

We wanted to determine the effects of TAK-228 on tumor samples. To do this, CAL-29, RT4, and T24 xenografts were excised and the samples were incubated *in vitro* with TAK-228. After treatment, the samples were paraffin-embedded and stained with p-S6 (Ser235/236), as a marker of mTORC1 activity. We observed that TAK-228 inhibited the phosphorylation of S6 in tumor xenograft samples. These results confirmed that TAK-228 is effective on tumor tissues *in vitro* (**Figure R.12.**).

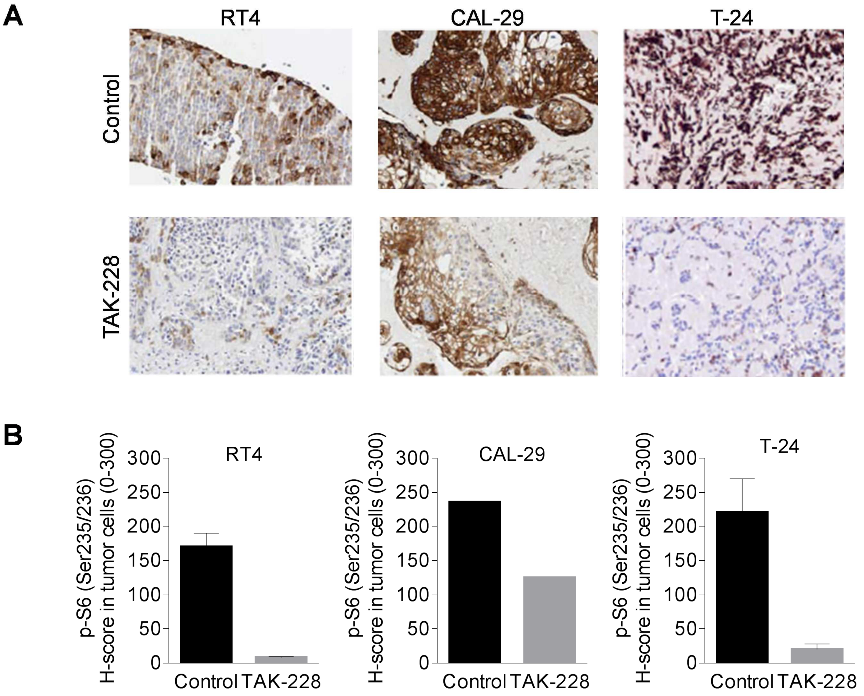
A
RT4
CAL-29
T-24
Control
TAK-228
B
RT4
CAL-29
T-24
p-S6 (Ser235/236)
H-score in tumor cells (0-300)
0
50
100
150
200
250
300
Control
TAK-228

Figure R.12. Molecular effects of TAK-228 added *ex vivo* to fresh xenografted tumors. A. Representative IHC images of p-S6 (235/236) staining in RT4, CAL-29, and T24 tumor samples treated *ex vivo* with TAK-228 [RT4 and T24 50nM; CAL-29 20nM] for 24 hours. **B.** Each column represents an effect on the p-S6 expression of the paired control- and TAK-228-treated samples measured as H-score.

R.3.1.3. In vivo effects of TAK-228 on the RT4 xenograft model

To confirm our in vitro data and determine the in vivo efficacy of TAK-228, we used the RT4 xenograft model. First, we treated the animals with TAK-228 at different doses and schedules, then we excised the tumors and checked several activity markers using immunohistochemistry.

R.3.1.3.1. Effect of TAK-228 on tumor growth

To evaluate TAK-228 efficacy as an anti-tumorigenic agent in vivo, we first used the RT4 xenograft model. We tested various doses and schedules of TAK-228, administered via oral gavage. The mice bearing suitably sized tumors were randomized into five groups (n= 8 mice per group) and treated: control (solvent PEG400); 6mg/Kg once a week; 3mg/Kg once a week; 1mg/Kg daily; and 0.6mg/Kg 5 days ON/2 days OFF. After 21 days of treatment, TAK-228 had significantly inhibited tumor xenograft growth both in the intermittent low dose (0.6mg/Kg 5 ON/2 OFF) and continuous low dose groups (1mg/Kg daily) (p= 0.049 and p= 0.012, respectively) compared to control mice. The sizes of the tumors in the group treated once a week with high doses (3mg/Kg and 6mg/Kg) were not significantly different from those of the control group. TAK-228 appeared to be well tolerated and no gross signs of toxicity or pathological changes were evident in the mice (**Figure R.13.**).

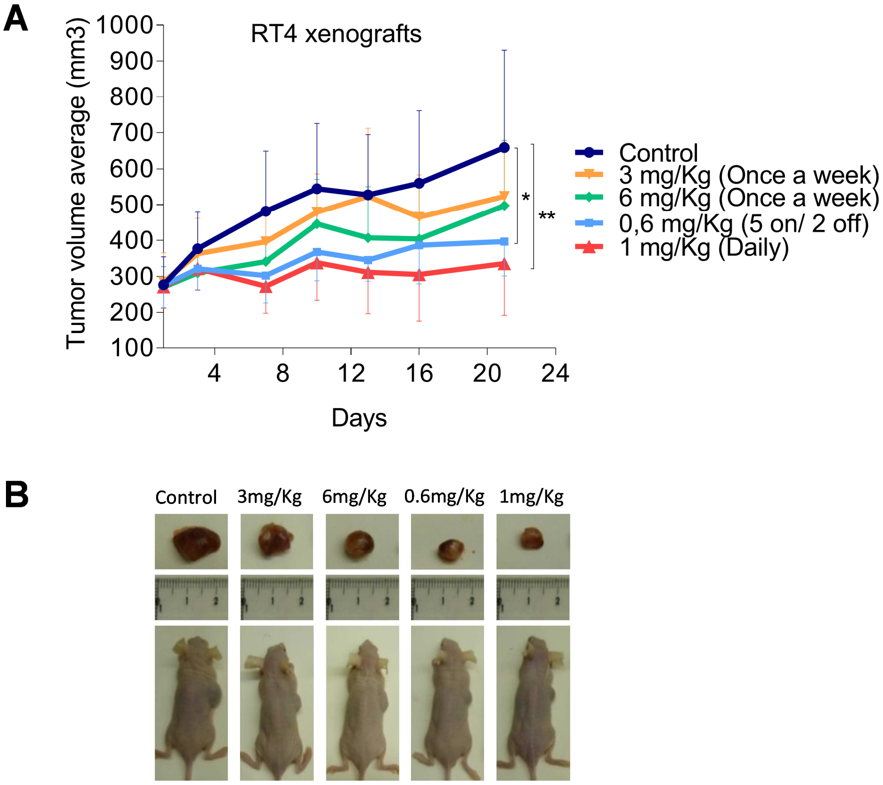

Figure R.13. Effects of TAK-228 on tumor growth *in vivo* in subcutaneous RT4 xenografts. A. Mice were treated for 21 days as indicated. Each treatment group consisted of eight mice. A plot of average tumor volume as a function of time in each treatment group is shown. *p<0.05, **p<0.01. **B.** Representative photographs of tumor-bearing mice and the excised tumors.

R.3.1.3.2. TAK-228 effects on tumor samples

The molecular effects of the drug were assessed on excised tumors from sacrificed mice on day 21 post-treatment. We determined the status of the PI3K/AKT/mTOR pathway activation in each group using IHC analysis. pS6 was used as a marker of TAK-228 activity. We observed that all treatments reduced the phosphorylation of S6 as well as its total levels. The strongest inhibitory effects were observed in tumors treated with intermittent low doses (0.6mg/Kg 5 ON/2 OFF) and continuous low doses (1mg/Kg daily) (**Figure R.14B**).

Sections were also stained for phosphorylated histone H3 (p-H3) and cleaved caspase-3 to assess effects on proliferation and apoptosis, respectively. A decrease in the cycling cell marker p-H3 (M phase) was found in all groups. In addition, the number of apoptotic cells had increased slightly after treatment. This increment was higher when the animals were treated on a daily basis (**Figure R.14B**).

We wondered whether TAK-228 was able to induce angiogenesis inhibition in this *in vivo* model. To check this, tumor specimens were immunohistochemically stained for three angiogenic markers: CD31 (also known as PECAM-1: Platelet Endothelial Cell Adhesion Molecule-1), VEGF-A, and p-KDR. The number of CD31 vascular structures was reduced, particularly in the groups treated with 0.6mg/kg and 1mg/Kg TAK-228. VEGF-A levels decreased when the animals were treated with TAK-228 with concomitant inhibition of KDR receptor phosphorylation (**Figure R.14A** and **Figure R.14B**).

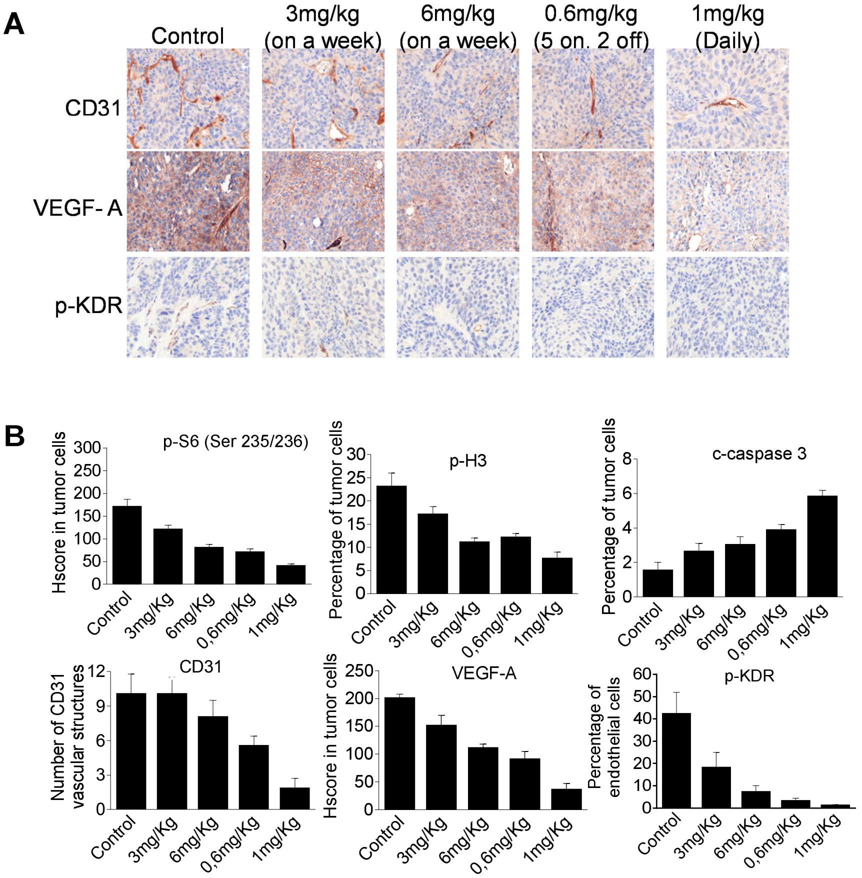
A
Control
3mg/kg (on a week)
6mg/kg (on a week)
0.6mg/kg (5 on. 2 off)
1mg/kg (Daily)
CD31
VEGF- A
p-KDR
B
p-S6 (Ser 235/236)
Hscore in tumor cells
300
250
200
150
100
50
0
Control
3mg/Kg
6mg/Kg
0,6mg/Kg
1mg/Kg
p-H3
Percentage of tumor cells
30
25
20
15
10
5
0
c-caspase 3
Percentage of tumor cells
8
6
4
2
0
CD31
Number of CD31 vascular structures
12
9
6
3
0
VEGF-A
Hscore in tumor cells
250
200
150
100
50
0
p-KDR
Percentage of endothelial cells
60
50
40
30
20
10
0

Figure R.14. TAK-228 effects in RT4 xenograft tumor sections. A. Representative IHC images of xenograft tumor sections stained with CD31, VEGF-A, and p-KDR. **B.** Box plots illustrating the staining results. Each graph is expressed as: H-score in tumor cells, p-pS6(Ser235/236), S6, and VEGF-A antibodies; percentage of stained-tumor (for Ser-10-phosphorylated histone H3 (H3P)), cleaved caspase-3 or endothelial cells (for p-KDR), and the number of stained tubular vascular structures (for CD31) within the tumor.

Based on these observations we can hypothesize that TAK-228 is an effective anti-tumorigenic agent in vivo that inhibits tumor proliferation through the inhibition of the PI3K pathway and by reducing angiogenesis.

R.3.2. Characterization of everolimus

In order to compare the effects of the dual mTOR inhibitor, TAK-228, with an mTORC1 inhibitor we used everolimus, a classical mTOR suppressor that has been widely studied in vitro for the treatment of different types of cancer.

To do this, we studied the cellular and molecular effects of everolimus on the BC cell lines.

R.3.2.1. Cellular effects of everolimus on BC cells

We analyzed the effects of everolimus on cell proliferation in the six BC cell lines.

R.3.2.1.1. Effect of everolimus on cell viability

Cells were treated with three concentrations of everolimus (10, 100 and 1000nM) and cell viability was determined. Everolimus reduced the proliferation of all BC cell lines in a non-dose-dependent manner. Similar effects were observed between cell lines (**Figure R.15.**). As we did not obtain a dose-response curve we could not calculate the IC50 values.

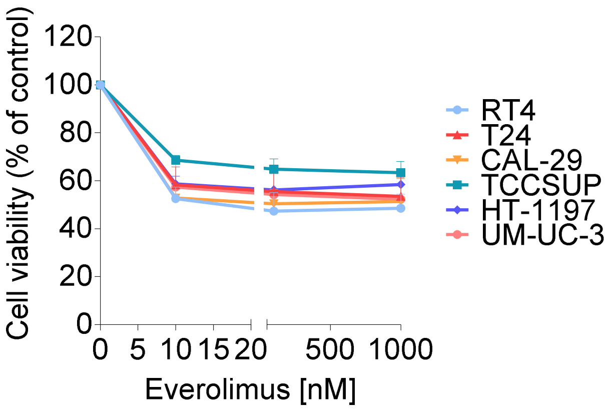

Figure R.15. Sensitivity of BC cell lines to everolimus. Sensitivity of BC to everolimus at 72 hours assessed using MTS assay. Values shown are the mean percentage +/- SD of cell viability relative to controls and plotted as dose-response curves using GraphPad Prism.

R.3.2.2. Molecular effect of everolimus on BC cells

To evaluate the inhibitory effects of everolimus on the PI3K/AKT/mTOR pathway we used three cell lines (RT4, CAL-29, and T24).

R.3.2.2.1. Molecular effect of everolimus on BC cells

As a direct marker of everolimus activity we checked the downstream effect on mTORC1 (S6 and 4E-BP1). However, we also analyzed AKT in order to compare the effects of everolimus with TAK-228.

Everolimus significantly inhibits the phosphorylation of S6 in the three cell lines. However, the phosphorylation of 4E-BP1 was not modified in RT4 cells after treatment with the drug and it actually increased in CAL-29 and T24 cells. In addition, AKT phosphorylation was upregulated in both sites (Ser473 and Thr308) in CAL-29 and T24 cells after treatment with everolimus.

We confirmed that everolimus is able to partially suppress mTORC1 activity by inhibiting only the phosphorylation of S6. Despite not being significant, we also observed a reactivation of the pathway by rephosphorylation of AKT (**Figure R.16.**).

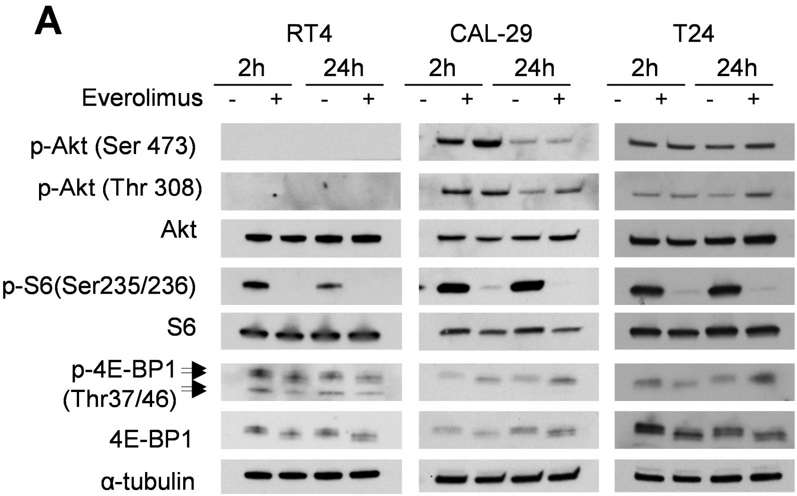
A
RT4
CAL-29
T24
2h
24h
2h
24h
2h
24h
Everolimus
- + - + - + - + - + - +
p-Akt (Ser 473)
p-Akt (Thr 308)
Akt
p-S6(Ser235/236)
S6
p-4E-BP1
(Thr37/46)
4E-BP1
α-tubulin

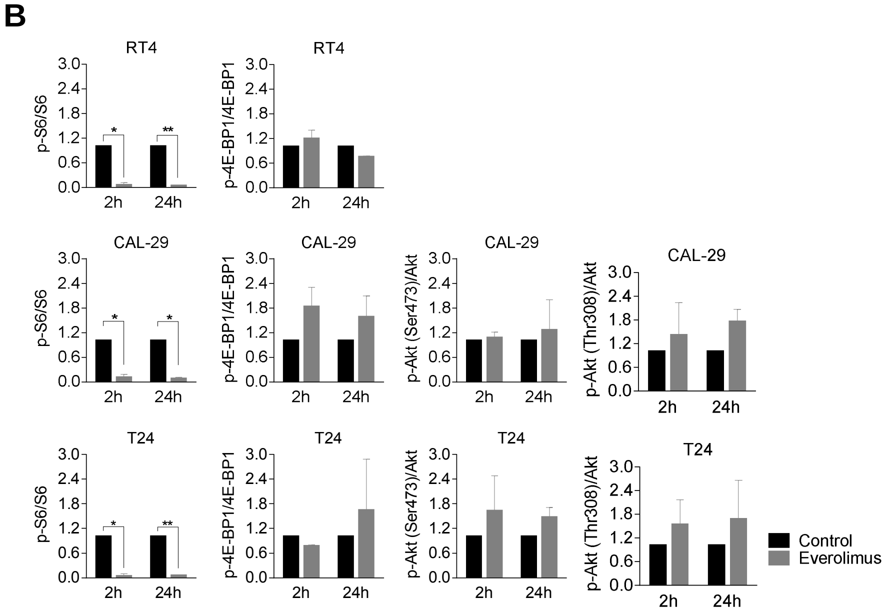

Figure R.16. Molecular effects of everolimus on the PI3K/mTOR signaling pathway. **A.** RT4, CAL-29 and T24 cells were treated with 100nM of everolimus for 2 and 24 hours. Whole-cell lysates were subjected to immunoblot analysis with the indicated antibodies. **B.** The graphs show the ratio of phosphorylated to total protein in each condition expressed as fold induction versus control arbitrarily set at 1.

These results suggest us that TAK-228 has more wide-reaching effects and is more effective than everolimus in inhibiting the PI3K signaling pathway.

R.3.3. Characterization of TAK-117

We wanted to analyze the effects of another agent targeting the PI3K/AKT/mTOR pathway. To do this, we used a PI3Kα inhibitor: TAK-117.

We first compared the effects of TAK-117 on cell proliferation and PI3K pathway inhibition with TAK-228. Then, to confirm the results obtained with the cells we tested the effects of the drug in vivo.

R.3.3.1. Cellular effect of TAK-117 on BC cell

We analyzed the effects of TAK-117 on cell proliferation in the six BC cell lines.

R.3.3.1.1. Effect of TAK-117 on cell viability

We tested the anti-proliferative effects of TAK-117 in our panel of six BC cell lines. The cells were treated with different concentrations of the drug and cell viability was determined via MTS assay to determine the IC50 of each cell line. All the cell lines showed sensitivity to the drug: CAL-29 cells and TCC-SUP cells had the lowest IC50 values (3.5 μM and 10.6μM, respectively), with CAL-29 cells being the most sensitive to the drug (**Figure R.17.**).

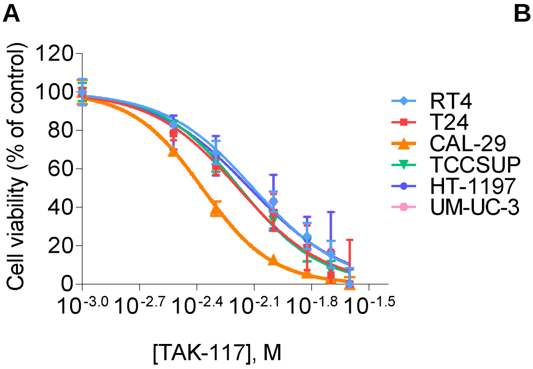

B

Cell line	IC50 TAK-117 [μM]
RT4	15.7 ± 1.1
T24	35.1 ± 10.9
CAL-29	3.5 ± 0.2
TCCSUP	10.6 ± 1.3
HT-1197	17.4 ± 5.7
UM-UC-3	19.7 ± 2.8

Figure R.17. Sensitivity of BC cell lines to TAK-117. A. Sensitivity of BC to TAK-117 at 72 hours assessed through MTS assay. Values shown are the mean percentage +/- SD of cell viability relative to controls and plotted as dose-response curves using GraphPad Prism. **B.** IC50 values of TAK-117 for the six cell lines. Incorporates data from three replicate experiments.

However, according to data provided by the company, doses higher than 3μM might show unspecific effects. For that reason, we confirmed these results with another method. We analyzed the effects of TAK-117 in the long-term (8-10 days). We observed varying sensitivities to TAK-117 between cell lines. CAL-29 and TCCSUP were the most sensitive to the drug, perhaps because of the mutations in their *PIK3CA* gene. However, the HT-1197 cell line, which is also mutated in *PIK3CA*, was not sensitive to TAK-117. This may be because it harbors a RAS mutation (**Figure R.18.**). These results confirm that TAK-117 is more effective in the tumor cell lines with mutations in the *PIK3CA* gene than in other cells with mutations in other members of the PI3K/AKT/mTOR pathway.

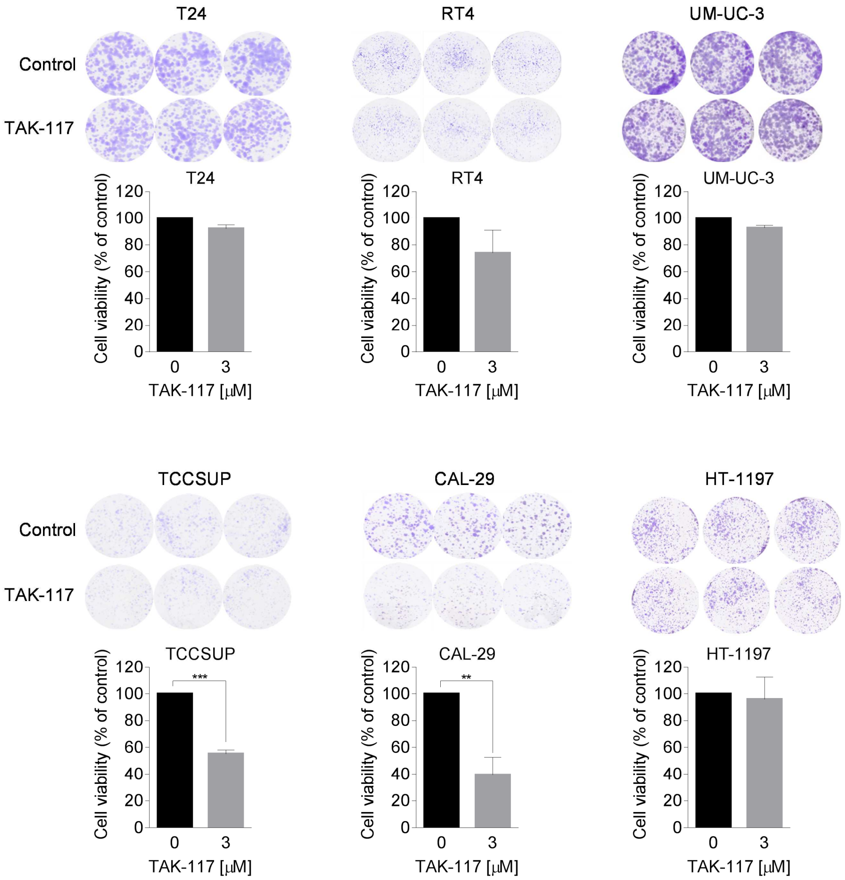

Figure R.18. Long-term *in vitro* exposure of tumor cells to TAK-117. Cells were treated with 3µM of TAK-177 for 8-10 days. Representative images of two independent experiments are shown. The results are shown as percentage of cells normalized to control.

R.3.3.2. Molecular effect of TAK-117 on BC cells

As a marker of TAK-117 activity we checked the activation of AKT by evaluating the phosphorylation at the Ser473 and Thr308 sites in three cell lines.

Phosphorylation of Akt at the Ser473 and Thr408 sites was suppressed by the drug after 2 hours and the inhibition was maintained until 24 hours in CAL-29 and T24 cells. Phosphorylation of AKT was not observed in basal conditions in RT4 cells. In addition we analyzed the other markers of the PI3K/AKT/mTOR pathway, and they remained unchanged after 2 and 24 hours of treatment (**Figure R.19.**).

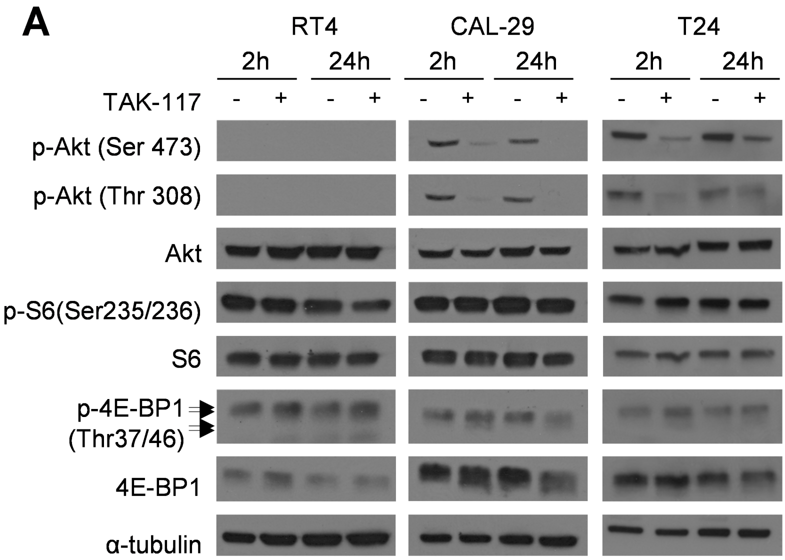
A
RT4
CAL-29
T24
2h
24h
2h
24h
2h
24h
TAK-117
- + - + - + - + - + - +
p-Akt (Ser 473)
p-Akt (Thr 308)
Akt
p-S6(Ser235/236)
S6
p-4E-BP1
(Thr37/46)
4E-BP1
α-tubulin

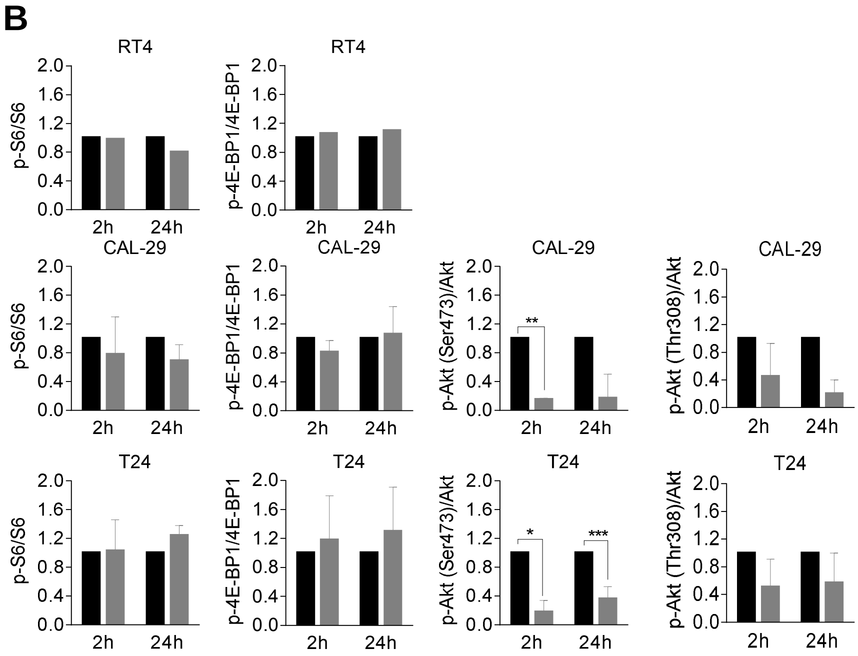

Figure R.19. Molecular effects of TAK-117 on the PI3K/mTOR signaling pathway. **A.** RT4, CAL-29 and T24 cells were treated with 100nM of everolimus for 2 and 24 hours. Whole-cell lysates were subjected to immunoblot analysis with the indicated antibodies. **B.** The graphs show the ratio of phosphorylated to total protein in each condition expressed as fold induction versus control arbitrarily set at 1.

R.3.3.3. In vivo effect of TAK-117 on the CAL-29 xenograft model

To confirm the results obtained for TAK-117 *in vitro* we used the CAL-29 xenograft model, since CAL-29 cells harbor the *PI3KCA* mutation and were the most sensitive to the drug.

Tumor growth of CAL-29 xenografts was very slow and the animals were treated for 54 days. TAK-117 inhibited the tumor growth in the CAL-29 xenografts, although this effect was not significant (**Figure R.20.**).

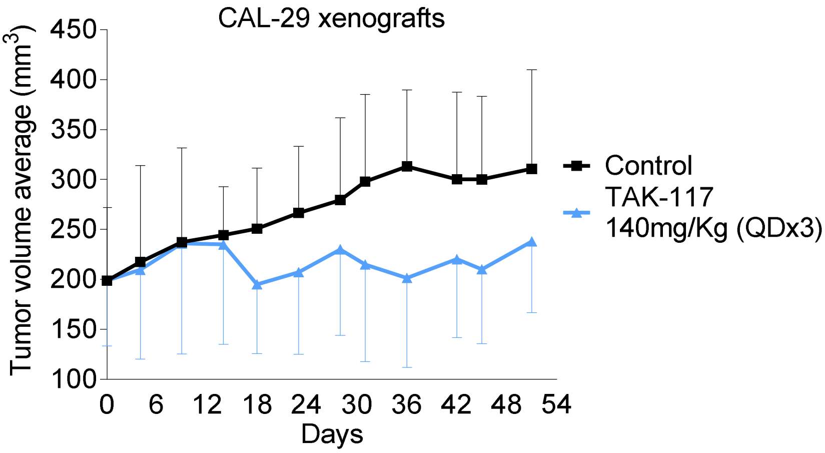

Figure R.20. *In vivo* exposure of subcutaneous CAL-29 xenografts to TAK-117. CAL-29 tumor-bearing mice were treated for 54 days as indicated. Each treatment group consisted of six mice. A plot of average tumor volume as a function of time in each treatment group is shown.

R.4. BIOMARKERS OF SENSITIVITY OR RESISTANCE TO TAK-228

Different biomarkers of sensitivity or resistance to PI3K/AKT/mTOR pathway inhibitors have been described [75, 87, 111, 112]. We wondered whether any of these markers could predict sensitivity to TAK-228 in our bladder cancer cells. To do this, we evaluated these markers in basal cell lysates using western blot. Correlation between protein expression and TAK-228 drug sensitivity (IC50 values) was assessed through Spearman's rank correlation coefficient (*r*). We considered there to be correlation when *r* was close to ± 1 and the level of significance was lower than 0.05.

R.3.4.1. Basal expression and correlation

TSC1 is the most relevant everolimus-response biomarker [75] and was the first one that we studied. TSC1 expression was present in five of the six cell lines, although absent in the TSC1 mutated RT4 cell line. However, no correlation was found between drug response and TSC1 expression.

We analyzed other members of the PI3K/Akt/mTOR pathway (p-S6 Ser235/236, S6, p-AKT Ser 473, AKT, and PTEN) and we found no correlation between these and the drug (**Figure R.21A**).

High GSK3 activity (low basal p-GSK3α/β (Ser61/9) levels) is associated with a better response to mTOR1/2 inhibitors including TAK-228 [87]. We observed that RT4, the most sensitive cell line to

TAK-228, has the highest GSK3 activity, however, this did not correlate with sensitivity to TAK-228 (**Figure R.21A**).

High 4E-BP1 levels and an elevated eIF4E/4E-BP ratio may predict resistance to dual mTOR inhibitors [111, 112]. The levels of total 4E-BP1 were increased in the three least sensitive of the six cell lines (higher IC50 values). We found strong positive correlation with TAK-228 response and 4E-BP1 levels (*r* = 0.814**). In addition, we observed a moderate negative correlation (*r* = -0.587*) with p-4E-BP1 (Thr37/46)/4E-BP1 and TAK-228 sensitivity. The ratio between eIF4E/4E-BP1 showed a strong negative correlation with drug sensitivity (*r* = -0.687*) (**Figure R.21B, Figure R.21C** and **Figure R.21D**).

Also, the incomplete dephosphorylation of 4E-BP1 could be associated with resistance to mTORC1/2 inhibitors. We also confirm that the most sensitive cells to the drug, RT4, are those that present the highest inhibition of 4E-BP1 when they are treated with TAK-228 (**Figure R.11C**).

Together, these results suggested we should further explore 4E-BP1, eIF4E/4E-BP1, and p-4E-BP1 (Thr37/46)/4E-BP1 as possible predictive biomarkers of response to TAK-228 in bladder cancer.

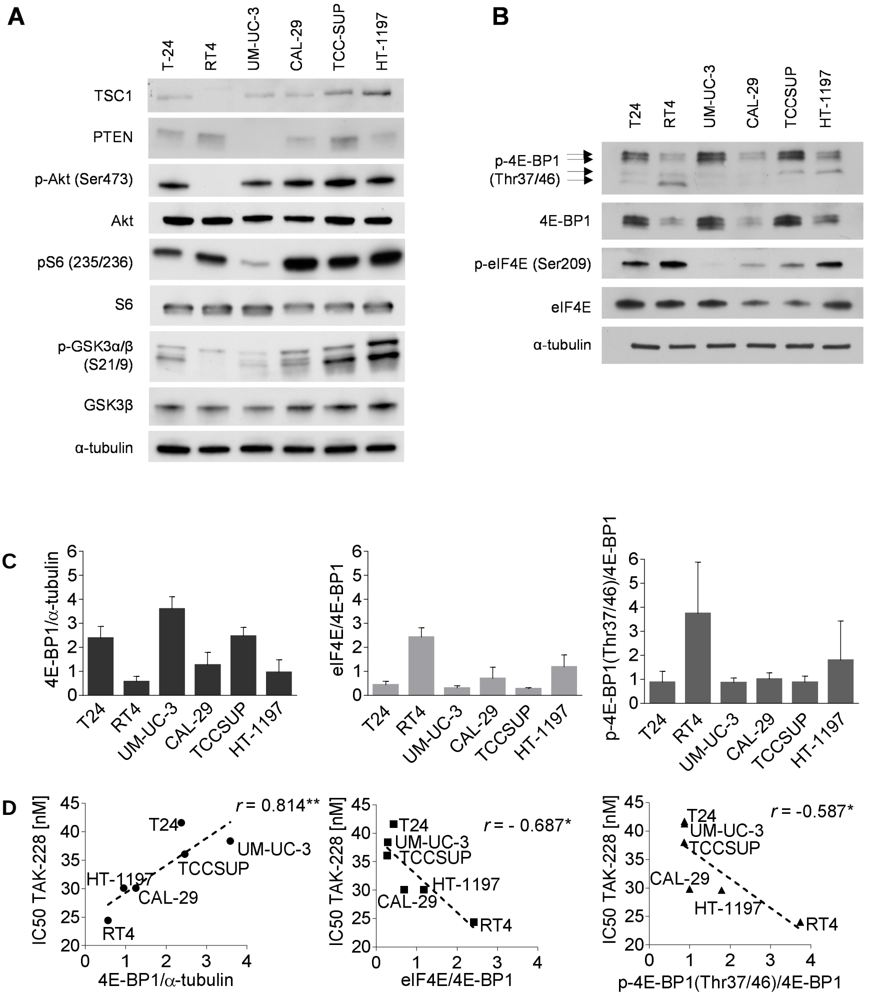

Figure R.21. Strategy for identifying potential biomarkers correlated with sensitivity to TAK-228. A-B. Baseline expression of PI3K/mTOR-associated pathway components in unstimulated BC cells. Whole-cell lysates were analyzed with antibodies indicated. The images are representative of three sets of biological replicates. **C.** Relative density of the bands was normalized to α-tubulin. Three ratios of protein levels were calculated and the reported values are averages of the three biological replicates; error bars indicate the standard error of the mean. **D.** Correlation of protein expression with sensitivity to TAK-228.

R.5. CHARACTERIZATION OF THE COMBINATION OF TAK-228 PLUS TAK-117

As we had demonstrated that TAK-228 and TAK-117 are effective on bladder cancer models, we further evaluated the effects of the combination looking for a more profound and stronger anti-proliferative activity.

R.5.1. Cellular effects of TAK-228 plus TAK-117 on BC cells

We analyzed the effects of the combination on cell proliferation in CAL-29, RT4, and T24 cells. Then, as we had previously shown that TAK-228 modulates cell cycle and autophagy, we investigated whether the combination had any additional effect on these two processes.

R.5.1.1. Effects of TAK-228 plus TAK-117 on cell viability

To determine the type of interaction between these two drugs, we first calculated the combinatorial index (CI) using Calcusyn (BioSoft). Cells were treated with serial dilutions of each drug on its own or with the two combined at a fixed ratio. Five dilutions ranging from one fourth of the IC50 to four times the IC50 doses of each drug, in combination, plus a control were tested. Cell viability was measured through MTS at 72 hours.

At IC50 conditions, in all 3 cell lines tested, the combination of TAK-228 and TAK-117 showed synergistic activity (CI<1). For the RT4 and CAL-29 cell lines, this synergistic effect was observed in the majority of the conditions tested. However, in T24 this synergistic effect was observed only in under certain conditions, suggesting that in T24 the combination is less effective than in the other cell lines (**Table R.4.**).

RT4				
Condition	**TAK-228 [nM]**	**TAK-117 [µM]**	**CI**	**Effect**
0.25x	6	3.9	0.72 ± 0.25	Moderate synergism
0.5x	12.2	7.9	0.64 ± 0.04	Synergism
0.75x	18.2	11.8	0.60 ± 0.01	Synergism
1x	24.0	15.8	0.57 ± 0.19	Synergism
2x	48.6	31.6	0.61 ± 0.08	Synergism
4x	97.2	63.2	0.66 ± 0.13	Synergism

CAL-29				
Condition	**TAK-228 [nM]**	**TAK-117 [µM]**	**CI**	**Effect**
0.25x	7.5	0.9	0.82 ± 0.33	Moderate synergism
0.5x	15	1.8	0.68 ± 0.22	Synergism
0.75x	22.5	2.7	0.58 ± 0.13	Synergism
1x	30.8	3.7	0.56 ± 0.06	Synergism
2x	61.6	7.4	0.71 ± 0.12	Synergism
4x	123.3	14.8	1.01 ± 0.23	Nearly additive

T24				
Condition	**TAK-228 [nM]**	**TAK-117 [µM]**	**CI**	**Effect**
0.25x	10.2	8.2	0.94 ± 0.07	Nearly additive
0.5x	20.5	16.5	0.97 ± 0.10	Nearly additive
0.75x	30.7	24.7	0.93 ± 0.05	Nearly additive
1x	41.0	33.0	0.83 ± 0.10	Moderate synergism
2x	82.1	66.0	0.87 ± 0.01	Slightly synergism
4x	164.7	132.0	1.21 ± 0.14	Moderate antagonism

Table R.4. Drug interaction determined using the TAK-228 and TAK-117 combination index. Three independent assays were performed for each cell line. Combination index (CI) values for RT4, CAL-29 and T24 were calculated employing Calcusyn software. Synergism (CI<1), additive effect (CI=1), and antagonism (CI>1).

In order to support these results, RT4 and CAL-29 cells were treated with the TAK combination, TAK-228, and TAK-117, at the corresponding IC50 doses for each drug/cell, and then the number of cells was quantified by automatic counting with Scepter. We confirmed that the combination significantly decreased cell proliferation compared to each drug on its own (**Figure R.22.**).

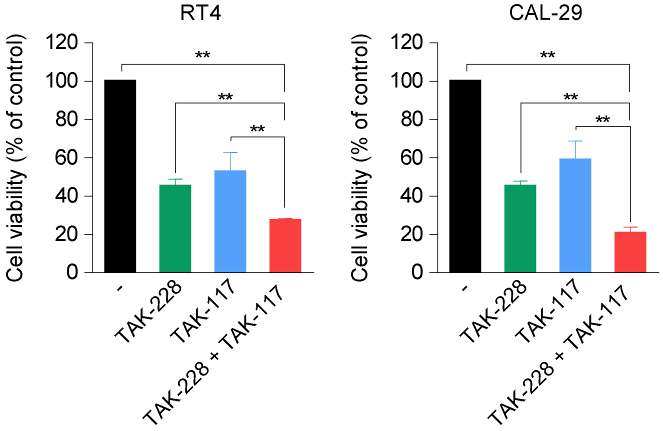

Figure R.22. Effects of TAK-228 combined with TAK-117 in RT4 and CAL-29 cells. Cells were treated with TAK-228 and TAK-117 at the corresponding IC50 values for each drug/cell [RT4: 24.3nM and 15.7µM; CAL29: 30.1nM and 3.5µM, respectively]. Cell viability was measured using the automatic Scepter 2.0 counter after 72 hours of treatment. The results are expressed as percentages of viable cells in the vehicle-treated control wells. **p<0.01

R.5.1.2. Effect of TAK-228 plus TAK-117 on cell cycle

The effects of the TAK combination on cell cycle were analyzed in RT4 cells. As we had demonstrated previously, TAK-228 increased the G0/G1 phase. We also observed a slight increment of this phase in the treatment with TAK-117. The greatest increase was with the combined treatment (**Figure R.23.**). The percentage of cells in each of the cell cycle phases is shown in **Table R.5.**

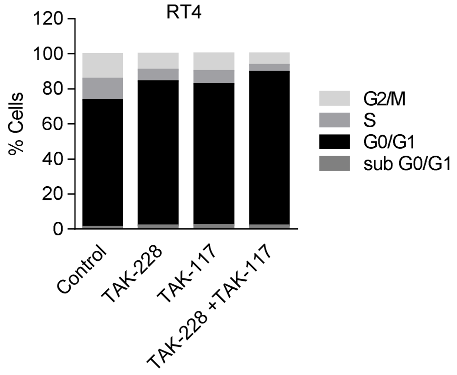

Figure R.23. Effects of TAK-228 combined with TAK-117 on cell cycle distribution. Cell cycle distribution after 24 hours of treatment with TAK-228 and TAK-117 at the corresponding IC50 values [24.3nM and 15.7µM, respectively], and the combination of the two drugs, for 24 hours. Fixed and propidium iodide stained cells were analyzed using flow cytometry. The bar chart shows the percentage of cells at different cell stages.

RT4				
Phase	**Control**	**TAK-228 [24.3nM]**	**TAK-117 [15.7µM]**	**TAK-228 + TAK-117**
G0/G1	72.2 ± 3.6	82.4 ± 4.1	80.0 ± 5.6	87.0 ± 1.1
S	12.2 ± 2.1	6.4 ± 0.2	7.4 ± 0.4	3.9 ± 0.2
G2/M	13.9 ± 6.0	9.2 ± 3.7	10.1 ± 4.6	6.6 ± 1.1
Sub G0/G1	0.8 ± 0.1	1.5 ± 0.6	1.9 ± 0.7	1.5 ± 0.2

Table R.5. Percentage of cells in each of the cell cycle phases after treatment with TAK-228, TAK-117, and TAK-228 + TAK-117. Each value represents the mean ± standard error of the mean.

R.5.1.3. Effects of TAK-228 plus TAK-117 on autophagy

The effects of the TAK combination on autophagy were analyzed in RT4 cells. TAK-117 slightly increased the levels of LC3-II and induced a small decrease in p62/SQSMT1 compared to the control. In the combined treatment we observed more LC3-II than in the other conditions, suggesting that the combination may enhance the activation of autophagy (**Figure R.24.**).

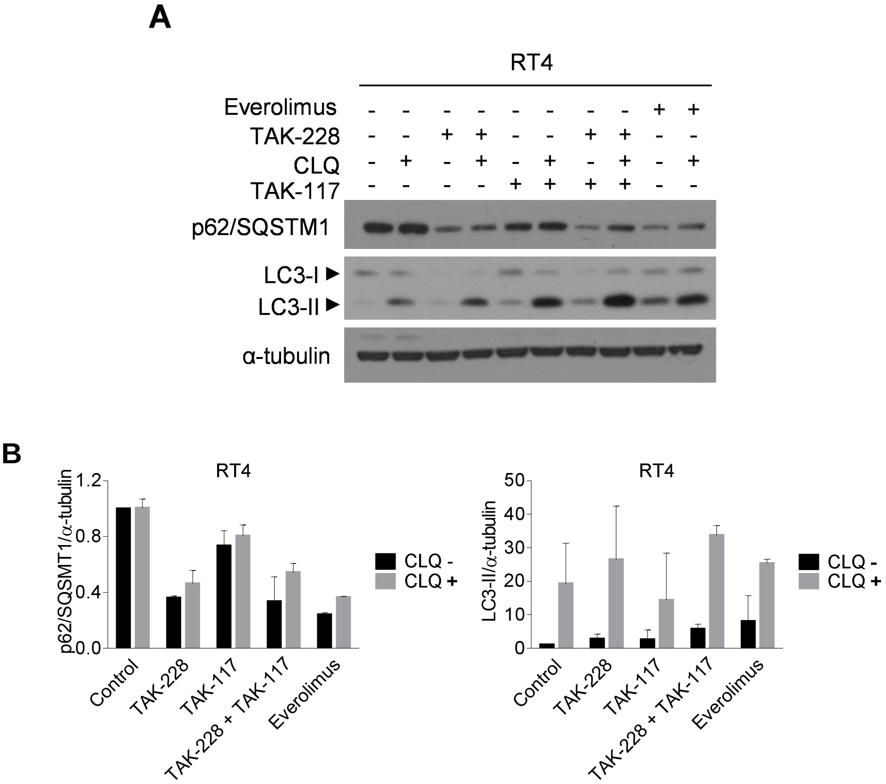

Figure R.24. The action of TAK-228 plus TAK-117 on autophagy. A. Cells were treated with TAK-228 and TAK-117 at the corresponding IC50 values [24.3nM and 15.7μM, respectively], or with a combination of the two drugs in the presence or absence of chloroquine (CLQ) [5μM], for 24

hours. Everolimus [100nM] was used as a control. Cell lysates were analyzed using western blot for p62/SQSMT1 and LC3-II. Representative images of two separate experiments are shown. **B.** The graphs show the levels of p62/SQSMT1 and LC3-II in each condition expressed as fold induction versus control arbitrarily set at 1.

R.5.2. Molecular effect of TAK-228 plus TAK-117 on BC cells

PI3K/AKT/mTOR pathway markers were analyzed in cell lysates of RT4 and CAL-29 cells treated with the drug combination. In both cell lines, at 24 hours, treatment with TAK-228 plus TAK-117 had significantly reduced S6 and 4E-BP1 phosphorylation, compared with each drug on its own. In CAL-29 cells, the combined treatment also led to a greater reduction in the phosphorylation of AKT (**Figure R.25.**).

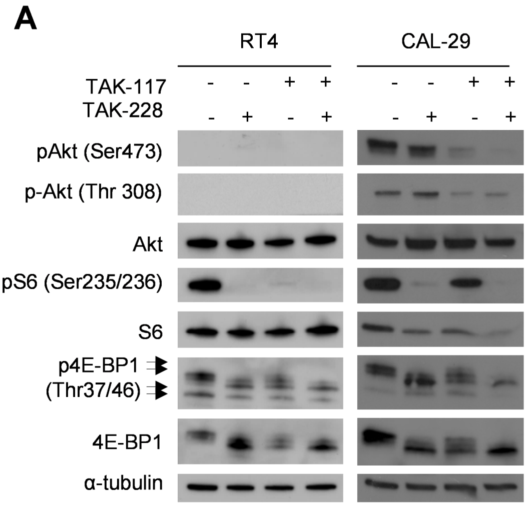
A
RT4
CAL-29
TAK-117 - - + + - - + +
TAK-228 - + - + - + - +
pAkt (Ser473)
p-Akt (Thr 308)
Akt
pS6 (Ser235/236)
S6
p4E-BP1
(Thr37/46)
4E-BP1
α-tubulin

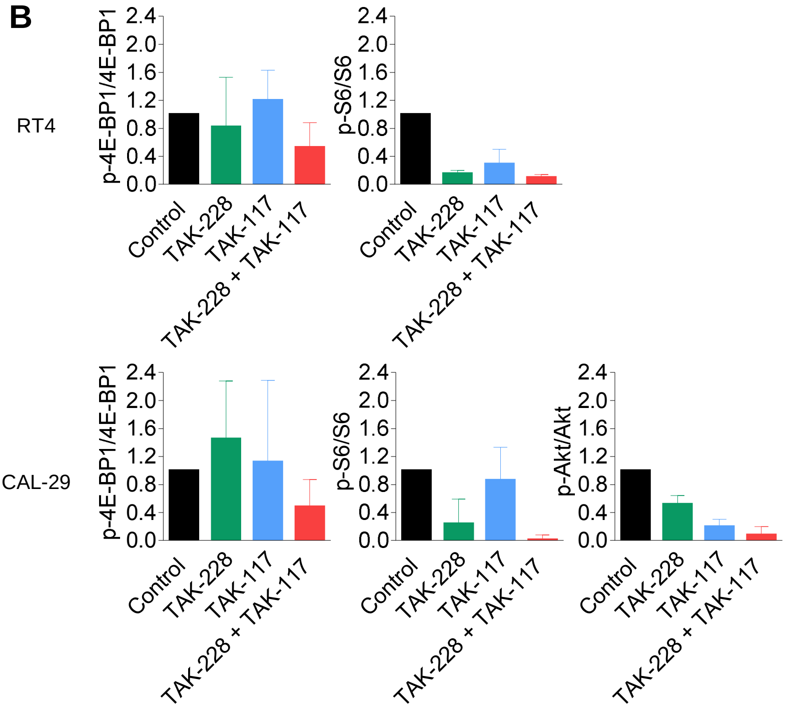

Figure R.25. Effect of TAK-228 and TAK-117 co-treatment on the PI3K/AKT/mTOR pathway *in vitro*. A. RT4 and CAL-29 cells were treated with TAK-228 and TAK-117 at the corresponding IC50 values, as well as the combination of the two drugs, for 24 hours. Cell lysates were assayed using western blot with the indicated antibodies. Representative images from two different experiments are shown. **B.** The graphs show the ratio of phosphorylated to total protein in each condition expressed as fold induction versus control arbitrarily set at 1.

We then used CAL-29 cells to analyze the effects of the combination over time. In the combined treatment, the inhibition of AKT, S6, and 4E-BP1 phosphorylation was higher than with each drug alone, and this effect was sustained until 72 hours, suggesting that there is greater inhibition of the pathway with the combination (**Figure R.26.**).

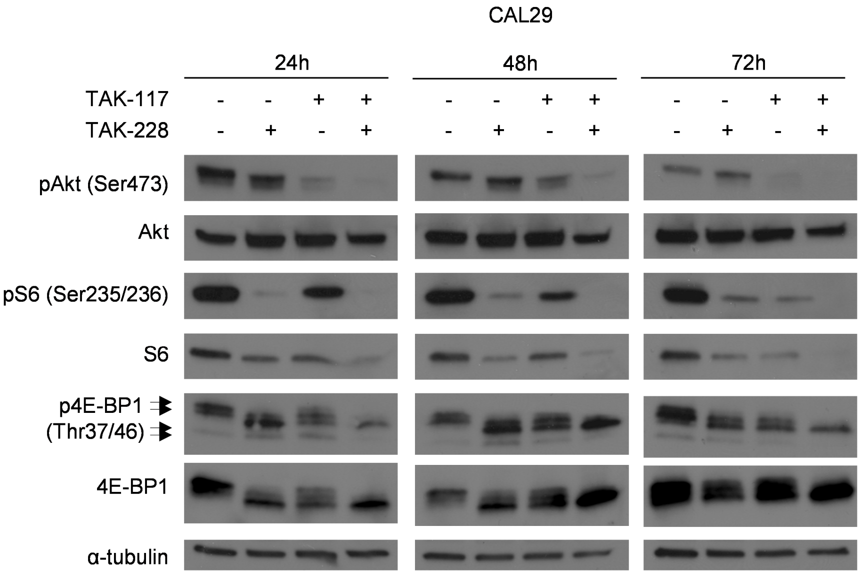
CAL29
24h
48h
72h
TAK-117 - - + + - - + + - - + +
TAK-228 - + - + - + - + - + - +
pAkt (Ser473)
Akt
pS6 (Ser235/236)
S6
p4E-BP1
(Thr37/46)
4E-BP1
α-tubulin

Figure R.26. Effect of continuous TAK-228 and TAK-117 co-treatment on the PI3K/AKT/mTOR pathway *in vitro*. CAL-29 cells were treated with TAK-228 and TAK-117 at the corresponding IC50 values, as well as the combination of the two drugs, for 24, 48 and 72 hours. Cell lysates were assayed using western blot with the indicated antibodies. Representative images from two different experiments are shown.

We can conclude that the combination acts synergistically *in vitro* in inhibiting cell proliferation and is superior to either of the drugs on their own.

R.5.3. *In vivo* effects of TAK-228 plus TAK-117 on the RT4 xenograft model

To validate our *in vitro* results, the antitumor effects of the combination were analyzed using the RT4 xenograft model.

R.5.3.1. Effects of TAK-228 plus TAK-117 on tumor growth

The mice were divided into four groups (sixteen animals each): control (PEG400 solvent); 1mg/Kg TAK-228 three times per week; 140mg/Kg TAK-117 three times per week; and 1mg/Kg TAK-228 + 140mg/Kg TAK-117 three times per week. In this model, the combination significantly (p=0.001) improved the antitumor effects compared to either of the drugs on their own (**Figure R.27.**).

We calculated the fold-change in tumor growth of each condition, obtaining the lowest value for the combination (2.5 for the control; 2.1 for TAK-228; 2.2 for INK1117; and 1.5 for TAK-228 + TAK-117). In addition, we calculated the TGI (tumor growth inhibition: TGI= 100-[(treated average volume /control average volume) x100]) for each condition, obtaining a 41.1% inhibition of tumor volume for the combination compared with the control group.

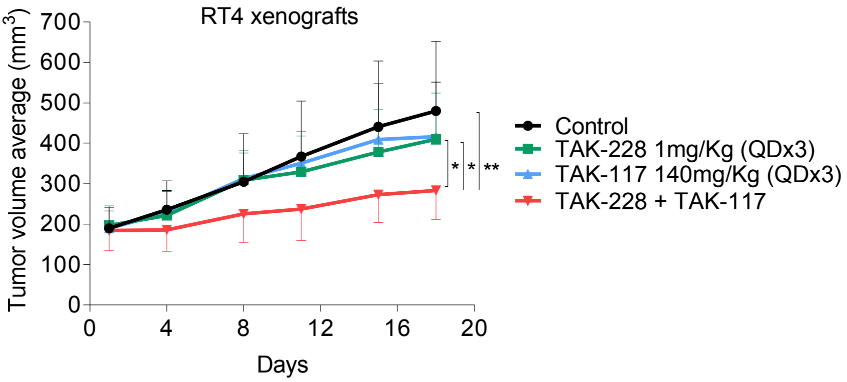

Figure R.27. Effects of TAK-228 combined with TAK-117 *in vivo*. Mice were treated for 3 weeks as indicated. Each treatment group consisted of sixteen mice. A plot of average tumor volume as a function of time in each treatment group is shown. * $p<0.05$, **$p<0.01$.

R.5.3.2. Effects of TAK-228 plus TAK-117 on tumor samples

Animals were sacrificed when the tumor mass of control group reached 700 mm^3. Tumors were excised and stained with pS6 Ser235/236, p-H3, and c-caspase 3. p-S6 decreased in tumors treated with either TAK-228 or TAK-117, with the greatest reduction in phosphorylation being seen with the combination. pH3 decreased in the treatments with the individual drugs but the largest decrease was seen with the combination. On the other hand, cleaved caspase-3 was found to increase with the combination compared to single agents. Individually, TAK-228 and TAK-117 had very little effect on cleaved caspase-3 (**Figure R.28.**).

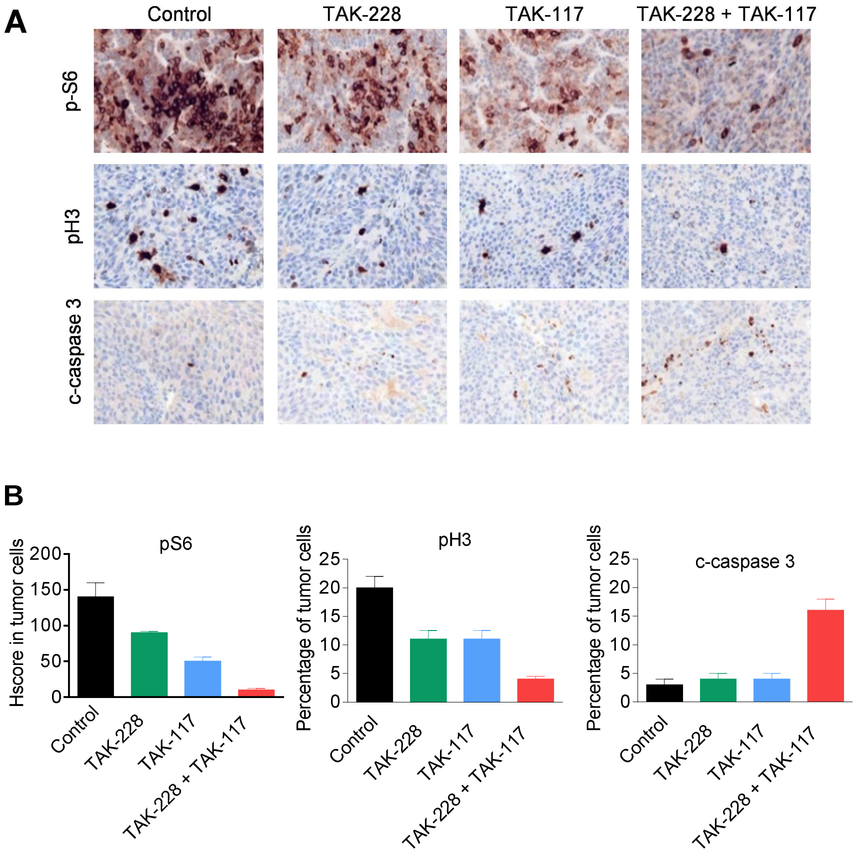
A
Control
TAK-228
TAK-117
TAK-228 + TAK-117
p-S6
pH3
c-caspase 3
B
pS6
Hscore in tumor cells
200
150
100
50
0
Control
TAK-228
TAK-117
TAK-228 + TAK-117
pH3
Percentage of tumor cells
25
20
15
10
5
0
Control
TAK-228
TAK-117
TAK-228 + TAK-117
c-caspase 3
Percentage of tumor cells
25
20
15
10
5
0
Control
TAK-228
TAK-117
TAK-228 + TAK-117

Figure R.28. Effect of TAK-228 combined with TAK-117 on xenograft tumor sections. **A.** Representative images of tumor samples stained for pS6 Ser235/236, p-H3, and cleaved caspase-3. The data are representative of independent tumors harvested from 5 mice. **B.** Box plots illustrate the staining results. Each graph is expressed as: H-score in tumor cells (p-S6(Ser235/236)) and percentage of stained-tumor for p-H3 (H3P) and cleaved caspase-3.

In addition, we used western blot to analyze the pathway markers in 3 representative tumors from each group. We observed a decrease in the phosphorylation of S6 and 4E-BP1 for each drug individually, as well as for the combination. The reduction of the proteins was slightly higher for the combination, although this was not significant (**Figure R.29.**). These results show the same trend as those obtained *in vitro* using cell lysates.

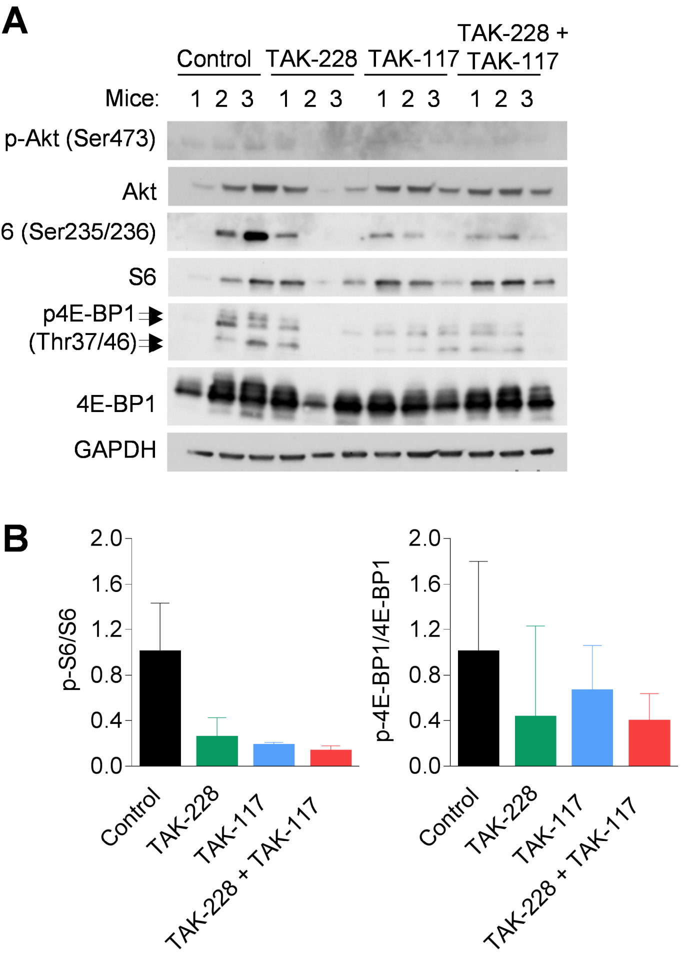

Figure R.29. Molecular effects of TAK-228 combined with TAK-117 in tumor samples. A. Tumor lysates were analyzed using western blot with the indicated antibodies. Tumors from three mice for each condition were checked. **B.** The graphs show the ratio of phosphorylated to total protein in each condition expressed as fold induction versus control arbitrarily set at 1.

We concluded that in the RT4 xenograft model, the combined TAK-228 plus TAK-117 treatment is more effective than either of the agents tested individually.

R.6. CHARACTERIZATION OF THE COMBINATION OF TAK-228 PLUS PACLITAXEL

We tested whether TAK-228 could enhance the effects of chemotherapy. To do this, we selected paclitaxel, as it is used as a second line treatment in BC.

R.6.1. Cellular effects of TAK-228 plus paclitaxel on BC cells

First, we analyzed the effect of the paclitaxel treatment on its own, followed by the effect of the TAK combination on cell viability in two BC cell lines. Finally, as we had done previously for TAK-228, to better characterize the combination, we analyzed its effects on cell cycle and autophagy.

R.6.1.1. Effects of TAK-228 plus paclitaxel on cell viability

First, we tested the effects of Paclitaxel on cell viability in RT4 and CAL-29 cells. As expected, we observed that both cell lines were sensitive to the drug (**Figure R.30.**).

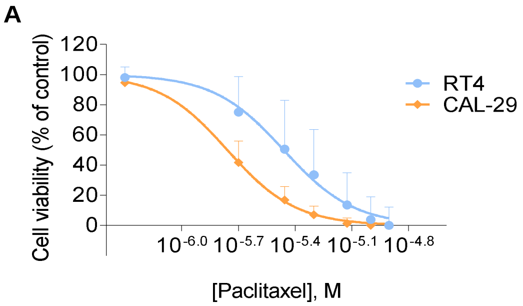

B

Cell line	**Paclitaxel [nM]**
RT4	5.3 ± 0.8
CAL-29	3.2 ± 1.2

Figure R.30. Sensitivity of RT4 and CAL-29 cells to Paclitaxel. A. Sensitivity of BC to Paclitaxel at 72 hours assessed through MTS assay. Values shown are the mean percentage +/- SD of cell viability relative to controls, plotted as dose-response curves using GraphPad Prism. **B.** IC50 values of Paclitaxel for RT4 and CAL-29. Incorporates data from three replicate experiments.

In order to analyze the proliferation effects of TAK-228 in combination with Paclitaxel we tested the drug combination on RT4 and CAL-29 cell lines. We treated the cells with two modalities: simultaneously with TAK-228 and paclitaxel; or first with just paclitaxel for 24 hours, after which time TAK-228 was added and cells were incubated for 48 hours. Concomitant treatment significantly improved the individual effects of the drugs in RT4 cells. The same trend was observed in CAL-29 cells, although this was only significant in TAK-228 versus TAK-228 plus paclitaxel.

We obtained similar results with both the concomitant treatment and sequential therapy. In both cell lines, the combination significantly reduced cell proliferation compared to each individual treatment.

CONCOMITANT TREATMENT: TAK-228 + Paclitaxel

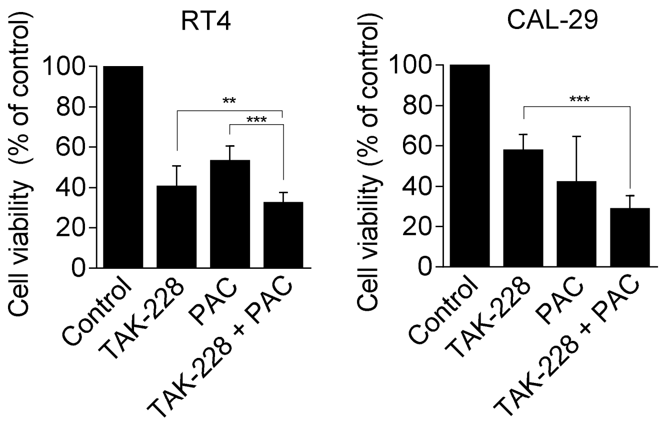

SEQUENTIAL TREATMENT: Paclitaxel ⟶ TAK-228

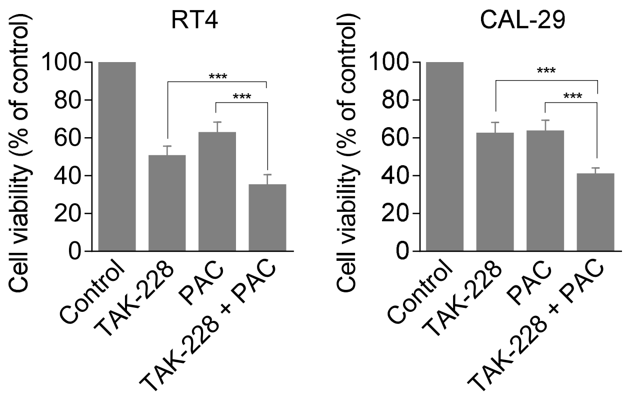

Figure R.31. Effects of TAK-228 combined with paclitaxel in RT4 and CAL-29 cells. Cells were treated with TAK-228 and paclitaxel (PAC) at the corresponding IC50 values for each drug/cell [RT4: 24.3nM and 5.3nM; CAL29: 30.1nM and 3.2nM, respectively]. Cells were treated in two ways: simultaneously with TAK-228 and paclitaxel (top), or first with paclitaxel for 24 hours, then TAK-228 was added and the cells were incubated for 48 hours (bottom). Cell viability was measured through MTS. The results are expressed as percentage of viable cells in the vehicle-treated control wells. **p<0.01, *** p<0.001.

R.6.1.2. Effects of TAK-228 plus Paclitaxel on cell cycle

The cell-cycle progression of RT4 cells was affected by both TAK-228 and paclitaxel. As we have described previously, TAK-228 increases the number of cells in the G0/G1 phase of the cell cycle. However, treatment with paclitaxel leads to an important reduction in the number of cells in the G0/G1 phase and induced cell cycle arrest in G2/M. Under control conditions 19.9 ± 4.1% of cells were in the G2/M phase, but when the cells were treated with paclitaxel the percentage of cells in this phase increased to 74.4± 3.0%. In the treatment with TAK-228 in combination with paclitaxel, we observed overlapping effects of TAK-228 and paclitaxel. We saw that the combination increases the G2/M phase and decreases the G0/G1 phase with respect to the control, but these changes were lower than with paclitaxel alone (**Figure R.32.**). The percentage of cells in each of the cell cycle phases is shown in **Table R.6.**

RT4				
Phase	**Control**	**TAK-228 [24nM]**	**Paclitaxel [7nM]**	**TAK-228 + paclitaxel**
G0/G1	67.8 ± 4.1	75.7 ± 8.5	17.1 ± 4.1	45.1 ± 2.8
S	11.5 ± 0.1	8.9 ± 3.6	6.8 ± 0.4	11.6 ± 0.9
G2/M	19.9 ± 4.1	14.8 ± 4.7	74.4 ± 3.0	42.7 ± 4.9

Table R.6. Percentage of cells in each of the cell cycle phases after treatment with TAK-228, paclitaxel, and TAK-228 + paclitaxel. Each value represents the mean ± standard error of the mean.

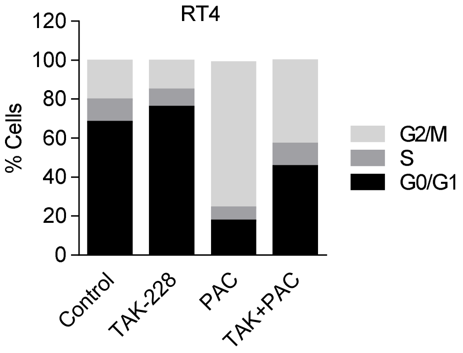

Figure R.32. Effects of TAK-228 combined with paclitaxel on cell cycle distribution. Cell cycle distribution after 24 hours of simultaneous treatment with TAK-228 and paclitaxel (PAC) at the corresponding IC50 values [24.3nM and 5.3nM, respectively], and the combination of the two drugs for 24 hours. Fixed and propidium iodide stained cells were analyzed using flow cytometry. The bar chart shows the percentage of cells at different cell stages.

After G2/M arrest, several tumor types exhibit significant apoptosis. We checked the effects of paclitaxel combined with TAK-228, and paclitaxel on its own on the RT4 cell line. Paclitaxel increased the number of apoptotic cells, although we did not find more apoptotic cells in the combined drug treatment (**Figure R.33.**).

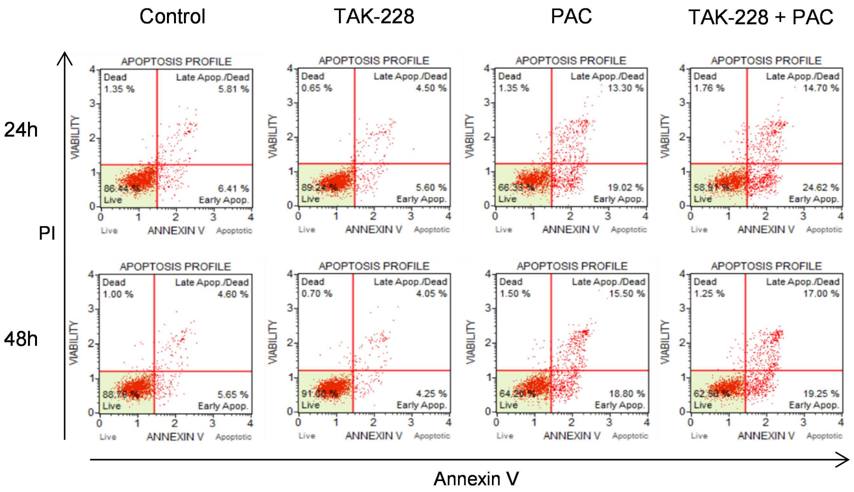

Figure R.33. The action of TAK-228 plus paclitaxel on apoptosis in RT4 cells. Representative flow cytometry dot plots of two independent experiments are shown after simultaneously treating the cells with TAK-228 and paclitaxel (PAC) at the corresponding IC50 values [24.3nM and 5.3nM, respectively], and the combination of the two drugs, for 24 and 48 hours.

Time	% of cells	Control	TAK-228 [24nM]	Paclitaxel [5.3nM]	TAK-228 + Paclitaxel
24h	**Live**	89.3 ± 4.1	91.2 ± 2.9	79.5 ± 18.7	77.1 ± 25.7
	Total apoptotic	9.5 ± 3.8	7.9 ± 3.2	19.1 ± 18.7	21.8 ± 21.8
48h	**Live**	89.4 ± 1.1	91.0 ± 0.0	68.7 ± 6.4	72.2 ± 13.7
	Total apoptotic	8.8 ± 1.9	7.9 ± 0.6	29.0 ± 7.5	25.5 ± 15.3

Table R.7. Percentage of live and apoptotic cells after the treatment with TAK-228, paclitaxel, and TAK-228 + paclitaxel. Each value represents the mean ± standard error of the mean.

R.6.1.3. Effects of TAK-228 plus Paclitaxel on autophagy

The effects on autophagy were also analyzed for this combination in RT4 cells. Paclitaxel used as single agent did not reduce p62/SQSMT1 levels, but did increase the levels of LC3-II. The combination of both drugs reduced the levels of p62/SQSMT1 and increased the levels of LC3-II, suggesting that the conversion of LC3-I to LC3-II is greater under this condition. It might be that the process of autophagy is more active when the cells are treated with the combination, however, with these results we could not conclude what role paclitaxel plays in the process of autophagy under the test conditions.

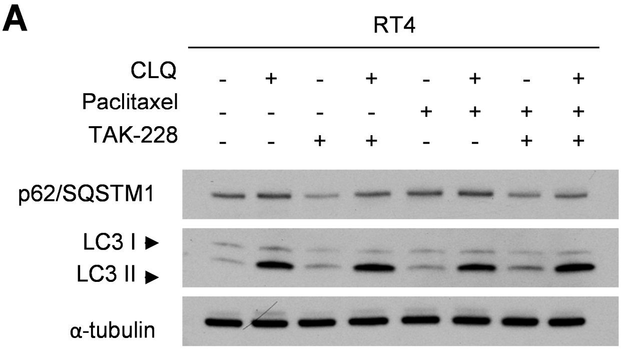

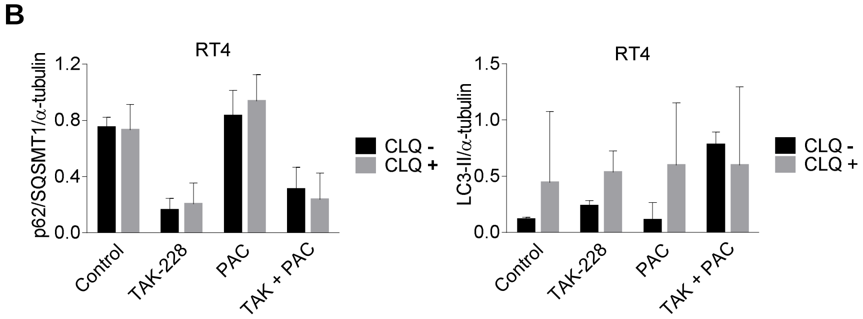

Figure R.34. The action of TAK-228 plus paclitaxel on autophagy. A. Cells were treated simultaneously with TAK-228 and paclitaxel (PAC) at the corresponding IC50 values [24.3nM and 5.3nM, respectively], as well as the combination of both drugs in the presence or absence of chloroquine (CLQ) [5µM], for 24 hours. Cell lysates were analyzed using western blot for p62/SQSMT1 and LC3-II. Representative images of two separate experiments are shown. **B.** The graphs show the levels of p62/SQSMT1 and LC3-II in each condition expressed as fold induction versus control arbitrarily set at 1.

R.6.2. Molecular effects of TAK-228 plus Paclitaxel in BC cells

The molecular effects on the PI3K/AKT/mTOR pathway of adding paclitaxel to TAK-228 treatment were analyzed in RT4 cells. We observed that the combination did not enhance the inhibitory effects of TAK-228 on this pathway under the conditions tested.

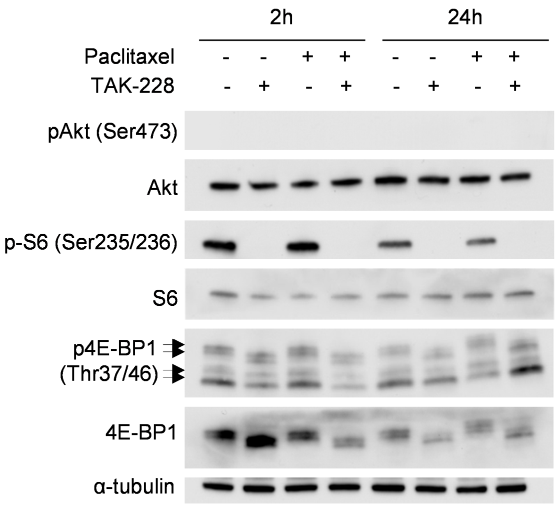

Figure R.35. Effect of TAK-228 and paclitaxel co-treatment on the PI3K/AKT/mTOR pathway *in vitro*. RT4 cells were treated simultaneously with TAK-228 and paclitaxel at the corresponding IC50 values, as well as the combination of both drugs, for 2 and 24 hours. Cell lysates were assayed using western blot with the indicated antibodies. Representative images from two different experiments are shown.

R.6.3. *In vivo* effects of TAK-228 plus Paclitaxel on the RT4 xenograft model

The combination of TAK-228 and paclitaxel was tested *in vivo* on the RT4 xenograft model to validate the results obtained *in vitro*. The first step was to experimentally determine the dose of paclitaxel suitable for use in the combined-drug experiment. We then evaluated the effects of TAK-228 plus paclitxel administered as a sequential combination.

R.6.3.1. Establishing treatment conditions for in vivo experiments with paclitaxel

For the experiments testing paclitaxel as a single agent, we tested several doses based on previous results from other groups. Mice were initially treated with 7mg/kg once per week, injected intraperitoneally. If there was no unacceptable toxicity, the next dose administered was increased to 10 mg/kg, followed by 15 mg/kg. In case of serious toxicity in one or more mice at 10 or 15 mg/kg, we planned to decrease the dose to the previously tolerated level. The optimal dose for the combined-drug experiments was defined as two consecutive doses with no toxicity.

We treated the animals with paclitaxel once a week following the established protocol. The mice showed no signs of toxicity at any dose. We administered 15mg/kg Paclitaxel three times: the dose was well tolerated and we also observed a slight decrease in tumor volume. We defined this dose as the optimal dose for the combined assays.

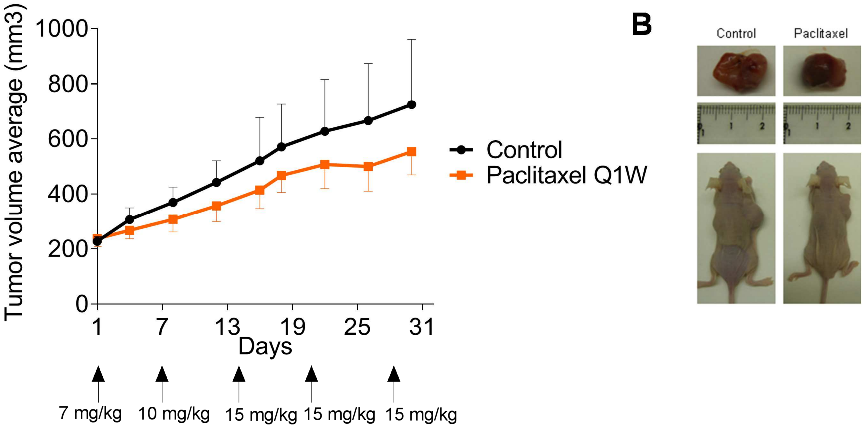

Figure R.36. Establishing the optimal dose of paclitaxel for the *in vivo* experiments. A. RT4 tumor-bearing mice were treated once a week with increasing doses of paclitaxel as indicated. Follow-up of the tumor was undertaken over 33 days. Each treatment group consisted of six mice. A plot of average tumor volume as a function of time in each treatment group is shown. **B.** Representative photographs of tumor-bearing mice and the excised tumors.

R.6.3.2. Effects of TAK-228 plus Paclitaxel on tumor growth

The mice were divided into four groups (eight animals in each): the control (PEG400 and water); Paclitaxel 15mg/Kg once per week; and TAK-228 1mg/Kg three times per week. In the fourth group, the combination group, the animals were treated with Paclitaxel and 24 hours later with TAK-228 1mg/Kg, three times per week.

Both drugs individually led to significantly smaller mean tumor volumes compared with the control. The reduction of tumor volume by the 2-drug combination was significantly higher than for each drug on its own (p<0.001). We calculated the reduction in tumor growth under the various conditions, obtaining the lowest value for the drug combination (4.7 for the control; 2.8 for Paclitaxel; 2.7 for TAK-228; and 1.9 for TAK-228 + Paclitaxel). In addition, we calculated TGI and obtained a 61.5% inhibition of tumor volume for the combination compared to the control.

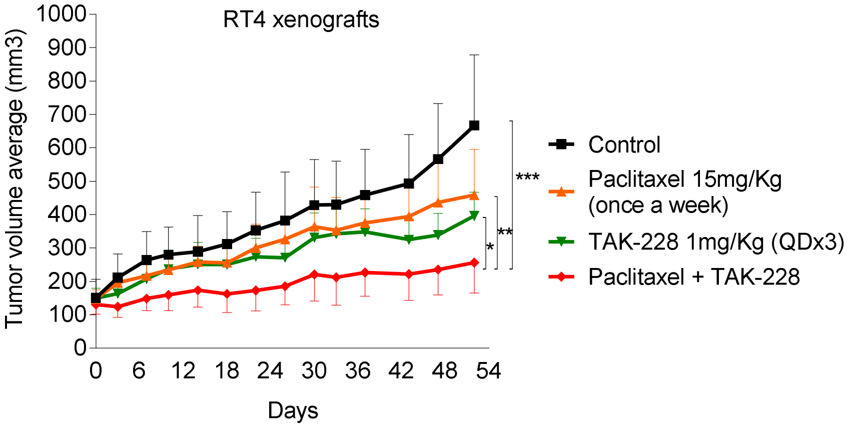

Figure R.37. Effects of TAK-228 combined with Paclitaxel *in vivo*. Mice were treated for 54 days as indicated. Each treatment group consisted of eight mice. A plot of average tumor volume as a function of time in each treatment group is shown. * p<0.05, **p<0.01, *** p<0.001.

Despite the fact we were unable to determine the exact mechanism by which TAK-228 potentiates the effect of paclitaxel, the *in vitro* results confirm that TAK-228 improves the effect of paclitaxel.

DISCUSSION

DISCUSSION

Current treatment for patients with advanced bladder cancer is mainly cisplatin-based combination chemotherapy with recent beneficial effects observed with the use of immune checkpoint inhibitors. Any other form of targeted therapy that use targeted agents to directly kill tumor cells is approved for bladder cancer, underscoring the need for more intensive research in this area. As genetic alterations in members of the PI3K/AKT/mTOR pathway have been found in bladder tumors [8] with some potential for therapeutic intervention, we focused our work on the study of TAK-228 (formely MLN0128/INK128), an investigational oral and selective adenosine triphosphate (ATP) site kinase inhibitor of both mTORC1 and mTORC2 as a possible option for bladder cancer patient [15]. In addition, we analyzed other strategies to inhibit the pathway. For that we studied two other small molecule inhibitors (everolimus and TAK-117) and compared their effects with the effects of TAK-228In our study, we used bladder cancer cells with different genetic features in the PI3K/AKT/mTOR pathway to mimic the diversity of gene mutations in BC patients.

TAK-228 as a possible treatment for bladder cancer

mTORC1/2 dual inhibitors, also known as the second generation of mTOR inhibitors, are widely studied both in preclinical and clinical settings as potential anti-cancer therapies various types of cancer [113-116]. In this work we characterized the effects of TAK-228 in preclinical models of BC.

Our study shows that TAK-228 inhibits cell growth *in vitro*of BC cells with diverse genetic backgrounds in the PI3K/AKT/mTOR pathway, more efficiently than everolimus/RAD0001To better understand which is the mechanism by TAK-228 induces antiproliferation effects we analyzed some of the most relevant cellular processes regulated by mTOR. The results obtained from flow cytometric assay clearly revealed that TAK-228 treatment *did* affect the distribution of cells in G0/G1 phase*.* This method did not identified apoptotic cells under our experimental conditions. Results of other groups are in accordance with ours instead there are some contradictory results. TAK-228 or other mTORC1/2 inhibitors induced G0/G1 arrest and activated apoptosis in some but not in all preclinical cancer models. TAK-228 induced apoptosis in breast, myeloma, pancreas and neuroblastoma cancer cells among others [85, 90, 108, 109] suggesting that the effects on apoptosis might depend on the cell type or the cell context. This leads to think that TAK-228 effects are more cytostatic than cytotoxic in our BC models.

We demonstrated that TAK-228 induces autophagy. The role of autophagy in cancer is complex and it is unclear whether autophagy suppresses or promotes tumorigenesis. Also can induce drug resistance or sensitize cells to therapies [61, 117-119]. It has been described that autophagy has cytotoxic effects and can contribute to cell death by a mechanism independent of apoptosis [118, 120]. We have analyzed the effects of TAK-228 on apoptosis, but not other mechanisms that could be related to autophagy death. In addition, it has been described that autophagy can produce cytostatic effects mediated by growth inhibition or associated with senescence [118]. We believe that TAK-228 exhibited anti-tumor effects at least in part though induction of authophagy. This possibility was not exhaustively elucidated in our investigations and will require future skillfully designed experiments *(*i.e. with autophagic inhibitors*)* to provide a clearer and complete confirmation. Modulation of autophagy represents a new opportunity for cancer treatment and inducers and/or inhibitors of autophagy in combination with other therapies are being studied in the clinic [61]. Both induction and inhibition of autophagy have been proven to be beneficial in the treatment of cancer. So, TAK-228 should be studied as an inductor of autophagy for the treatment of cancer.

We demonstrated the efficiency of TAK-228 on inhibiting the downstream targets of mTORC1 and mTORC2 (S6, 4E-BP1 and AKT). The mTORC1 pathway and its downstream effectors (S6K1 and 4E-BP1) have a key role in cell growth and cell cycle progression [28, 121, 122]. These processes may be affected when mTORC1 is inactivated by TAK-228. In addition, in the most sensitive cell line to the drug, RT4, we observed high inhibition of 4E-BP1 by TAK-228. 4E-BP1 protein acts as a repressor of the translation initiation factor eIF4E and therefore plays an important role on protein synthesis [48]. eIF4E regulates the translation of mRNAs whose protein products are well recognized to contribute to malignancy, among them c-*myc*, cyclin D1, angiogenesis factors (FGF-2 and VEGF), and and MMP-9 [123]. Dephosphorylated 4E-BP1 binds with eIF4E preventing mRNA translation. We think that the inhibitory effects of TAK-228 may contribute to repress the protein synthesis of these mRNAs.

We observed reduction of the phosphorylation of AKT, a direct downstream target of mTORC2, suggesting that the AKT activity is decreased and consequently its signaling might be inhibited. However, we observed a slightly recover in the phosphorylation of the threonine site, consistent with previous studies, that could be explained by reactivation of PI3K due to RTKs [124]. It may be a limitation of this kind of mTOR inhibitors.

mTORC2 is a critical regulator of cytoskeleton reorganization [28]. Moreover it has been implicated in invasion and metastasis in colon and breast cancer [125, 126]. It is described that mTORC2 is a central regulator of cell migration and invasion in BC [127]. Thus makes it an attractive target for cancer therapy. We have not studied the effects of TAK-228 on these processes but we hypothesize that the inhibition of mTORC2 induced by TAK-228 might affect these processes and prevent or limit invasion.

More strikingly, we also demonstrated the drug's efficacy *in vivo*. TAK-228 treatment significantly results in dose-dependent growth inhibition on tumor growth in RT4-tumor bearing nude mice model.

We also studied markers of angiogenesis in the tumor samples after the treatment with TAK-228 since it is known that PI3K/AKT/mTOR pathway plays a key role in angiogenesis [128]. Rapamycin and rapalogues reduce VEGF-A levels in renal cancer models and inhibit primary or metastatic tumor growth by angiogenesis [129, 130]. We also demonstrated in the RT4 xenograft model that TAK-228 reduces angiogenesis. We think that it could be translated in clinical benefit for patients with alterations in this pathway.

Several preclinical studies demonstrated that TAK-228 is efficient in solid tumors and hematological malignancies [66, 86, 88, 90, 108, 109, 131-133].

TAK-228 has potential to be a potent anti-cancer agent due to its effects on cell proliferation, cell cycle, tumor growth and angiogenesis. TAK-228 is able to strongly inhibit the PI3K/AKT/mTOR pathway in cells with alterations in members of this route and affects important cellular processes regulated by mTOR.

TAK-228 is superior than everolimus

mTORC1/2 inhibitors were developed to improve the effects of the classic mTOR inhibitors (mTORC1 inhibitors). We compared TAK-228 with everolimus in our BC models in order to analyse the differences between the two types of drugs targeting mTOR.

Previous preclinical studies suggest that inhibition of mTOR by mTORC1 inhibitors results in inhibition of BC cell growth [72, 73, 134]. However, rapalogues have modest clinical activity against various tumors which is sometimes attributed to their incomplete inhibition of 4E-BP1 phosphorylation and/or the lack of mTORC2 inhibition [135].

TAK-228 shows greater reduction of the cell proliferation and the inhibition of the PI3K/AKT/mTOR pathway than everolimus. TAK-228 has stronger effects on mTORC1 downstreams (S6 and 4E-BP1) than everolimus. The fact that everolimus only induces inhibition of mTORC1 limits its efficacy and therefore induces incomplete inhibition of the pathway. This limitation could be explained by the disruption of the feedback loop (via S6K) that occurs after the mTORC1 inhibition and that induces the AKT activation [63]. TAK-228 inhibits the phosphorylation of AKT and prevents the compensatory loop that occurs when mTORC1 is inhibited. In conclusion, TAK-228 inhibits TORC1/2-dependent signaling in preclinical models of bladder cancer. TAK-228 appears to be superior in blocking mTORC1/2-signaling in contrast to rapamycin.

Preclinical studies with other dual mTORC1/2 inhibitors (PP242, OXA-01, OSI-027) in other tumor cell types demonstrated that dual inhibitors are better inhibitors of the PI3K/AKT/mTOR pathway than rapalogues [78, 80, 82, 136].

TAK-228 improves the effects and overcome the limitations of the classical mTOR inhibitors suggesting that it might have better effects in the clinic than everolimus.

TAK-117 as a possible treatment for bladder cancer

PI3K inhibitors are being studied as a possible therapy in solid tumors due to the important role of PI3K in cancer. The first-generation of PI3K inhibitors, pan-PI3K inhibitors that target all the isoforms of the protein, may be better suited to treating PI3K pathway–activated tumors associated with heterogeneous molecular alterations [62]. However, pan-PI3K inhibitors have encountered problems in clinical trials. The pan-PI3K inhibitors have limitations because of the unspecific effects (inhibition of other PI3K-related kinase family) and the possible toxicities. In addition, it is recognized that the four isoforms of the class I PI3K play different roles depending on the type of malignancy and the genetic aberrations it harbors. This has led to the development of isoform-selective inhibitors that are expected that they might be more specific and better tolerated than the pan-PI3K inhibitors [137].

The frequency of mutations in the *PI3KCA* gene in BC and the development of the new generation of PI3K inhibitors led us to study TAK-117, a selective PI3Kα, as a possible treatment for BC.

We demonstrated the efficiency of TAK-117 as an antitumor agent that reduces the proliferation of some BC cell lines (CAL-29 and TCCSUP) and also inhibits the tumor growth of the CAL-29 xenografts. We observed different sensitivities to TAK-117, with the greater effects in the cells mutated in the *PI3KCA* gene, CAL-29 (*PI3KCA* H1047R) and TCCSUP (*PI3KCA* E545K). On the other hand, HT-1197 cells, mutated in the *PI3KCA* gene (E545K) and also RAS mutated, were primary resistant to TAK-117.

Our results are in accordance with published data that suggests some alterations in the PI3K gene as possible biomarkers of response to these drugs. Mutation of *PI3KCA* gene (E545K and H1047R), and *PI3KCA* amplification or *ERBB2* amplification correlate with sensitivity to PI3Kα inhibitors, whereas *PTEN* and *BRAF* mutations, and coexistent *PIK3CA* and *KRAS* mutations are associated with resistance [62, 138]. Furthermore, a PI3K inhibitor (GDC-0941) has been shown to be effective in preclinical BC models [94], particularly in cell lines and xenografts with mutations in the PI3KCA gene.

All these results together suggested us to consider TAK-117 as a therapeutic strategy for tumors with over activation of the PI3K/AKT/mTOR pathway especially if they harbor activating mutations in the *PI3KCA* gene. Furthermore, these genetic alterations should be validated as possible predictive biomarkers of response to this drug in BC.

Biomarkers of sensitivity or resistance to TAK-228

The lack of predictive biomarkers of response to PI3K/AKT/mTOR inhibitors makes difficult the selection of the patients and therefore the success of these drugs in the clinic. Identification of biomarkers to help select patients who are most likely to benefit from these drugs is essential and it is being evaluated in the ongoing clinical trials.

TSC1 is the most relevant biomarker of response described for everolimus in BC. TSC1 mutations in bladder cancer are associated to more efficacious responses to everolimus in clinical trials [75]. For that reason we studied this protein as a possible biomarker of TAK-228. We not find correlation between TSC1 and TAK-228 response, probably because of the different inhibitory effects of the drugs on the pathway. However, RT4 cells, that are mutated in TSC1 and do not express the protein, are the most sensitive cells to TAK-228. Considering these results, TSC1 should not be dismissed as a possible biomarker and should be studied in clinical trials with mTORC1/2 inhibitors.

On the other hand, mTORC1/2 inhibitors have recently entered in the clinic and no response biomarkers have been defined yet. In contrast, in preclinical studies, some markers have been proposed [87, 111, 112, 139, 140]. Based on our results we propose two types of biomakers. In first place, basal levels of 4E-BP1, p-4E-

BP/4E-BP1 and eIF4E/4E-BP1 are possible biomarkers that might predict sensitivity to TAK-228. Interestingly, expression of 4E-BP1, p-4E-BP1 and eIF4E were found to be elevated in tumor samples from patients with BC compared to normal bladder tissues [123, 141, 142]. The outcome of these alterations is diverse but they may represent therapeutic targets. Also they may help to stratify patients and select the most suited for the therapy.

And secondly, the inhibition of the phosphorylation of 4E-BP1 after TAK-228 treatment might be a predictive biomarker of the action of the drug.

We could not analysed these biomarkers in patient samples, for that reason further studies should be done to better define whether these markers could predict response to TAK-228 in BC patients.

TAK-228 in combination with other therapies as a possible treatment for bladder cancer

Despite the fact that PI3K/AKT/mTOR pathway inhibitors are promising anticancer agents, clinical data show limited activity of AKT, mTOR, PI3K inhibitors as single-agent [35]. Better effects were observed in combination with other therapies and are studied in clinical trials [67]. It is necessary to define rational combinations with other therapies to maximize the potential of these small-molecule inhibitors.

The cross-talk with other therapies lead to test PI3K/AKT/mTOR pathway inhibitors in combination with other targeted therapies, such as the drugs targeting the RAS-RAF-MEK-ERK cascade [143-

145]. Also are tested in combination with autophagy inhibitors [146-148] or poly(ADP-ribose) polymerase (PARP) inhibitors [149, 150].

It makes sense to combine PI3K/AKT/mTOR pathway inhibitors with the standard chemotherapy used in the clinical practice.

TAK-228 or other dual mTOR inhibitors showed synergistic efficacy in combination with other therapies in several cancer cells *in vitro* [83, 85, 87, 151-154].

We studied two possible combinations between TAK-228 and other therapies looking for improve the TAK-228 effects and establish the best therapy for patients with advanced BC whose tumors have overactivation of the PI3K/AKT/mTOR pathway.

TAK-228 plus TAK-117

We found that the combination with TAK-228 and TAK-117 is synergistic *in vitro* in BC cells and in *in vivo* in the RT4 xenograft model. The combination of both drugs induces higher effects on cell cycle, autophagy and causes a stronger inhibition of the pathway that might maintain prolong inhibition of it. Our results suggest that the double targeting of the pathway is more effective than each drug as single-agent. The combination may be effective in tumors with constitutive activation of the route.

TAK-228 in combination with TAK-117 is tested in clinical trials for solid malignancies according to ClinicalTrials.gov. Taking our results into account, this combination might be interesting to evaluate for the treatment of bladder cancer.

Characterization of the combination of TAK-228 plus Paclitaxel

Taxanes are second line chemotherapy in management of metastatic BC in USA [155]. We studied the combination of TAK-228 and paclitaxel as a possible therapeutic option for patients with advanced BC with mutations in the PI3K pathway.

Paclitaxel has been demonstrated to be an effective mitotic inhibitor and apoptosis inducer to treat aggressive malignancies [156, 157]. We demonstrated that paclitaxel as single agent inhibits the proliferation, induces apoptosis, and increases the G2/M cell cycle phase in BC cells.

The combination of TAK-228 and paclitaxel significantly improves the effects of paclitaxel alone, *in vitro* and *in vivo*. We did different approaches to elucidate the mechanism by which the combination reduces cell proliferation. In the combination treatment we observed apoptosis, cell cycle arrest and activation of autophagy. However, we did not define a clear mechanism of action for the combination. We tested the combination *in vivo* as a sequential treatment and we observed tumor growth inhibition suggesting that it would be a regime to test in clinical trials. These results encourage us to consider this combination as new strategy to further study for the treatment of bladder cancer.

Moreover, TAK-228 demonstrated efficiancy in combination with Paclitaxel in patients with advanced solid malignancies [158].

A clinical trial in patients will be ongoing soon at our Institution (expected data December 2017). The agents that will be investigated in the trial are TAK-228 and paclitaxel and the title is: Phase II Study of Paclitaxel and TAK-228 in metastatic urothelial carcinoma (UC) and the impact of PI3K-mTOR pathway genomic alterations. This is an Investigator initiated study (IIS), the IP is Dr. Joaquim Bellmunt and Hospital del Mar will be the Coordinating Center. At this moment it is in the process of final acceptance and will shortly be presented to the Spanish Sanitary Authorities.

Emergent alternative therapies

A third generation of mTOR inhibitors, known as RapaLink-1, have been recently developed to overcome the mTOR-intrinsec mechanism of resistance. Primary or acquired mutations located in the kinase and the RBD domains of mTOR can reduce the sensitivity to mTOR inhibitors [159]. RapaLinks target the catalytic domain of mTOR and also act as allosteric inhibitors. These drugs may be more effectively delaying the acquisition of mTOR resistance mechanisms than mTOR inhibitors [160].

Other components associated with the PI3K/AKT/mTOR signalling pathway may be useful targets for anticancer therapy. Deregulation in the protein synthesis [47, 123, 161-163] is found in tumors and therapeutic agents that target components of the translational machinery are attractive as anti-cancer therapy [163].

Translational relevance

Our results show that TAK-228 and TAK-117 may represent valuable therapeutic options in patients with advanced bladder cancer. TAK-228 exhibits potential to be combined with other therapies for the treatment of BC.

Patients whose tumors harbor genetic events or proteins alterations that induce uncontrolled constitutively activation of the PI3K/AKT/mTOR pathway, are expected to be sensitive to drugs targeting the pathway. We define specific potential biomarkers of response for TAK-228 or TAK-117 that should be validated in more preclinical studies, as well as in future clinical trials in order to be able to predict which patients are likely to receive the most benefit from PI3K inhibitors or mTORC1/2 inhibitors.

Further studies with TAK-228 alone or in combination with other therapies will be needed to see if this preclinical therapeutic efficacy is translated into clinical benefit for selected bladder cancer patients.

CONCLUSIONS

CONCLUSIONS

1. TAK-228 inhibits cell proliferation of bladder cancer cells with diverse genetic background consistent with activation of the PI3K/AKT/mTOR pathway. RT4 cell line, harboring a TSC1 gene mutation, is significantly more sensitive than the others.

2. TAK-228 induces cell cycle arrest at G0/G1 phase and activates autophagy. However, apoptosis induction was not detected with drug treatment under our experimental conditions.

3. TAK-228 strongly reduces the activation of the PI3K/AKT/mTOR pathway by inhibiting mTORC1 and mTORC2 complexes.

4. The cytostatic and molecular effects of TAK-228 are superior than the effects of everolimus in bladder cancer cells.

5. TAK-228 inhibits, in a dose-dependent manner tumor growth *in vivo* in the RT4 xenograft model and further reduces angiogenesis in the TAK-228 treated tumors compared to vehicle-treated controls.

6. Three possible biomarkers of response to TAK-228 (basal levels of 4E-BP1, p-4E-BP1/4E-BP1 and eIF4E/4E-BP1) were found to be of relevance and should be studied in

more detail in additional preclinical models and patient samples.

7. TAK-117 significantly reduces the cell proliferation of bladder cancer cells that have a *PIK3CA* mutation and no *RAS*. CAL-29 and TCC-SUP cells are the two most sensitive cells to the drug. TAK-117 reduces the activation of the PI3K/AKT/mTOR pathway by dephosphorilating AKT.

8. The combination of TAK-228 plus TAK-117 results in synergistic antiproliferative effects in bladder cancer cell lines and in the RT4 xenograft model in vivo. The molecular inhibition of the pathway is stronger with the combination than with each drug alone.

9. TAK-228 potentiates the antiproliferative effects of paclitaxel *in vitro* and in the RT4 xenograft model *in vivo*.

10. Our preclinical results demonstrate that TAK-228 alone or in combination with other therapies might represent a therapeutic strategy for patients with advanced bladder cancer with tumors with PI3K/AKT/mTOR pathway activation. A clinical trial in patients will be ongoing soon at our Institution.

MATERIAL AND METHODS

MATERIAL AND METHODS

M.1. CELL LINES AND CELL CULTURE

Six bladder cancer cell lines were used in this study. T24, HT-1197, TCC-SUP, UM-UC3 and RT4 were obtained from ATCC. CAL-29 was purchased from DSMZ. All cell lines were grown in Minimum Essential Medium (Live Technologies, Inc. Ltd.) supplemented with 10% fetal bovine serum (FBS, Sigma-Aldrich), 2 mM/L L-glutamine (Live Technologies, Inc. Ltd.) and penicillin (100units/ml), streptomycin (100µg/ml) (Live Technologies, Inc. Ltd.). All cell lines were maintained at 37ºC in a humidified atmosphere containing 5% CO_2.

M.2. DRUGS

TAK-228 and INK1117 were provided by Millennium Pharmaceuticals, Inc. For *in vitro* studies, drugs were prepared as a 10mM stock solution in DMSO and stored at -20ºC. The stock solution was diluted in culture media for use in the experiments. For *in vivo* studies in mice, TAK-228 and INK1117 were resuspended in PEG400, were sonicated ~15min and then were placed on a rotor and rotated between 1-24 hours until the material was fully dissolved. It could be stored at room temperature during one week.

Paclitaxel was purchased from MerkMillipore and was prepared as a 10mM stock solution in DMSO and stored at -20ºC. The stock solution was diluted in culture media for use in the experiments.

For *in vivo* studies Paclitaxel was obtained from Hospital del Mar (Paclitaxel from Teva, 6mg/ml concentrate for solution for infusion). Paclitaxel was diluted in physiological saline solution for injection (B.Braun Medical).

Everolimus (RAD001) was purchased from Selleckchem and was prepared as a 10mM stock solution in DSMO and stored at -20ºC. The stock solution was diluted in culture media for use in the experiments.

M.3. CELL PROLIFERATION AND CELL VIABILITY

Several approaches were used to assess the effects of different treatments on cell proliferation and viability. MTS assay, which measures the metabolic activity of cells, automated cell counting and crystal violet staining to determine the number of living cells.

M.3.1. MTS assay

To measure the effects of the drugs alone and in combination on the viability of bladder cancer cell lines, cells were seeded at a density of 1.000 to 7.000 per well in 100µl of culture media (based on optimal density for each cell line) in 96-well flat-bottomed plates. After 24 hours of incubation, cells were treated with the drugs alone or in combination. 100µl of 2x drug containing media was added in each well.

After 72h of treatment, cell viability was measured by the MTS CellTiter 96 AQ One solution Cell proliferation assay (Promega) as described by the manufacturer. MTS (tetrazolium compound [3-(4,5-dimethylthiazol-2-yl)-5-(3-carboxymethoxyphenyl)-2-(4-sulfophenyl)-2H-tetrazolium) is bioreduced by cells into a formazan product. Cells that are metabolically active can accomplish by dehydrogenase enzymes the conversion of MTS into aqueous, soluble formazan product.

40µL of 96 AQ One solution reagent were added to each well and the cells were further incubated from 1-4 hours at 37ºC and then recording absorbance at 490nm and 690nm with a microplate spectrophotometer. The percentage of surviving cells to each treatment was estimated by dividing the A490nm-A690nm of treated cells with the A490nm- A690nm of control cells.

All drugs and drug combinations were performed in three independent assays for each cell line.

M.3.1.1. Single agents assays

Cells were treated with escalating doses of TAK-228 (5, 10, 15, 20, 50, 60, 80, 100nM), INK1117 (1,3,5,10,15,20,25 µM) and Paclitaxel (0.5, 2, 3.5, 5, 7.5,10,12.5,15 nM) as single agents.

IC50 (the half maximal inhibitory concentration) values for each drug were determined using Calcusyn (BioSoft).

Drug effects are plotted using dose-response curve by GraphPad Prism Software (GraphPad Software).

M.3.1.2. Combinatorial assays

For combinatorial assays, cells were treated with the combination drugs at their equipotent ratio (e.g. at the ratio of their IC50’s). After the ratio is set, we make a mixture of the two drugs at 4-fold of their IC50’s and serially dilute the mixture (e.g. 2-fold dilutions to 2-fold, 1-fold, 0.5-fold, 0.25-fold and 0.125 fold) to obtain a good dosage range and dose density. This practice provides, in most curves, at least two points in the middle range of approximately 20 to 80% effect.

CI (combinatorial index) values for synergy were determined using Calcusyn (BioSoft) that utilises the methodology applied by Chou and Talalay [164] for formal synergy analysis and using computerized simulations determines the combination index (CI) for quantitative definition of synergism (CI<1), additive effect (CI=1) and antagonism (CI>1). Drug effects are plotted by Graphpad Prism Software.

CI values obtained for each cell line were summarize in a table.

M.3.2. Automatic cell counting

To provide experimental confirmation in some conditions, cell viability was measured by automated counting. Cells were seeded in triplicate in 6-well plates at a density of 20.000 to 90.000 per well (based on optimal density for each cell line) in 3ml. After 24 hours, cells were treated with drugs alone or in combination during 72 hours. Then, cells were tripsinized and resuspended in PBS for counting using the Scepter Automated Cell Counter (Millipore, Billerica, MA). The number of viable cells in each treatment was plotted as percentage of control.

M.3.3. Crystal violet assays

For long-term viability assays (8-10 days), cell viability was determined by Crystal Violet staining. Cells were seeded in triplicate in 6-well plates at a density of 6.000 to 40.000 cells per well in 3ml. The drug is added 24 hours later of platting the cells. After the first treatment, the treatment is repeated every three days in culture. After 7-10 days, culture media was carefully removed and the wells were washed with PBS. Then, Crystal violet solution (10% Acetic acid, 10% Absolute Ethanol and 0,06% Crystal violet) was added in an amount sufficient to cover the surface culture area during at least 1 hour. After that, the plates were washed five times by filling the wells with PBS. Plates were inverted and dried on paper towels. Images of each plate were scanned and quantify. Blue intensity was measured in arbitrary units using ImageJ. The number of viable cells in each treatment was plotted as percentage of control.

M.4. PROTEIN DETECTION

To analyze the expression of different proteins in basal conditions or after the treatment of the drugs, proteins were analyzed by western blot.

First, cells were lysated and the quantity of protein on the cell extracts were determined. Then, western blot was performed.

M.4.1. Total protein extraction

For whole-cell protein extracts, cells were cultured in 100 mm2 plates at a density of $2.5x10^5$ -$1x10^6$ based on optimal density for each cell line. Cells were lysed in ice-cold Lysis buffer (Tris-HCL (pH = 7.4) 50mM, NaCl 150mM, 1 % NP40, EDTA 5mM, NaF 5mM) supplemented with protease inhibitors (Complete Mini EDTA-free Protease inhibitor Cocktail, Sigma) mechanically with the help of an scrapper. After shaking during 20min at 4ºC, the samples were centrifuged 10min at 13.200rpm and the supernatant was aliquoted and stored at -20°C.

M.4.2. Protein quantification

The Bio-Rad Protein Assay based of the method of Bradford was used to determine the concentration of solubilised proteins.

An acidic dye was added to the whole-cell protein extracts and then recording absorbance at 750nm with a microplate spectrophotometer. Comparison to a standard curve of BSA (bovine serum albumin) provides a relative measurement of protein concentration.

M.4.3. Western blot analysis

To determine the expression of specific proteins in different cells or different conditions, the same quantity of protein for each sample (20-40µg) was adjusted to the same volume with lysis buffer. An equal amount of 2X 5% b-mercaptoethanol Laemmly-sample buffer was added to each sample. Samples were denaturalized by 5 minutes at 95ºC. Samples (30µg/lane) were subjected to SDS-page and transferred to PDVF membranes using pre-cast gels and membranes (Bio-Rad). The transfer was done using the Trans-Blot Turbo and the Transfer Packs (including on optimized buffer, membrane, and filter paper) which is a system designed to provide rapid transfers (maximum 10 minutes).

Immunoblotting was carried out according to standard procedure. To block unspecific detection, PDVF membranes were incubated with 5% Milk TBS-T for 1 hour at room temperature. Then, membranes were incubated overnight at 4oC with the specific primary antibody (listed below). After washing 3 times with TBS-T, horseradish peroxidase-conjugated secondary antibodies were used to detect primary antibodies. Membranes were washed again 2 times with TBS-T and 1 time with TBS, and target proteins were visualized after enhanced chemoluminescence treatment (Amersham) of membranes and subsequent exposure to X-ray film.

The following antibodies were purchased from the manufacturers listed below and used for Western blot assay: p-Akt (Ser473), p-Akt (Thr308), Akt, p-S6 (Ser235/236), S6, p-4E-BP1 (Thr37/46), 4E-BP1, eIF4E, p-eIF4E (Ser209), LC3-II, p62/SQSTM1, cleaved-PARP, cyclin D1, TSC1, PTEN and p-GSK3α/β (S21/9) (Cell

Signaling), α-tubulin (Sigma-Aldrich), GAPDH (Santa Cruz) and GSK3β (BD. Biosciences). Mouse and rabbit horseradish peroxidise (HRP)-conjugated secondary antibodies (GE Healthcare Life Sciences) were used.

M.4.4. Western blot quantification by QuantityOne

Bands were scanned from the films and intensities were measured using QuantityOne software. The anti-α-tubulin antibody was used as control to verify equal protein loading across samples. Values corrected for loading were expressed as fold change of a control condition arbitrarily set to 1.

M.5. CELL CYCLE ANALYSIS

The effects of the drugs on cell cycle progression were analyzed by flow cytometry and western blot.

M.5.1. Cell cycle analysis by flow cytometry

Flow cytometry allows to distinguish cells in different phases of the cell cycle measuring the DNA content. Propidium iodide is used to label the DNA and it permits to distinct three main groups: G0/G1 (2n) phases, S (2n~4n) phase, and G2/M (4n) phases.

Cells were seeded in 100 mm^2 dishes at a density of $2.5x10^5$ - $1x10^6$ based on optimal density for each cell line and after 24 hours of incubation cells were treated with the drugs. Then, cells were harvested by tripsinitzation and counted. After washing three times with PBS by 8 minutes of centrifugation at 1500 rpm's, approximately $1x10^6$ cells were resuspended and fixed on 70% ethanol with PBS overnight. Ethanol was removed by washing 3 times with PBS, by 10.000 rpms 2 minutes, and DNA was stained with PBS containing 50µg/ml propidium iodide and 100µg/ml of RNAse during 3 days at 4ºC protected from light. Cell-cycle distribution was profiled by flow cytometry. A total of 10.000 cells were acquired on a FACSCalibur flow cytometer (Beckton Dickinson) and analyzed with Cell Quest Software.

Results were plotted in a graph as the percentage of cells at different cell stages.

M.5.2. Cell cycle analysis by western blot

Cyclin D1 levels were assessed as mean of cell cycle status since cyclin D1 is required for cell cycle G0/G1 phase.

Cells were seeded in 100 mm^2 dishes at a density of $2.5x10^5$ - $1x10^6$ based on optimal density for each cell line and after 24 hours of incubation cells were treated with the drugs. The levels of the protein were analyzed at 24 and 48 hours after the treatment by western blot.

M.6. APOPTOSIS ANALYSIS

During apoptosis, or programmed cell death, cells respond to specific induction signals by initiating intracellular processes that result in characteristic physiological changes. Among these are the apperance of membrane-associated apoptotic bodies (such as phosphatidylserine (PS)), cleavage of specific cellular proteins (such as PARP), compaction and fragmentation of nuclear chromatin, and loss of membrane integrity.

The effects of the drugs on the process of apoptosis were assessed by flow cytometry and by western blot.

M.6.1. Apoptosis analysis by flow cytometry

Apoptosis analysis by flow cytometry was performed using the Muse Cell Analyzer (Millipore) and the Muse Annexin V and dead cell kit following the protocol provided in the user’s guide. This kit allows for the quantitative analysis of live, early and late apoptosis, and cell death.

The kit uses Annexin V and 7-AAD to staind the cells and distingish the cells in different apoptosis statges. Annexins are a family of calcium-dependent phospho-lipid binding proteins that preferentially bind PS. Molecules of PS are normally localized to the internal face of the membrane and are translocated to the outer surface of the cell during the apoptosis. Annexin V is abble to detect PS in the external membrane of apoptotic cells. 7-AAD is a fluorescent chemical compound with a strong affinity for DNA.

Four populations of cells can be distinguished in this assay: non-apoptotic cells, early apoptotic cells, late stage apoptotic and dead cells, and nuclear debris.

Cells were seeded in 100 mm^2 dishes at a density of 2.5x10^5 - 1x10^6 based on optimal density for each cell line and after 24 hours of incubation cells were treated with the drugs during 24 and 48 hours. After the incubation, cells were tripsinized and mixed the Muse™ Annexin V & Dead Cell Reagent. Samples were incubated for 20 minuts at room temperature and the analyzed by the Muse Cell Analyzer.

M.6.2. Apoptosis analysis by western blot

PARP-cleavage was assessed by western blot as a marker of cells undergoing apoptosis. PARP is nuclear poly (ADP-ribose) polymerase, which is an enzyme implicated in the repair of DNA strand breaks and helps cells to maintain their viability.

M.7. AUTOPHAGY ANALYSIS

Autophagy is a dynamic, multi-step process that can be modulated at several steps, both positively and negatively that make it difficult to analyze.

According to the guidelines for monitoring autophagy, the effects of the drugs on autophagy flux were determined by detection of stained autophagic vesicles and by immunoblot analysis of proteins involved in the process.

The autophagic flux begins with the formation of a double membrane (fagophore), whic expands around a portion of cytoplasm and fuses to form the autophagosome. Then, the autophagosme fuses with lysosome to generate an autolysosome that at the end is degraded [165].

These experiments were performed in the presence and in the absence of chloroquine, a classical autophagy inhibitor used to block the process at the final step. Chloroquine prevents the acidification of lysosomes impeding the fusion and the degradation of the autophagic vesicles. As autophagy is a dynamic process, blocking the degradation of the vesicles allows us to detect them.

M.7.1. Autophagic vesicles by microscopy

In general, the amounts of cellular autophagosomes is an indicator of the level of cellular autophagic activity. Staining the autophagosomes allows to detect them by microscopy [166].

Cells were seeded on tissue culture treated slides and after 24 hours of incubation cells were treated with the drugs. After 24 hours of treatment, cells were stained with the Cyto-ID autophagy detection kit (Enzo Life Sciences). Cells were stained with the dye reagent, which includes titratable moieties specific for selectively staining autophagic vesicles, and subsequently analyzed by fluorescence microscopy according to manufacturer’s protocol.

High fluorescent intensity punctuate pattern corresponds to the production of autophagic vesicles.

M.7.2. Autophagy analysis by western blot

Immunoblot analysis of LC3 and p62/SQSTM1, among other proteins, has been widely used to monitor autophagic flux [167]. LC3 (Light chain 3) is a homolog protein of the yeast ATG8 protein whic is critical for autophagy. During the process of autophagosome formation LC3-I is converted to LC3-II through lipidation by a ubiquitin-like system. LC3-II form is recruited to the autophagosome membrane and it is believed to be involved in autophagosome membrane expansion and fusion events. The conversion of LC3-I to LC3-II has been used as an indicator of autophagy. LC3-I (14-16kDa) and LC3-II (16-18kDa) are detected by western blot.

The p62 protein, also called sequestosome 1 (SQSTM1) is an autophagic cargo receptor that may serve to link ubiquitinated proteins to the autophagic machinery. Also, p62/SQSTM1 binds directly to LC3 proteins.

The protein is internalized into the autophagosomes and itself degraded by autophagy. Since p62 accumulates when autophagy is inhibited, and decreased levels can be observed when autophagy is induced, p62 has been used as a marker to study autophagic flux.

M.8. *IN VIVO* STUDIES

M.8.1. Animals

Five-week-old male BALB/c nude mice were purchased from Charles River Laboratories (Wilmington, MA) and hosted in the pathogen-free animal facility at the Barcelona Biomedical Research Park (PRBB). Animal treatments were done according to institution-approved protocols.

M.8.2. Set-up: Subcutaneous xenograft model in BALB/c nude mice

We have been working in the establishment *in vivo* models of human urothelial cancer. As few or no reports addressing how to generate these models were available at the start of the project, we first conducted a pilot study to test whether the maximum number of cells that could be reasonably for subcutaneous injection was able to form tumors. A total of $20x10^6$ cells (1:1 in matrigel; in 100 µl) were injected into the right flanks of mice (5 mice/cell line). Four of the six BC cell lines were tested *in vivo*. Animals were examined twice a week for signs of tumor growth and tumors were measured using vernier calipers. Tumor volume was determined from caliper measurements of tumor length (L) and width (W) according to the formula $((L \times W^2)/2)$. Tumor weights were also recorded at the time of sacrifice.

M.8.3. Survival studies

To evaluate the efficacy of the drugs as antitumorigenic agents *in vivo,* tumours were allowed to grow until the tumor volume reached approximately 200 mm^3. Then, mice were randomized to 4 or 5 groups with 8-10 mice in each group. The treatment groups were described in each experiment in RESULTS section.

The tumor volume was analysed every 3 or 4 days during the studies. Also, the TGI (tumor growth inhibition: TGI= 100-[(treated average volume /Control average volume)x100]) and the fold change in tumor growth (the ratio of the difference between final tumor volume and the initial tumor volume) were calculated.

M.9. TUMOR SAMPLES ANALYSIS

To determine the effects of the drugs in tumor samples two types of analysis were done: ex vivo treatment of tumor samples in culture or treatment of animals in vivo. After the treatment of drugs, a portion of tumor was formalin fixed and paraffin-embedded for immunohistochemical (IHC) study.

In one experiment of animals treated in vivo, samples also were analysed by western blot.

M.9.1. Tumor samples analysis by immunohistochemistry

For ICH, five-μm tissue sections from formalin-fixed and paraffin embedded samples were obtained, mounted onto charged slides and then, deparaffinised in xylene and hydrated. After heat antigen retrieval performed at high pH solution using PT Link platform (Dako), slides for immunohistochemistry were incubated with primary antibodies for 1 h. After that, slides were incubated with an anti-rabbit Ig dextran polymer (Flex+, Dako) and 3,3′-diaminobenzidine used as a chromogen in a Dako Link platform. Samples were analysed by microscopy by a pathologist. Representative images of the staining are shown and H-score (was calculated as follows: the percentage of cells at *each* staining intensity) or the percentage of stained-tumor cells were calculated.

M.9.1.1. IHC analysis of tumor samples treated ex vivo

Tumor cells (RT4, CAL-29 and T24) were injected into the flank of the mice as described above. Tumors grew up to a volume of 300-600mm^3. Tumors were excised and *tumor pieces* were cryopreserved (for future cell lines establishment or tumor implantation) or tumors were sliced and cultured in vitro.

Samples were treated with or without TAK-228 [RT4 and T24 50nM, CAL-29 20nM]- during 24 hours and routinely formalin-fixed and paraffin-embedded. Slides were prepared and pS6 (Ser235/236) was assayed by immunohistochemistry and H-score in tumor samples was measured.

M.9.1.2. IHC analysis of tumor samples from survival studies

We have determined the status of the PI3K/Akt/mTOR pathway activation in each group using IHC analysis. The histological tumor sections were stained to ascertain the levels of phosphorylated S6 (Ser 235/236) and S6, as well as total protein levels. We also performed staining for phospho histone H3 (p-H3), a marker of cells in M phase, and hence a marker of cycling cells. In addition, for the detection of apoptotic events, we used the active form of caspase-3 (cleaved caspase 3). As a markers of angiogenesis VEGF-A, p-KDR in endothelial cells and the the number of stained tubular vascular structures (for CD31) within the tumor. H-score was calculated for p-S6 (Ser235/236), S6 and VEGF-A) and the percentage of stained-tumor cells was measure for p-H3, p-KDR and CD31. The antibodies used for the IHC were purchased from Cell Signaling.

M.9.2. Tumor samples analysis by western-blot

A portion of the tumor was snap-frozen in liquid and stored at -80°C until were used for protein extraction. Tumors were disaggregated with in Lysis buffer. Then, samples were shacked during 20min at 4ºC and the samples were centrifuged 10min at 13.200rpm and the supernatant was aliquoted and stored at -20°C.

Western blot for p-Akt (Ser473), Akt, p-S6 (Ser235/236), S6, p-4E-BP1 (Thr37/46), 4E-BP1 antibodies was performed from 3 mice of each treatment group.

M.10. STATISTICAL ANALYSIS

Statistical analysis was carried out with SPSS version 18.0 (SPSS, Inc.).

M.10.1. Statistics for *in vitro* and *in vivo* assays

Student's *t*-test or independent sample *t*-test is used for the comparisons of the means between two unrelated groups. This test was used for the *in vitro* experiments when two variables were compared.

One-Way analysis of variance (ANOVA) is used to test whether there are any statistically significant differences between the means of groups. Tukey's and Bonferroni Post Hoc tests were used to perform pairwise comparison. One-Way ANOVA was used to assess differences in the effects between combined treatments with multiple conditions for the *in vitro* and *in vivo* experiments. All the statistical test were performed at the two-sided 0,05 level of significance.

M.10.2. Statistics for biomarkers and drug response correlation

The Spearman’s rank correlation coefficient or Spearman’s rho (*r*) is a measure of the linear correlation between two variables X and Y.

The Spearman’s rank correlation was used to correlate protein expression levels between the IC50 values for TAK-228. Positive correlation was considered when *r* is closer to +1 and negative correlation when *r* is closer to -1; and the level of significance was lower than 0,05.

BIBLIOGRAPHY

BIBLIOGRAPHY

1. Jemal, A., et al., *Global cancer statistics.* CA Cancer J Clin, 2011. **61**(2): p. 69-90.
2. Burger, M., et al., *Epidemiology and risk factors of urothelial bladder cancer.* Eur Urol, 2013. **63**(2): p. 234-41.
3. Witjes, J.A., et al., *EAU guidelines on muscle-invasive and metastatic bladder cancer: summary of the 2013 guidelines.* Eur Urol, 2014. **65**(4): p. 778-92.
4. Dahm, P. and J.E. Gschwend, *Malignant non-urothelial neoplasms of the urinary bladder: a review.* Eur Urol, 2003. **44**(6): p. 672-81.
5. Knowles, M.A. and C.D. Hurst, *Molecular biology of bladder cancer: new insights into pathogenesis and clinical diversity.* Nat Rev Cancer, 2015. **15**(1): p. 25-41.
6. Bellmunt, J., et al., *Long-term survival results of a randomized phase III trial of vinflunine plus best supportive care versus best supportive care alone in advanced urothelial carcinoma patients after failure of platinum-based chemotherapy.* Ann Oncol, 2013. **24**(6): p. 1466-72.
7. Ismaili, N., M. Amzerin, and A. Flechon, *Chemotherapy in advanced bladder cancer: current status and future.* J Hematol Oncol, 2011. **4**: p. 35.
8. *Comprehensive molecular characterization of urothelial bladder carcinoma.* Nature, 2014. **507**(7492): p. 315-22.
9. Bader, A.G., et al., *Oncogenic PI3K deregulates transcription and translation.* Nat Rev Cancer, 2005. **5**(12): p. 921-9.
10. Polivka, J., Jr. and F. Janku, *Molecular targets for cancer therapy in the PI3K/AKT/mTOR pathway.* Pharmacol Ther, 2014. **142**(2): p. 164-75.
11. Samuels, Y., et al., *High frequency of mutations of the PIK3CA gene in human cancers.* Science, 2004. **304**(5670): p. 554.
12. Engelman, J.A., *Targeting PI3K signalling in cancer: opportunities, challenges and limitations.* Nat Rev Cancer, 2009. **9**(8): p. 550-62.
13. Askham, J.M., et al., *AKT1 mutations in bladder cancer: identification of a novel oncogenic mutation that can co-operate with E17K.* Oncogene, 2010. **29**(1): p. 150-5.
14. Iyer, G., et al., *Prevalence and co-occurrence of actionable genomic alterations in high-grade bladder cancer.* J Clin Oncol, 2013. **31**(25): p. 3133-40.

15. Bellmunt, J., et al., *Molecular targets on the horizon for kidney and urothelial cancer.* Nat Rev Clin Oncol, 2013. **10**(10): p. 557-70.
16. Chaux, A., et al., *High epidermal growth factor receptor immunohistochemical expression in urothelial carcinoma of the bladder is not associated with EGFR mutations in exons 19 and 21: a study using formalin-fixed, paraffin-embedded archival tissues.* Hum Pathol, 2012. **43**(10): p. 1590-5.
17. Wulfing, C., et al., *A single-arm, multicenter, open-label phase 2 study of lapatinib as the second-line treatment of patients with locally advanced or metastatic transitional cell carcinoma.* Cancer, 2009. **115**(13): p. 2881-90.
18. Pruthi, R.S., et al., *A phase II trial of neoadjuvant erlotinib in patients with muscle-invasive bladder cancer undergoing radical cystectomy: clinical and pathological results.* BJU Int, 2010. **106**(3): p. 349-54.
19. Kamat, A.M., *Commentary on "Phase II trial of cetuximab with or without paclitaxel in patients with advanced urothelial tract carcinoma." Wong YN, Litwin S, Vaughn D, Cohen S, Plimack ER, Lee J, Song W, Dabrow M, Brody M, Tuttle H, Hudes G, University of Pennsylvania, Philadelphia, PA: J Clin Oncol 2012;30(28):3545-51 [Epub 2012 Aug 27].* Urol Oncol, 2013. **31**(5): p. 719.
20. Milowsky, M.I., et al., *Phase 2 trial of dovitinib in patients with progressive FGFR3-mutated or FGFR3 wild-type advanced urothelial carcinoma.* Eur J Cancer, 2014. **50**(18): p. 3145-52.
21. Crew, J.P., et al., *Urinary vascular endothelial growth factor and its correlation with bladder cancer recurrence rates.* J Urol, 1999. **161**(3): p. 799-804.
22. Kopparapu, P.K., et al., *Expression of VEGF and its receptors VEGFR1/VEGFR2 is associated with invasiveness of bladder cancer.* Anticancer Res, 2013. **33**(6): p. 2381-90.
23. Gallagher, D.J., et al., *Phase II study of sunitinib in patients with metastatic urothelial cancer.* J Clin Oncol, 2010. **28**(8): p. 1373-9.
24. Grivas, P.D., et al., *Double-blind, randomized, phase 2 trial of maintenance sunitinib versus placebo after response to chemotherapy in patients with advanced urothelial carcinoma.* Cancer, 2014. **120**(5): p. 692-701.
25. Hahn, N.M., et al., *Phase II trial of cisplatin, gemcitabine, and bevacizumab as first-line therapy for metastatic urothelial carcinoma: Hoosier Oncology Group GU 04-75.* J Clin Oncol, 2011. **29**(12): p. 1525-30.

26. Petrylak, D.P., et al., *Docetaxel As Monotherapy or Combined With Ramucirumab or Icrucumab in Second-Line Treatment for Locally Advanced or Metastatic Urothelial Carcinoma: An Open-Label, Three-Arm, Randomized Controlled Phase II Trial.* J Clin Oncol, 2016. **34**(13): p. 1500-9.
27. Bellmunt, J., T. Powles, and N.J. Vogelzang, *A review on the evolution of PD-1/PD-L1 immunotherapy for bladder cancer: The future is now.* Cancer Treat Rev, 2017. **54**: p. 58-67.
28. Laplante, M. and D.M. Sabatini, *mTOR signaling in growth control and disease.* Cell, 2012. **149**(2): p. 274-93.
29. Chiarini, F., et al., *Current treatment strategies for inhibiting mTOR in cancer.* Trends Pharmacol Sci, 2015. **36**(2): p. 124-35.
30. Courtney, K.D., R.B. Corcoran, and J.A. Engelman, *The PI3K pathway as drug target in human cancer.* J Clin Oncol, 2010. **28**(6): p. 1075-83.
31. Hawkins, P.T., et al., *Signalling through Class I PI3Ks in mammalian cells.* Biochem Soc Trans, 2006. **34**(Pt 5): p. 647-62.
32. Liu, P., et al., *Targeting the phosphoinositide 3-kinase pathway in cancer.* Nat Rev Drug Discov, 2009. **8**(8): p. 627-44.
33. Katso, R., et al., *Cellular function of phosphoinositide 3-kinases: implications for development, homeostasis, and cancer.* Annu Rev Cell Dev Biol, 2001. **17**: p. 615-75.
34. New, D.C. and Y.H. Wong, *Molecular mechanisms mediating the G protein-coupled receptor regulation of cell cycle progression.* J Mol Signal, 2007. **2**: p. 2.
35. Fruman, D.A. and C. Rommel, *PI3K and cancer: lessons, challenges and opportunities.* Nat Rev Drug Discov, 2014. **13**(2): p. 140-56.
36. Gagliardi, P.A., A. Puliafito, and L. Primo, *PDK1: At the crossroad of cancer signaling pathways.* Semin Cancer Biol, 2017.
37. Manning, B.D. and L.C. Cantley, *AKT/PKB signaling: navigating downstream.* Cell, 2007. **129**(7): p. 1261-74.
38. Manning, B.D. and A. Toker, *AKT/PKB Signaling: Navigating the Network.* Cell, 2017. **169**(3): p. 381-405.
39. Hers, I., E.E. Vincent, and J.M. Tavare, *Akt signalling in health and disease.* Cell Signal, 2011. **23**(10): p. 1515-27.
40. Guertin, D.A. and D.M. Sabatini, *Defining the role of mTOR in cancer.* Cancer Cell, 2007. **12**(1): p. 9-22.
41. Huang, J. and B.D. Manning, *The TSC1-TSC2 complex: a molecular switchboard controlling cell growth.* Biochem J, 2008. **412**(2): p. 179-90.

42. Inoki, K., et al., *TSC2 is phosphorylated and inhibited by Akt and suppresses mTOR signalling.* Nat Cell Biol, 2002. **4**(9): p. 648-57.
43. Benjamin, D., et al., *Rapamycin passes the torch: a new generation of mTOR inhibitors.* Nat Rev Drug Discov, 2011. **10**(11): p. 868-80.
44. Hoeffer, C.A. and E. Klann, *mTOR signaling: at the crossroads of plasticity, memory and disease.* Trends Neurosci, 2010. **33**(2): p. 67-75.
45. Schalm, S.S., et al., *TOS motif-mediated raptor binding regulates 4E-BP1 multisite phosphorylation and function.* Curr Biol, 2003. **13**(10): p. 797-806.
46. Gingras, A.C., et al., *Regulation of 4E-BP1 phosphorylation: a novel two-step mechanism.* Genes Dev, 1999. **13**(11): p. 1422-37.
47. Ruggero, D. and N. Sonenberg, *The Akt of translational control.* Oncogene, 2005. **24**(50): p. 7426-34.
48. Musa, J., et al., *Eukaryotic initiation factor 4E-binding protein 1 (4E-BP1): a master regulator of mRNA translation involved in tumorigenesis.* Oncogene, 2016. **35**(36): p. 4675-88.
49. Tavares, M.R., et al., *The S6K protein family in health and disease.* Life Sci, 2015. **131**: p. 1-10.
50. Magnuson, B., B. Ekim, and D.C. Fingar, *Regulation and function of ribosomal protein S6 kinase (S6K) within mTOR signalling networks.* Biochem J, 2012. **441**(1): p. 1-21.
51. Ruvinsky, I. and O. Meyuhas, *Ribosomal protein S6 phosphorylation: from protein synthesis to cell size.* Trends Biochem Sci, 2006. **31**(6): p. 342-8.
52. Hay, N. and N. Sonenberg, *Upstream and downstream of mTOR.* Genes Dev, 2004. **18**(16): p. 1926-45.
53. Carracedo, A. and P.P. Pandolfi, *The PTEN-PI3K pathway: of feedbacks and cross-talks.* Oncogene, 2008. **27**(41): p. 5527-41.
54. Cheung, M. and J.R. Testa, *Diverse mechanisms of AKT pathway activation in human malignancy.* Curr Cancer Drug Targets, 2013. **13**(3): p. 234-44.
55. Crowell, J.A., V.E. Steele, and J.R. Fay, *Targeting the AKT protein kinase for cancer chemoprevention.* Mol Cancer Ther, 2007. **6**(8): p. 2139-48.
56. Markman, B., et al., *Status of PI3K inhibition and biomarker development in cancer therapeutics.* Ann Oncol, 2010. **21**(4): p. 683-91.
57. Greer, E.L. and A. Brunet, *FOXO transcription factors at the interface between longevity and tumor suppression.* Oncogene, 2005. **24**(50): p. 7410-25.

58. Milne, D., et al., *A novel site of AKT-mediated phosphorylation in the human MDM2 onco-protein.* FEBS Lett, 2004. **577**(1-2): p. 270-6.
59. Abukhdeir, A.M. and B.H. Park, *P21 and p27: roles in carcinogenesis and drug resistance.* Expert Rev Mol Med, 2008. **10**: p. e19.
60. Sardiello, M., et al., *A gene network regulating lysosomal biogenesis and function.* Science, 2009. **325**(5939): p. 473-7.
61. Yang, Z.J., et al., *The role of autophagy in cancer: therapeutic implications.* Mol Cancer Ther, 2011. **10**(9): p. 1533-41.
62. Dienstmann, R., et al., *Picking the point of inhibition: a comparative review of PI3K/AKT/mTOR pathway inhibitors.* Mol Cancer Ther, 2014. **13**(5): p. 1021-31.
63. O'Reilly, K.E., et al., *mTOR inhibition induces upstream receptor tyrosine kinase signaling and activates Akt.* Cancer Res, 2006. **66**(3): p. 1500-8.
64. Maira, S.M., et al., *Identification and characterization of NVP-BEZ235, a new orally available dual phosphatidylinositol 3-kinase/mammalian target of rapamycin inhibitor with potent in vivo antitumor activity.* Mol Cancer Ther, 2008. **7**(7): p. 1851-63.
65. Serra, V., et al., *NVP-BEZ235, a dual PI3K/mTOR inhibitor, prevents PI3K signaling and inhibits the growth of cancer cells with activating PI3K mutations.* Cancer Res, 2008. **68**(19): p. 8022-30.
66. Janes, M.R., et al., *Effective and selective targeting of leukemia cells using a TORC1/2 kinase inhibitor.* Nat Med, 2010. **16**(2): p. 205-13.
67. LoRusso, P.M., *Inhibition of the PI3K/AKT/mTOR Pathway in Solid Tumors.* J Clin Oncol, 2016.
68. Meric-Bernstam, F. and A.M. Gonzalez-Angulo, *Targeting the mTOR signaling network for cancer therapy.* J Clin Oncol, 2009. **27**(13): p. 2278-87.
69. Choi, J., et al., *Structure of the FKBP12-rapamycin complex interacting with the binding domain of human FRAP.* Science, 1996. **273**(5272): p. 239-42.
70. Hartford, C.M. and M.J. Ratain, *Rapamycin: something old, something new, sometimes borrowed and now renewed.* Clin Pharmacol Ther, 2007. **82**(4): p. 381-8.
71. Hare, S.H. and A.J. Harvey, *mTOR function and therapeutic targeting in breast cancer.* Am J Cancer Res, 2017. **7**(3): p. 383-404.

72. Chiong, E., et al., *Effects of mTOR inhibitor everolimus (RAD001) on bladder cancer cells.* Clin Cancer Res, 2011. **17**(9): p. 2863-73.
73. Mansure, J.J., et al., *Inhibition of mammalian target of rapamycin as a therapeutic strategy in the management of bladder cancer.* Cancer Biol Ther, 2009. **8**(24): p. 2339-47.
74. Efeyan, A. and D.M. Sabatini, *mTOR and cancer: many loops in one pathway.* Curr Opin Cell Biol, 2010. **22**(2): p. 169-76.
75. Iyer, G., et al., *Genome sequencing identifies a basis for everolimus sensitivity.* Science, 2012. **338**(6104): p. 221.
76. Milowsky, M.I., et al., *Phase II study of everolimus in metastatic urothelial cancer.* BJU Int, 2013. **112**(4): p. 462-70.
77. Vilar, E., J. Perez-Garcia, and J. Tabernero, *Pushing the envelope in the mTOR pathway: the second generation of inhibitors.* Mol Cancer Ther, 2011. **10**(3): p. 395-403.
78. Feldman, M.E., et al., *Active-site inhibitors of mTOR target rapamycin-resistant outputs of mTORC1 and mTORC2.* PLoS Biol, 2009. **7**(2): p. e38.
79. Thoreen, C.C., et al., *An ATP-competitive mammalian target of rapamycin inhibitor reveals rapamycin-resistant functions of mTORC1.* J Biol Chem, 2009. **284**(12): p. 8023-32.
80. Bhagwat, S.V., et al., *Preclinical characterization of OSI-027, a potent and selective inhibitor of mTORC1 and mTORC2: distinct from rapamycin.* Mol Cancer Ther, 2011. **10**(8): p. 1394-406.
81. Garcia-Martinez, J.M., et al., *Ku-0063794 is a specific inhibitor of the mammalian target of rapamycin (mTOR).* Biochem J, 2009. **421**(1): p. 29-42.
82. Falcon, B.L., et al., *Reduced VEGF production, angiogenesis, and vascular regrowth contribute to the antitumor properties of dual mTORC1/mTORC2 inhibitors.* Cancer Res, 2011. **71**(5): p. 1573-83.
83. Becker, M.N., et al., *The combination of an mTORc1/TORc2 inhibitor with lapatinib is synergistic in bladder cancer in vitro.* Urol Oncol, 2013.
84. Houede, N. and P. Pourquier, *Targeting the genetic alterations of the PI3K-AKT-mTOR pathway: its potential use in the treatment of bladder cancers.* Pharmacol Ther, 2015. **145**: p. 1-18.
85. Garcia-Garcia, C., et al., *Dual mTORC1/2 and HER2 blockade results in antitumor activity in preclinical models of breast cancer resistant to anti-HER2 therapy.* Clin Cancer Res, 2012. **18**(9): p. 2603-12.
86. Gokmen-Polar, Y., et al., *Investigational drug MLN0128, a novel TORC1/2 inhibitor, demonstrates potent oral antitumor activity in*

human breast cancer xenograft models. Breast Cancer Res Treat, 2012. **136**(3): p. 673-82.

87. Koo, J., et al., *Maintaining glycogen synthase kinase-3 activity is critical for mTOR kinase inhibitors to inhibit cancer cell growth.* Cancer Res, 2014. **74**(9): p. 2555-68.
88. Li, C., et al., *The preclinical evaluation of the dual mTORC1/2 inhibitor INK-128 as a potential anti-colorectal cancer agent.* Cancer Biol Ther, 2015. **16**(1): p. 34-42.
89. Hsieh, A.C., et al., *The translational landscape of mTOR signalling steers cancer initiation and metastasis.* Nature, 2012. **485**(7396): p. 55-61.
90. Maiso, P., et al., *Defining the role of TORC1/2 in multiple myeloma.* Blood, 2011. **118**(26): p. 6860-70.
91. Hernandez-Aya, L.F. and A.M. Gonzalez-Angulo, *Targeting the phosphatidylinositol 3-kinase signaling pathway in breast cancer.* Oncologist, 2011. **16**(4): p. 404-14.
92. Miller, T.W., J.M. Balko, and C.L. Arteaga, *Phosphatidylinositol 3-kinase and antiestrogen resistance in breast cancer.* J Clin Oncol, 2011. **29**(33): p. 4452-61.
93. Zardavas, D., J. Baselga, and M. Piccart, *Emerging targeted agents in metastatic breast cancer.* Nat Rev Clin Oncol, 2013. **10**(4): p. 191-210.
94. Ross, R.L., et al., *PIK3CA dependence and sensitivity to therapeutic targeting in urothelial carcinoma.* BMC Cancer, 2016. **16**: p. 553.
95. Vora, S.R., et al., *CDK 4/6 inhibitors sensitize PIK3CA mutant breast cancer to PI3K inhibitors.* Cancer Cell, 2014. **26**(1): p. 136-49.
96. Tao, J.J., et al., *Antagonism of EGFR and HER3 enhances the response to inhibitors of the PI3K-Akt pathway in triple-negative breast cancer.* Sci Signal, 2014. **7**(318): p. ra29.
97. Juric, D., et al., *A First-in-Human, Phase I, Dose-Escalation Study of TAK-117, a Selective PI3Kalpha Isoform Inhibitor, in Patients with Advanced Solid Malignancies.* Clin Cancer Res, 2017.
98. Jessen, K., *A potent and selective PI3K inhibitor, INK1117, targets human cancers harboring oncogenic PIK3CA mutations.* Molecular Cancer therapeutics, 2011.
99. Fechner, G., et al., *Rapamycin inhibits in vitro growth and release of angiogenetic factors in human bladder cancer.* Urology, 2009. **73**(3): p. 665-8; discussion 668-9.

100. Hansel, D.E., et al., *Mammalian target of rapamycin (mTOR) regulates cellular proliferation and tumor growth in urothelial carcinoma.* Am J Pathol, 2010. **176**(6): p. 3062-72.
101. Seront, E., et al., *Phase II study of everolimus in patients with locally advanced or metastatic transitional cell carcinoma of the urothelial tract: clinical activity, molecular response, and biomarkers.* Ann Oncol, 2012. **23**(10): p. 2663-70.
102. Gerullis, H., et al., *Long-term response in advanced bladder cancer involving the use of temsirolimus and vinflunine after platin resistance.* Anticancer Drugs, 2011. **22**(9): p. 940-3.
103. Niegisch, G., et al., *Second-Line Treatment of Advanced Urothelial Cancer with Paclitaxel and Everolimus in a German Phase II Trial (AUO Trial AB 35/09).* Oncology, 2015. **89**(2): p. 70-8.
104. Wagle, N., et al., *Activating mTOR mutations in a patient with an extraordinary response on a phase I trial of everolimus and pazopanib.* Cancer Discov, 2014. **4**(5): p. 546-53.
105. Guo, Y., et al., *TSC1 involvement in bladder cancer: diverse effects and therapeutic implications.* J Pathol, 2013. **230**(1): p. 17-27.
106. Barretina, J., et al., *The Cancer Cell Line Encyclopedia enables predictive modelling of anticancer drug sensitivity.* Nature, 2012. **483**(7391): p. 603-7.
107. Cattan, N., et al., *Establishment of two new human bladder carcinoma cell lines, CAL 29 and CAL 185. Comparative study of cell scattering and epithelial to mesenchyme transition induced by growth factors.* Br J Cancer, 2001. **85**(9): p. 1412-7.
108. Zhang, H., et al., *mTOR ATP-competitive inhibitor INK128 inhibits neuroblastoma growth via blocking mTORC signaling.* Apoptosis, 2015. **20**(1): p. 50-62.
109. Lou, H.Z., et al., *The novel mTORC1/2 dual inhibitor INK-128 suppresses survival and proliferation of primary and transformed human pancreatic cancer cells.* Biochem Biophys Res Commun, 2014. **450**(2): p. 973-8.
110. Montagut, C., et al., *Identification of a mutation in the extracellular domain of the Epidermal Growth Factor Receptor conferring cetuximab resistance in colorectal cancer.* Nat Med, 2012. **18**(2): p. 221-3.
111. Alain, T., et al., *eIF4E/4E-BP ratio predicts the efficacy of mTOR targeted therapies.* Cancer Res, 2012. **72**(24): p. 6468-76.
112. Hsieh, A.C., et al., *Cell type-specific abundance of 4EBP1 primes prostate cancer sensitivity or resistance to PI3K pathway inhibitors.* Sci Signal, 2015. **8**(403): p. ra116.

113. Don, A.S. and X.F. Zheng, *Recent clinical trials of mTOR-targeted cancer therapies.* Rev Recent Clin Trials, 2011. **6**(1): p. 24-35.
114. Wander, S.A., B.T. Hennessy, and J.M. Slingerland, *Next-generation mTOR inhibitors in clinical oncology: how pathway complexity informs therapeutic strategy.* J Clin Invest, 2011. **121**(4): p. 1231-41.
115. Wacheck, V., *mTOR pathway inhibitors in cancer therapy: moving past rapamycin.* Pharmacogenomics, 2010. **11**(9): p. 1189-91.
116. Albert, S., et al., *New inhibitors of the mammalian target of rapamycin signaling pathway for cancer.* Expert Opin Investig Drugs, 2010. **19**(8): p. 919-30.
117. Kondo, Y., et al., *The role of autophagy in cancer development and response to therapy.* Nat Rev Cancer, 2005. **5**(9): p. 726-34.
118. Gewirtz, D.A., *The four faces of autophagy: implications for cancer therapy.* Cancer Res, 2014. **74**(3): p. 647-51.
119. Ravanan, P., I.F. Srikumar, and P. Talwar, *Autophagy: The spotlight for cellular stress responses.* Life Sci, 2017. **188**: p. 53-67.
120. Denton, D., T. Xu, and S. Kumar, *Autophagy as a pro-death pathway.* Immunol Cell Biol, 2015. **93**(1): p. 35-42.
121. Fingar, D.C. and J. Blenis, *Target of rapamycin (TOR): an integrator of nutrient and growth factor signals and coordinator of cell growth and cell cycle progression.* Oncogene, 2004. **23**(18): p. 3151-71.
122. Fingar, D.C., et al., *mTOR controls cell cycle progression through its cell growth effectors S6K1 and 4E-BP1/eukaryotic translation initiation factor 4E.* Mol Cell Biol, 2004. **24**(1): p. 200-16.
123. De Benedetti, A. and J.R. Graff, *eIF-4E expression and its role in malignancies and metastases.* Oncogene, 2004. **23**(18): p. 3189-99.
124. Rodrik-Outmezguine, V.S., et al., *mTOR kinase inhibition causes feedback-dependent biphasic regulation of AKT signaling.* Cancer Discov, 2011. **1**(3): p. 248-59.
125. Gulhati, P., et al., *mTORC1 and mTORC2 regulate EMT, motility, and metastasis of colorectal cancer via RhoA and Rac1 signaling pathways.* Cancer Res, 2011. **71**(9): p. 3246-56.
126. Li, H., et al., *Targeting of mTORC2 prevents cell migration and promotes apoptosis in breast cancer.* Breast Cancer Res Treat, 2012. **134**(3): p. 1057-66.
127. Gupta, S., et al., *Mammalian Target of Rapamycin Complex 2 (mTORC2) Is a Critical Determinant of Bladder Cancer Invasion.* PLoS One, 2013. **8**(11): p. e81081.

128. Karar, J. and A. Maity, *PI3K/AKT/mTOR Pathway in Angiogenesis.* Front Mol Neurosci, 2011. **4**: p. 51.

129. Guba, M., et al., *Rapamycin inhibits primary and metastatic tumor growth by antiangiogenesis: involvement of vascular endothelial growth factor.* Nat Med, 2002. **8**(2): p. 128-35.

130. Dodd, K.M., et al., *mTORC1 drives HIF-1alpha and VEGF-A signalling via multiple mechanisms involving 4E-BP1, S6K1 and STAT3.* Oncogene, 2015. **34**(17): p. 2239-50.

131. Slotkin, E.K., et al., *MLN0128, an ATP-competitive mTOR kinase inhibitor with potent in vitro and in vivo antitumor activity, as potential therapy for bone and soft-tissue sarcoma.* Mol Cancer Ther, 2015. **14**(2): p. 395-406.

132. Jiang, S.J. and S. Wang, *Dual targeting of mTORC1 and mTORC2 by INK-128 potently inhibits human prostate cancer cell growth in vitro and in vivo.* Tumour Biol, 2015. **36**(10): p. 8177-84.

133. Zhang, S., et al., *Pan-mTOR inhibitor MLN0128 is effective against intrahepatic cholangiocarcinoma in mice.* J Hepatol, 2017.

134. Vasconcelos-Nobrega, C., et al., *In vivo and in vitro effects of RAD001 on bladder cancer.* Urol Oncol, 2013. **31**(7): p. 1212-21.

135. Dowling, R.J., et al., *Dissecting the role of mTOR: lessons from mTOR inhibitors.* Biochim Biophys Acta, 2010. **1804**(3): p. 433-9.

136. Janes, M.R., et al., *Efficacy of the investigational mTOR kinase inhibitor MLN0128/INK128 in models of B-cell acute lymphoblastic leukemia.* Leukemia, 2013. **27**(3): p. 586-94.

137. Wang, X., J. Ding, and L.H. Meng, *PI3K isoform-selective inhibitors: next-generation targeted cancer therapies.* Acta Pharmacol Sin, 2015. **36**(10): p. 1170-6.

138. Weigelt, B. and J. Downward, *Genomic Determinants of PI3K Pathway Inhibitor Response in Cancer.* Front Oncol, 2012. **2**: p. 109.

139. Ducker, G.S., et al., *Incomplete inhibition of phosphorylation of 4E-BP1 as a mechanism of primary resistance to ATP-competitive mTOR inhibitors.* Oncogene, 2014. **33**(12): p. 1590-600.

140. Fan, Q.W., T.P. Nicolaides, and W.A. Weiss, *Inhibiting 4EBP1 in glioblastoma.* Clin Cancer Res, 2017.

141. Schultz, L., et al., *Expression status and prognostic significance of mammalian target of rapamycin pathway members in urothelial carcinoma of urinary bladder after cystectomy.* Cancer, 2010. **116**(23): p. 5517-26.

142. Nishikawa, M., et al., *Significance of 4E-binding protein 1 as a therapeutic target for invasive urothelial carcinoma of the bladder.* Urol Oncol, 2015. **33**(4): p. 166 e9-15.

143. She, Q.B., et al., *4E-BP1 is a key effector of the oncogenic activation of the AKT and ERK signaling pathways that integrates their function in tumors.* Cancer Cell, 2010. **18**(1): p. 39-51.
144. Engelman, J.A., et al., *Effective use of PI3K and MEK inhibitors to treat mutant Kras G12D and PIK3CA H1047R murine lung cancers.* Nat Med, 2008. **14**(12): p. 1351-6.
145. Posch, C., et al., *Combined targeting of MEK and PI3K/mTOR effector pathways is necessary to effectively inhibit NRAS mutant melanoma in vitro and in vivo.* Proc Natl Acad Sci U S A, 2013. **110**(10): p. 4015-20.
146. Fan, Q.W., et al., *Akt and autophagy cooperate to promote survival of drug-resistant glioma.* Sci Signal, 2010. **3**(147): p. ra81.
147. Rosich, L., D. Colomer, and G. Roue, *Autophagy controls everolimus (RAD001) activity in mantle cell lymphoma.* Autophagy, 2013. **9**(1): p. 115-7.
148. Bokobza, S.M., et al., *Combining AKT inhibition with chloroquine and gefitinib prevents compensatory autophagy and induces cell death in EGFR mutated NSCLC cells.* Oncotarget, 2014. **5**(13): p. 4765-78.
149. Ibrahim, Y.H., et al., *PI3K inhibition impairs BRCA1/2 expression and sensitizes BRCA-proficient triple-negative breast cancer to PARP inhibition.* Cancer Discov, 2012. **2**(11): p. 1036-47.
150. Juvekar, A., et al., *Combining a PI3K inhibitor with a PARP inhibitor provides an effective therapy for BRCA1-related breast cancer.* Cancer Discov, 2012. **2**(11): p. 1048-63.
151. Hayman, T.J., et al., *The ATP-Competitive mTOR Inhibitor INK128 Enhances In Vitro and In Vivo Radiosensitivity of Pancreatic Carcinoma Cells.* Clin Cancer Res, 2014. **20**(1): p. 110-9.
152. Yang, C., et al., *PDK1 inhibitor GSK2334470 exerts antitumor activity in multiple myeloma and forms a novel multitargeted combination with dual mTORC1/C2 inhibitor PP242.* Oncotarget, 2017. **8**(24): p. 39185-39197.
153. Rubens, J.A., et al., *The TORC1/2 inhibitor TAK228 sensitizes atypical teratoid rhabdoid tumors to cisplatin-induced cytotoxicity.* Neuro Oncol, 2017. **19**(10): p. 1361-1371.
154. Miyahara, H., et al., *The dual mTOR kinase inhibitor TAK228 inhibits tumorigenicity and enhances radiosensitization in diffuse intrinsic pontine glioma.* Cancer Lett, 2017. **400**: p. 110-116.
155. Nadal, R. and J. Bellmunt, *New treatments for bladder cancer: when will we make progress?* Curr Treat Options Oncol, 2014. **15**(1): p. 99-114.

156. Wang, T.H., H.S. Wang, and Y.K. Soong, *Paclitaxel-induced cell death: where the cell cycle and apoptosis come together.* Cancer, 2000. **88**(11): p. 2619-28.
157. Shi, X. and X. Sun, *Regulation of paclitaxel activity by microtubule-associated proteins in cancer chemotherapy.* Cancer Chemother Pharmacol, 2017.
158. Burris, H.A., 3rd, et al., *TAK-228 (formerly MLN0128), an investigational dual TORC1/2 inhibitor plus paclitaxel, with/without trastuzumab, in patients with advanced solid malignancies.* Cancer Chemother Pharmacol, 2017. **80**(2): p. 261-273.
159. Rodrik-Outmezguine, V.S., et al., *Overcoming mTOR resistance mutations with a new-generation mTOR inhibitor.* Nature, 2016. **534**(7606): p. 272-6.
160. Fan, Q., et al., *A Kinase Inhibitor Targeted to mTORC1 Drives Regression in Glioblastoma.* Cancer Cell, 2017. **31**(3): p. 424-435.
161. Ruggero, D., et al., *The translation factor eIF-4E promotes tumor formation and cooperates with c-Myc in lymphomagenesis.* Nat Med, 2004. **10**(5): p. 484-6.
162. Siddiqui, N. and N. Sonenberg, *Signalling to eIF4E in cancer.* Biochem Soc Trans, 2015. **43**(5): p. 763-72.
163. Bhat, M., et al., *Targeting the translation machinery in cancer.* Nat Rev Drug Discov, 2015. **14**(4): p. 261-78.
164. Chou T-C, T.P., *Analysis of combined drug effects: a new look at a very old problem.* Trends Pharmacol Sci. , 1983: p. 4:450–454.
165. Hansen, T.E. and T. Johansen, *Following autophagy step by step.* BMC Biol, 2011. **9**: p. 39.
166. Mizushima, N., T. Yoshimori, and B. Levine, *Methods in mammalian autophagy research.* Cell, 2010. **140**(3): p. 313-26.
167. Jiang, P. and N. Mizushima, *LC3- and p62-based biochemical methods for the analysis of autophagy progression in mammalian cells.* Methods, 2015. **75**: p. 13-8.

ANNEX

ANNEX

Poster presentation

Title: Targeting the PI3K/AKT/mTOR pathway with a dual mTORC1/2 inhibitor in bladder cancer. Rationale for its testing in clinical trials.

Authors: A.Hernández-Prat, A. Martinez, O. Arpí, S. Menéndez, N. Iarchoukc, F. Rojo, J. Albanell, R. Brake, A. Rovira, J. Bellmunt.

Congress: Poster presented al 24th Biennial Congress of the European Association for Cancer, Manchester, UK, 9-12 julio 2016.

Reference: EJC, July 2016, Volume 61, Supplement 1, Page S141). Abstract 629.

Article in preparation

Hernandez-Prat A. et.al., *Targeting the PI3K/AKT/mTOR pathway with a dual mTORC1/2 inhibitor in bladder cancer. Rationale for its testing in clinical trials*

Collaboration

I have also collaborated in another project of the group during the Thesis research period. This work is not included in the PhD Thesis, but we are preparing a manuscript of this work (*Increasing the in vitro and in vivo efficacy of T-DM1 by modulating the mTOR pathway in HER2-positive breast cancer*).